ZINC-LEAD MINERALIZATION AT PERING MINE

IN THE GRIQUALAND WEST SUB-BASIN

- AN ISOTOPIC STUDY

by

Audrey Michelle Turner

Submitted in fulfilment of the
requirements for the degree of
Masters of Science,
in the
Department of Geology and Applied Geology,
University of Natal
1992

Durban
1992

ABSTRACT

Detailed studies, both chemical and physical, have been performed on various dolomites and vug-filling carbonates, to determine the pathways and extent of the mineralizing fluids associated with the Pering Zn-Pb deposit within the Griqualand West sub-basin. Three carbonate phases were identified within the vugs using cathodoluminescence microscopy. The first phase formed a reaction rim on the host dolomites during the deposition of sphalerite and oscillatory zoned carbonate. Finally calcite was deposited, which is associated with post-mineralizing fluids. The vug-filling carbonates have very radiogenic $^{87}Sr/^{86}Sr$ values (0.72-0.76) compared with the host dolomites (0.70-0.73). The gangue carbonate minerals deposited within the vugs have similar radiogenic $^{87}Sr/^{86}Sr$ values to the gangue minerals of the main Pering orebody, indicating that the vugs formed part of the aquifer system through which the mineralizing fluids migrated. Radiogenic ^{87}Sr was not acquired from the surrounding host dolomite. The mineralizing fluids may have picked up radiogenic ^{87}Sr when migrating through porous rocks such as the Makwassie Quartz Porphyry of the Ventersdorp Supergroup or felsic rocks forming the Kaapvaal Craton. In addition, radiogenic Sr may have been acquired from dewatering of the Lokammona shales within the area, or expelled from amphibolite and granulite rocks involved in the Kheis or Namaqua Tectonic events.

Two models are proposed to explain the genesis of the main Pering deposit and the occurrence of sphalerite in the vug-filling carbonates surrounding the deposit: 1) Mixing Model; and 2) Single Fluid Model. The Single Fluid Model is preferred which involves a single fluid migration and interaction with the carbonate host rock and/or pore fluid. The metals were probably transported as chloride complexes together with reduced sulphur at temperatures greater than 200° C. Deposition of the ore minerals resulted from either a dilution of the fluid, a pH increase or a temperature decrease. Both dolomites and vug-filling carbonates have a model Pb age between 2.0 and 2.7. Secondary 1Ga model ages indicate a minor Namaqua tectonic influence. Carbon and oxygen isotopes indicate that the fluids originated in a deep burial environment.

Future exploration work using cathodoluminescence microscopy and staining techniques will be both useful and cost-effective. Isotopic work should concentrate on the Rb-Sr system as radiogenic $^{87}Sr/^{86}Sr$ values are the best indicators of the path of the mineralizing fluid, and the proximity to ore concentrations.

PREFACE

The research described in this thesis was carried out in the Department of Geology and Applied Geology, University of Natal, Durban, from January 1991 to May 1991 and October 1991 to December 1992, under the supervision of Dr M.J. Duane and Dr F.J. Kruger. The research was interrupted for 4 months due to back injuries sustained in a serious motor vehicle accident near Pering Mine.

These studies represent original work by the author and have not been submitted in any form to another University. Where use was made of the work of others it has been duly acknowledged in the text.

ACKNOWLEDGEMENTS

Shell Metals South Africa, for funding this project. Thank you to Peter Steadman and Gavin Whitfield.

Dr M. Duane for initiating this project, for supplying various references, and editing the various drafts of this thesis.

Dr F. Kruger for his supervision with the laboratory work when preparing samples for Pb and Rb-Sr isotopic analysis. For help in running the Rb samples, and for running the Sr and Pb samples on the mass spectrometer. For editing the third and forth drafts of this thesis. Thank you for your constant enthusiasm, patience and willingness to help with this project.

Prof. T. Mason for editing the third draft of this thesis and for your constant help, support and encouragement.

Mr S. Nicolescou for editing the third draft of this thesis, for your willingness to help and for the valuable discussions.

Mr. F. Dooge at Pering Mine for providing accommodation at the exploration camp and allowing me access to the Shell exploration boreholes.

Mr G. Chetty and Mr V. Pakkiri at the University of Natal, Durban, for cutting endless polished thin sections and providing constant help with technical matters.

Prof. B. Verhagen for allowing me to do the C and O isotopic work at the Schonland Centre and for his help with this work. Thank you to Osborne Malinga for his help in preparing the C and O samples for analysis, and for running the samples on the mass spectrometer. This help is greatly appreciated.

Dr C. Harris for analysing two quartz samples at the University of Cape Town.

Mr J. Holtzhausen for patiently sawing the core samples to be used for analysis into millimetre size slices.

Joseph Aphane, Craig Smith, Ingaborg Swinley, Janet Moyes and Erica Barton for help with various problems experienced while doing work at the Bernard Price Institute of Geophysics, Johannesburg.

Prof. N. Beukes for allowing access to the cathodoluminescence microscope at the Rand Afrikaans University, Johannesburg.

Mr D. Hattingh for drafting the borehole location map and part of the Pering Mine location map

Mr and Mrs Kruger for providing accommodation while working at the B.P.I. Geophysics. Thank you for putting up with me for the months spent doing laboratory work. Your kind hospitality is greatly appreciated.

Mr and Mrs Basson for providing accommodation in Reivilo. Thank you for being there to help me after the motor vehicle accident. Thank you for your kindness, support and willingness to help. All you have done for me is greatly appreciated.

Mr K. Pietersen for your constant support and help with this project. Thank you for helping me through the tough times.

UNITS, SYMBOLS AND ABBREVIATIONS

A ..... amps
Å ..... angstroms
As ..... arsenic
Ba ..... barium
C ..... carbon
Ca ..... calcium
$CaCO_3$ ..... calcium carbonate
Cd ..... cadmium
CH_4 ..... methane
Cl ..... chlorine
cm ..... centimetre
CO_2 ..... carbon dioxide
Cu ..... copper
Fe ..... iron
fO_2 ..... oxygen fugacity
Ga ..... billion years
g ..... grams
HBr ..... hydrobromic acid
HCl ..... hydrochloric acid
HNO_3 ..... nitric acid
H_2S ..... hydrogen sulphide
J-type ..... Joplin-type
K ..... potassium
KCl ..... potassium chloride
km ..... kilometres
kV ..... kilovolts
LB1 ..... borehole LB1
Ma ..... million years
Mg ..... magnesium
$MgCO_3$ ..... magnesium carbonate
ml ..... millilitre
µA ..... micro-amps
µl ..... microlitre
µg ..... micrograms
Mn ..... manganese
ng ..... nanograms
N ..... normal
Na ..... sodium
NaCl ..... sodium chloride
Na_2S ..... sodium sulphide
Ni ..... nickel
O ..... oxygen
Pb ..... lead
pg ..... picograms

ppm ..... parts per million
Rb ..... rubidium
Re ..... rhenium
σ ..... sigma
S ..... sulphur
Sr ..... strontium
S26 ..... borehole S26
Ta ..... tantalum
Th ..... thorium
U ..... uranium
Zn ..... zinc

CONTENTS

LIST OF FIGURES

LIST OF PLATES

LIST OF TABLES

CHAPTER 1
INTRODUCTION

1.1 The General Geology of the Transvaal Supergroup

The Lower Proterozoic Transvaal Supergroup is preserved within the Griqualand West and Transvaal sub-basins (Figure 1). The combined area occupied by these two sub-basins is approximately 250 000km^2, although Button (1973) estimated that the original area may have been twice this size. According to Tankard *et al.* (1982), the extensive carbonates, iron-formation and minor siliclastics were deposited within shallow epeiric seas. The sedimentary and volcanic rocks of these two sub-basins have been correlated due to their basic similarities, hence the incorporation of the lithologies within the Transvaal Supergroup (Beukes, 1986; Clendenin, 1989). The Griqualand West and Transvaal sub-basins were either partly or completely separated by an archlike structure which exposes the underlying Ventersdorp Supergroup and which also acted as a basement high during the deposition of the Transvaal Supergroup (Clendenin *et al.*, 1988). Zn-Pb mineralization occurs at several localities within Lower Proterozoic carbonates of the Transvaal Supergroup. This study concentrated on the mineralization within the vicinity of Pering Mine, which is currently the only economic Zn-Pb deposit in the Griqualand West sub-basin.

In the Griqualand West sub-basin the Transvaal Supergroup comprises the Ghaap Group, which includes the dolomitic Schmidtsdrif and Campbellrand Subgroups (Figure 2). The lower Schmidtsdrif Subgroup, consists mostly of shale with minor interbedded dolomite. A precursor carbonate platform sequence to the Campbellrand Subgroup, namely the Boomplaas Formation, is developed in the Schmidtsdrif Subgroup (Beukes, 1983 a&b). The Campbellrand Subgroup conformably overlies the Schmidtsdrif Subgroup, and is in turn conformably overlain by the Kuruman iron-formation, Asbesheuwels Subgroup (Beukes, 1987). The Campbellrand Subgroup represents a major carbonate buildup, up to 1500m thick, covering 80 000km^2 along the western margin of the Kaapvaal Craton in the northern Cape (Figure 3). Its correlative in the Transvaal sub-basin, the Malmani Subgroup, covers an additional 110000km^2 and is up to 1700m thick (Button, 1973). The original extent of the carbonate buildup is not known, but it probably extended, at least, across the entire 600 000km^2 surface of the Kaapvaal Craton (Beukes, 1983a). The Campbellrand Subgroup is younger than 2600Ma and older than 2300Ma (Beukes, 1983a, Walraven *et al.*, 1990a). The most reliable date available for the Schmidtsdrif Formation is 2557±49Ma (Pb-Pb) which was obtained by Jahn *et al.* (1990).

Towards the east the Campbellrand Subgroup is virtually undeformed, dipping at 1-2° to the west on the Ghaap Plateau, but structural deformation intensifies towards the edge of the Kaapvaal Craton. Locally the carbonates are tightly folded, as in the Prieska area, or thrust over Middle Proterozoic red beds of the Olifantshoek Group (Beukes, 1987). South of Prieska the Campbellrand Subgroup is faulted out against the Doringberg shear zone (Coward and Potgieter, 1983).

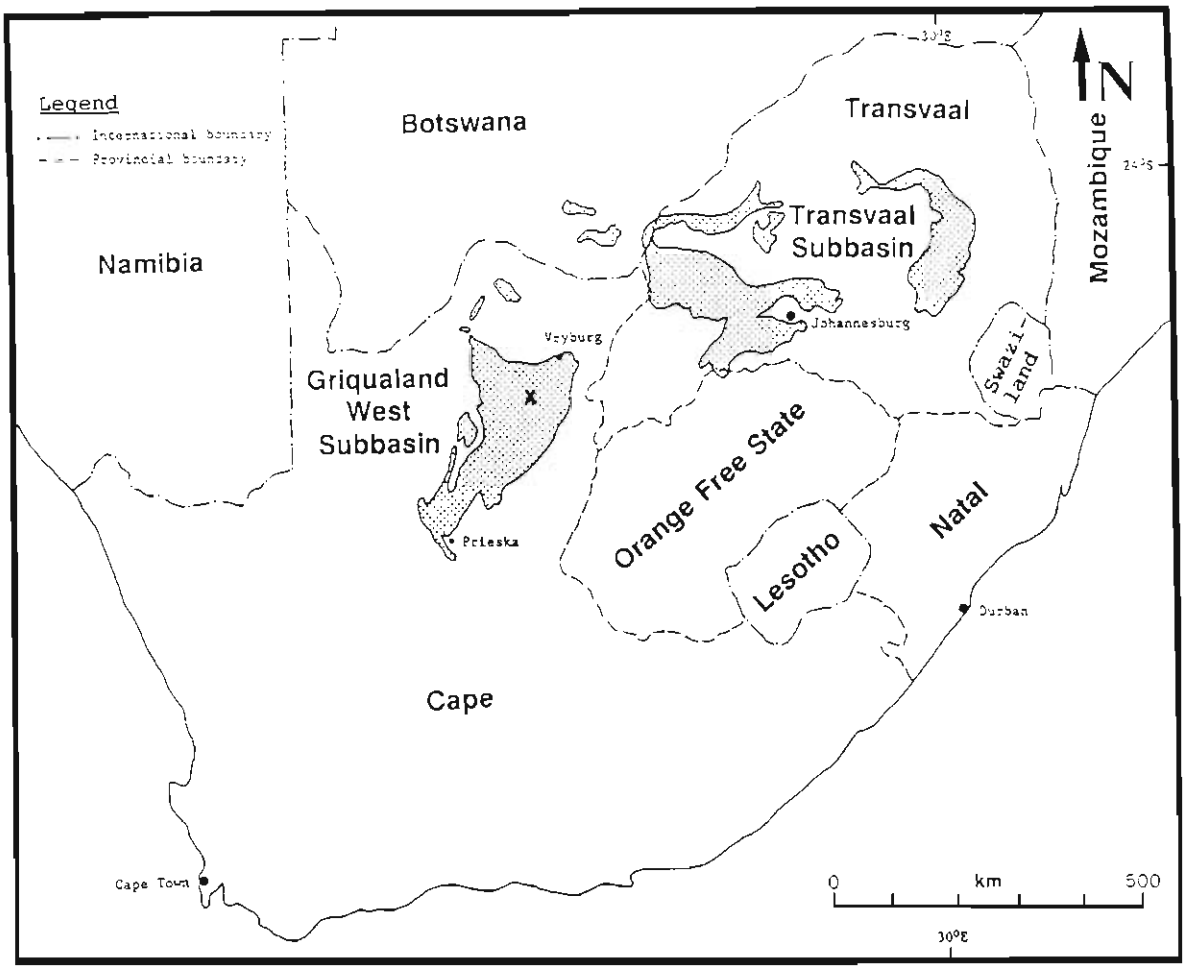

Figure 1. Distribution of the Transvaal Supergroup in the Griqualand West and Transvaal sub-basins. x = Pering Mine. [From Tyler (1979)].

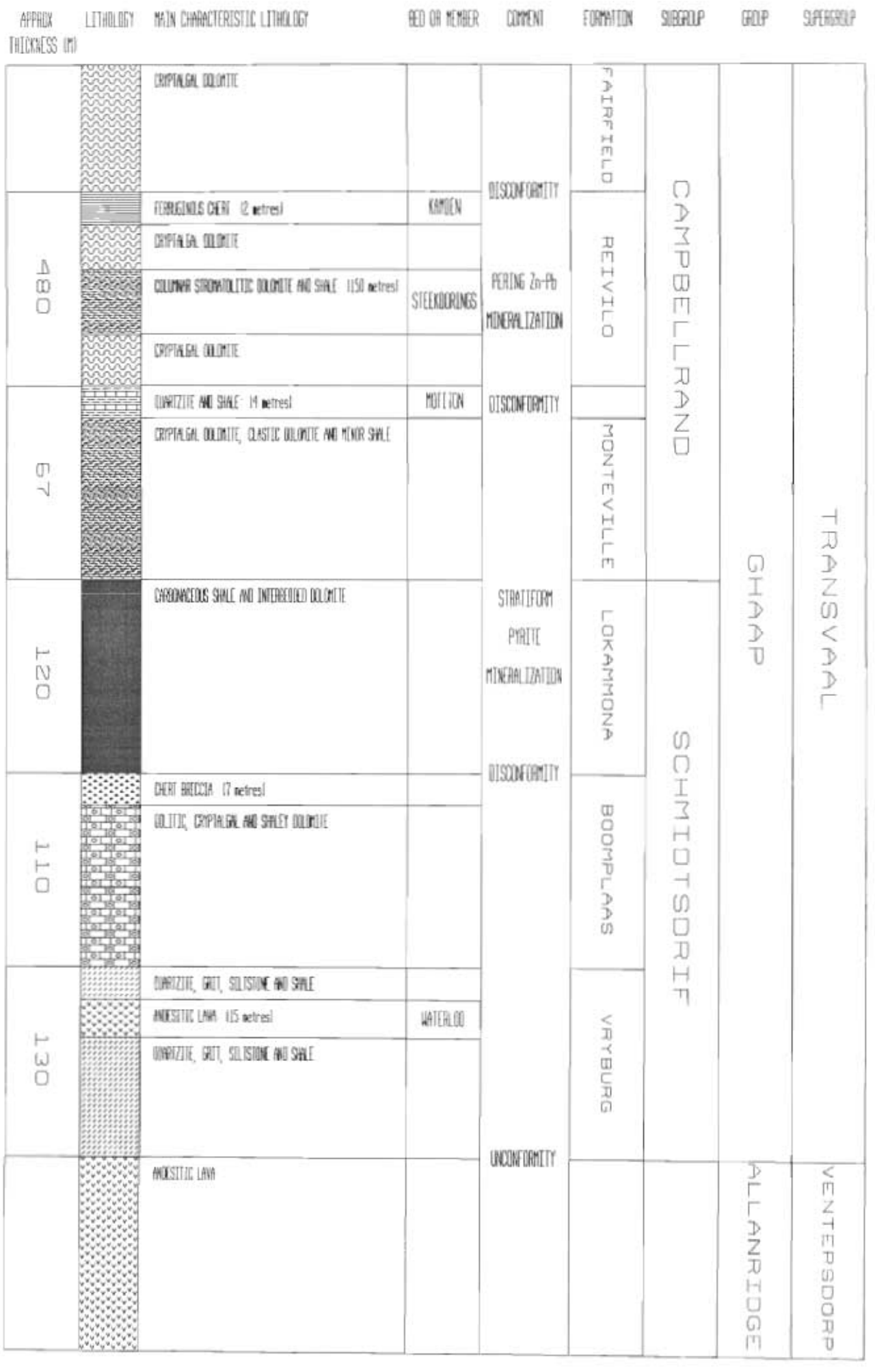

Figure 2. Generalized lithostratigraphic column of the Vryburg Trough in the Pering Mine area. [From Reuber 1978)]

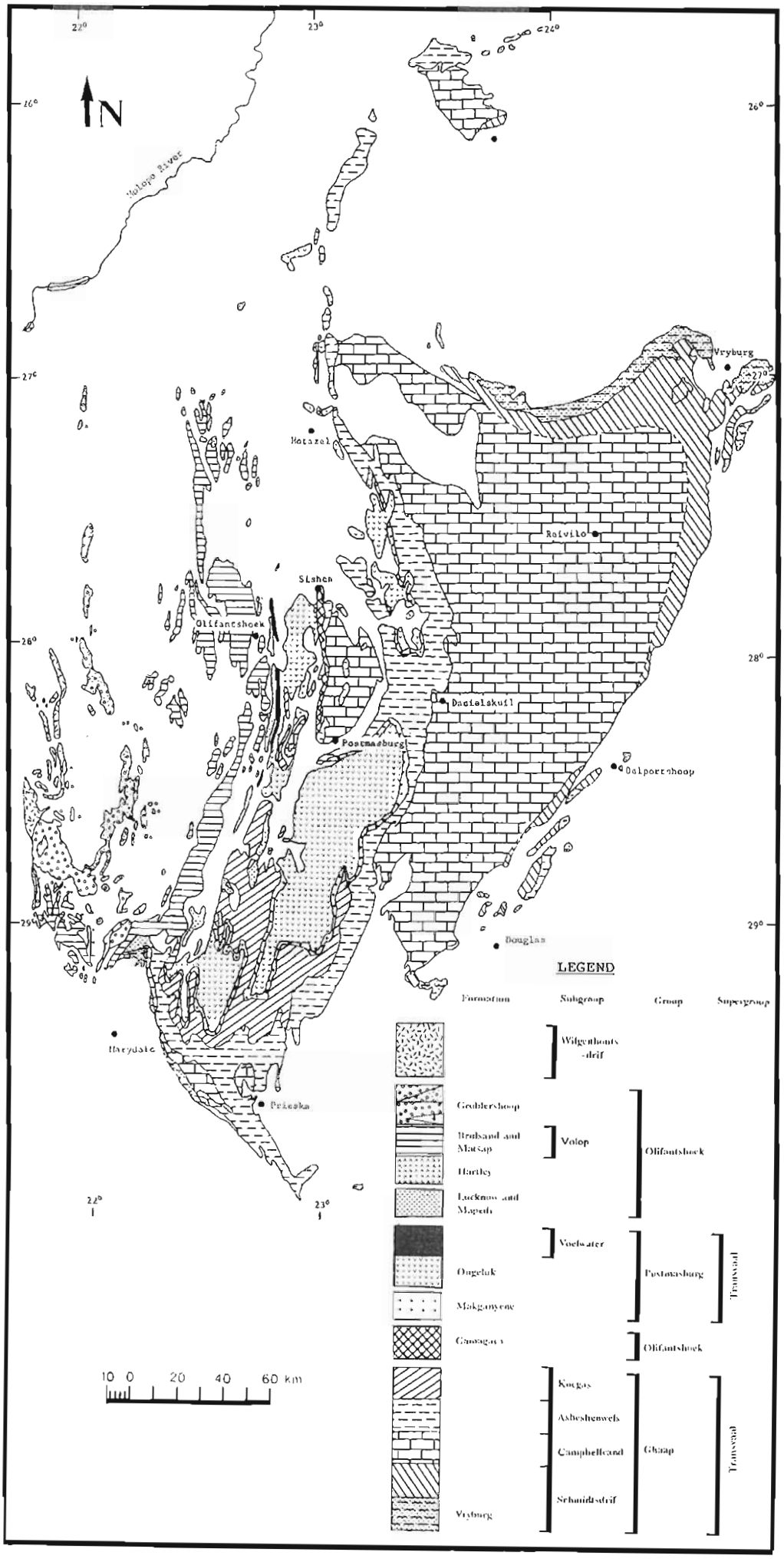

Figure 3. Geological map of the Transvaal Supergroup and Olifantshoek Group in

1.2 Zn-Pb Mineralization at the Pering Mine

The Pering Zn-Pb Mine is situated on the Ghaap Plateau approximately 20km north-east of Reivilo and 40km south-west of Vryburg (Figure 4). The mineralization occurs within the Steekdorings Member, Reivilo Formation, Campbellrand Subgroup (Figure 2). The main orebody is concentrated around the perimeter of a large (200 x 300m) collapsed karst structure and also occurs in sub-horizontal, stratabound layers (Wheatley *et al.*, 1986). This mineralization occurs within a small basin-like downwarp, approximately 2km in diameter. The deposit has estimated reserves of 18 million tons with grades of 3.6% Zn and 0.6% Pb (Wheatley *et al.*, 1986). The orebody is thought to be a Mississippi Valley-type deposit, which requires that the ore-bearing components were transported in solution, within areas of net permeability (aquifers), and deposited as carbonate-hosted sulphide minerals. Deposition of the sulphide minerals occurs as open-space fillings, and is clearly epigenetic.

Several boreholes in the vicinity of Pering Mine show evidence of the passage of the ore-forming fluids. It was therefore considered plausible that these channels contained isotopic signatures that revealed the proximity to ore deposition. Detailed isotopic investigations were therefore undertaken to determine the isotopic signatures of these channels and their significance to ore deposition.

1.3 Aims of this Study

The specific aims of this project are listed below.

(1) Examine various formations within the Ghaap Group to locate possible fossil aquifers that may have fed Zn-Pb bearing brines to the Pering and other associated base-metal deposits;

(2) Identify the distinguishing features of these aquifer structures; and

(3) Determine the composition and signatures of the mineralizing fluids using detailed Pb, Sr, C and O isotopic data.

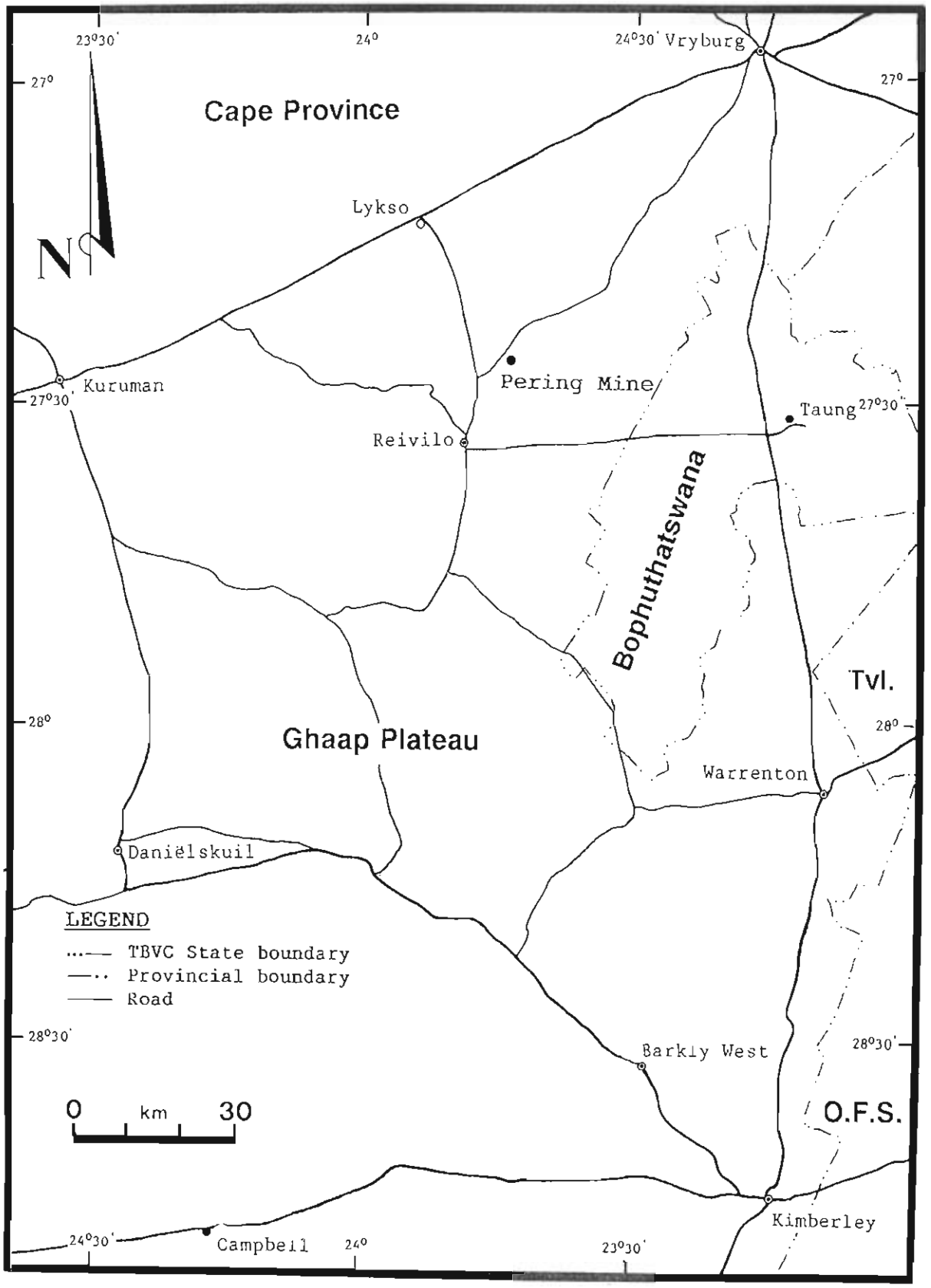

Figure 4. The location of Pering Mine.

CHAPTER 2
METHODS OF ANALYSIS

2.1 Borehole Samples

Drillcore provided by Shell exploration around Pering Mine were examined and sampled (Figure 5). The drillcore logs prepared by Shell and Swennen (1986) were used as references. The core was cut with a rotary saw and sampled; the remaining half was retained for reference. The samples were numbered according to the borehole number and a letter was assigned to each sample, from the top (A) to the base (Z). In some cases a subscript letter was also used, for example, $S26G_b$. The geology, reference logs and number of samples collected from each drillcore are listed in Appendix 1.

The main aim of sampling the drillcores was to identify structures that had the potential for being conduits for the migration of Zn-Pb-rich fluids. The most feasible structures identified were the vugs or druses which are found throughout the drillcore successions, particularly above and below the thin shale horizons (Plate 1). Boreholes LB1 and S26 were chosen for detailed study to determine the effect of fluid movement close to Pering Mine (S26) and at some distance from the mine (LB1). In addition, Swennen (1986) recommended that LB1 should be studied in detail, as this area may be a prime exploration target. A composite stratigraphic column is plotted in Figure 6. This was originally compiled by the mine staff at Pering Mine. The drillcore logs, sample locations and sample numbers of S26 and LB1 are shown in Figures 7 and 8.

2.2 Polished Thin Sections

Forty-nine polished thin sections were cut from the samples of LB1 and 91 polished thin sections from S26. These sections were examined using reflected- and transmitted-light microscopy. Under reflected-light the main ore minerals identified were sphalerite, pyrite and galena. Galena, which is quantitatively subordinate to sphalerite and pyrite, is found within the dolomite. The sphalerite, which is Fe-poor, is found within the vugs of S26. Although Swennen (1986) has identified sphalerite within LB1, no sphalerite was found in the vugs studied from this borehole. Pyrite is associated with the carbonaceous shales intersected in both boreholes. The individual carbonate phases within the vugs, in particular those associated with sphalerite mineralization, were difficult to identify using transmitted-light microscopy. Cathodoluminescence microscopy which allows carbonate phases to be distinguished by their trace element concentrations, was therefore undertaken.

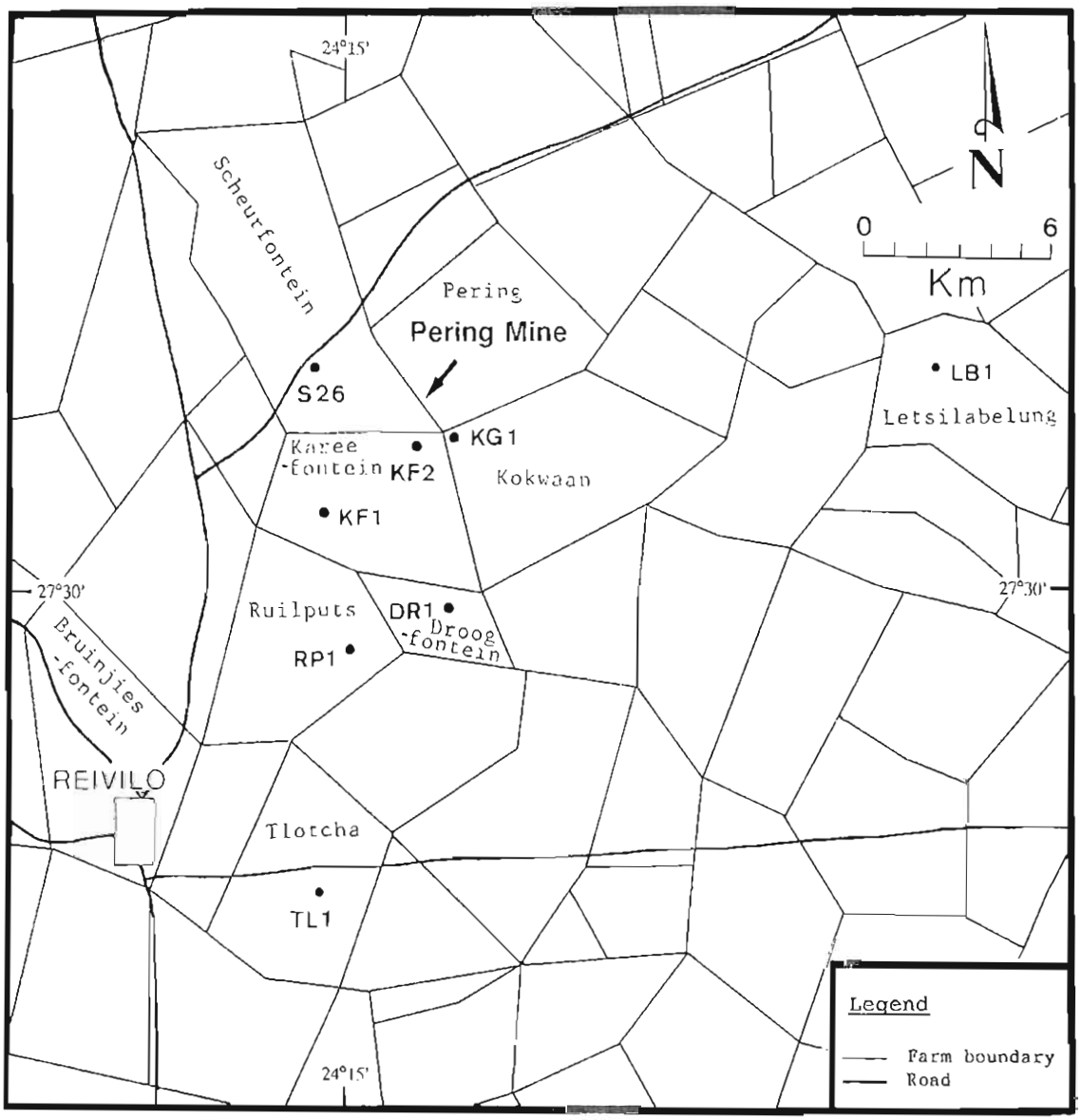

Figure 5. Shell exploration boreholes examined and sampled around Pering Mine.

Plate 1. Scanning electron micrograph of a typical vug within which equant carbonate crystals have grown.

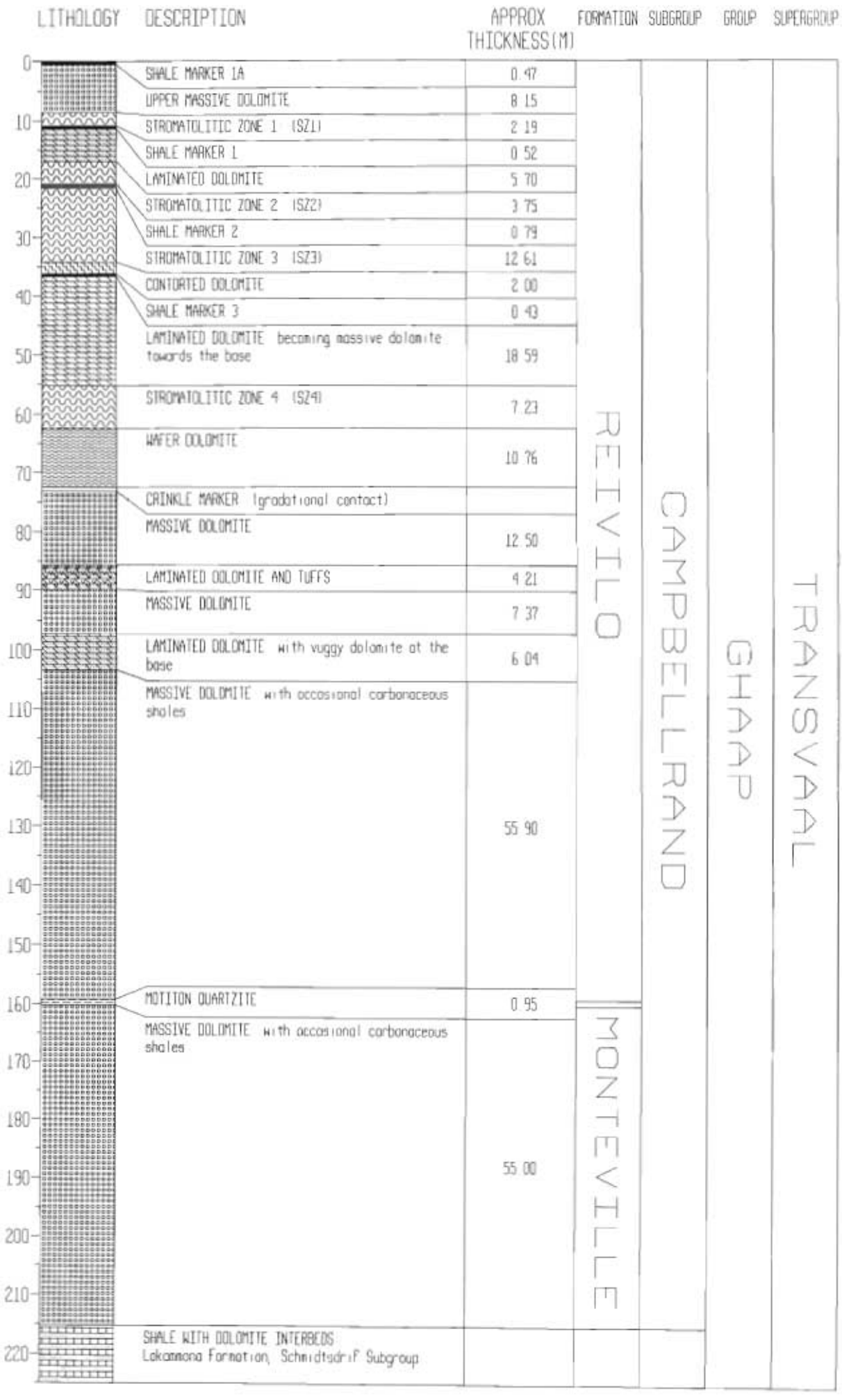

Figure 6. Composite stratigraphic column compiled for Pering Mine.

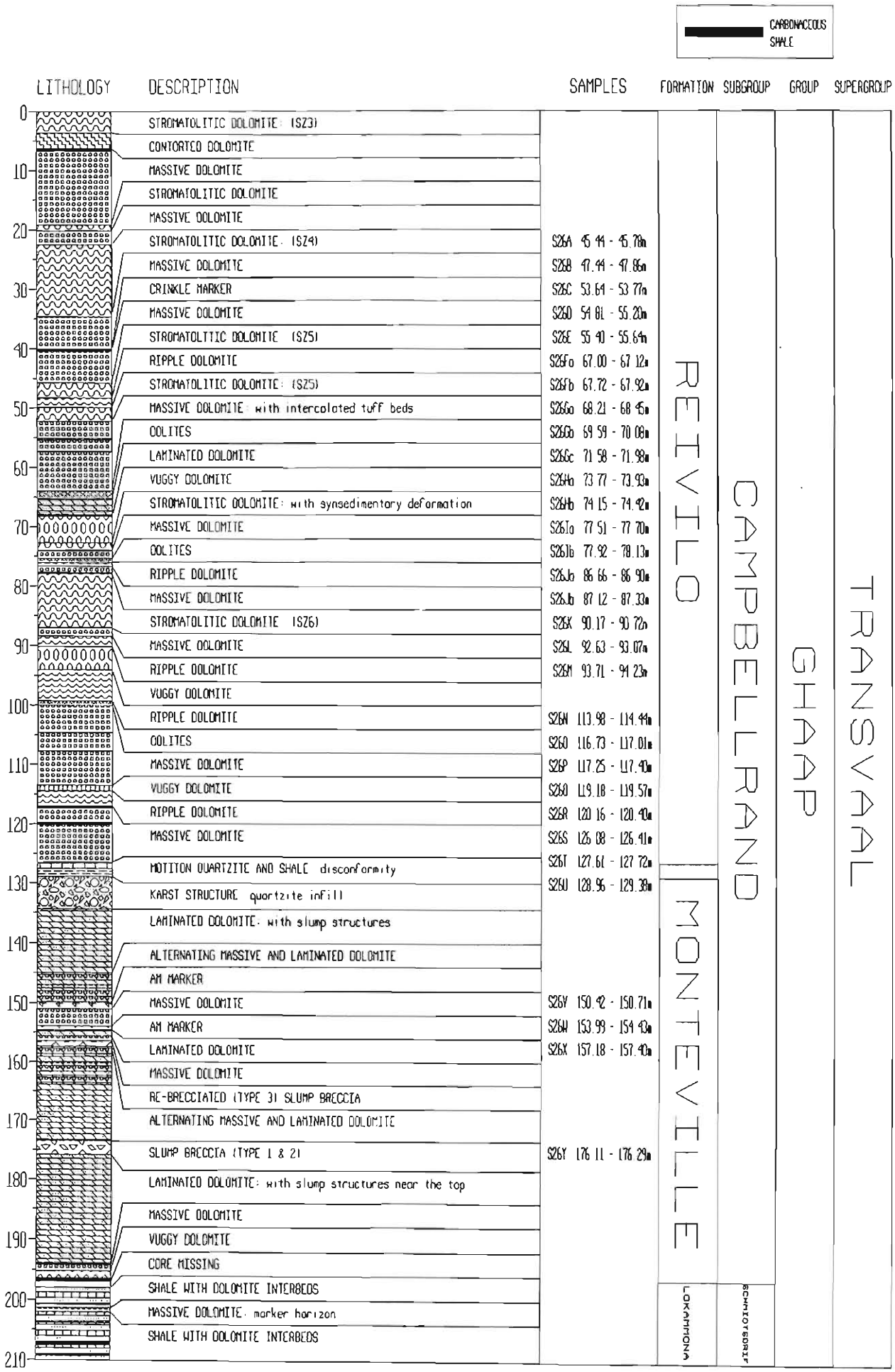

Figure 7. Detailed lithology and sample locations of borehole S26.

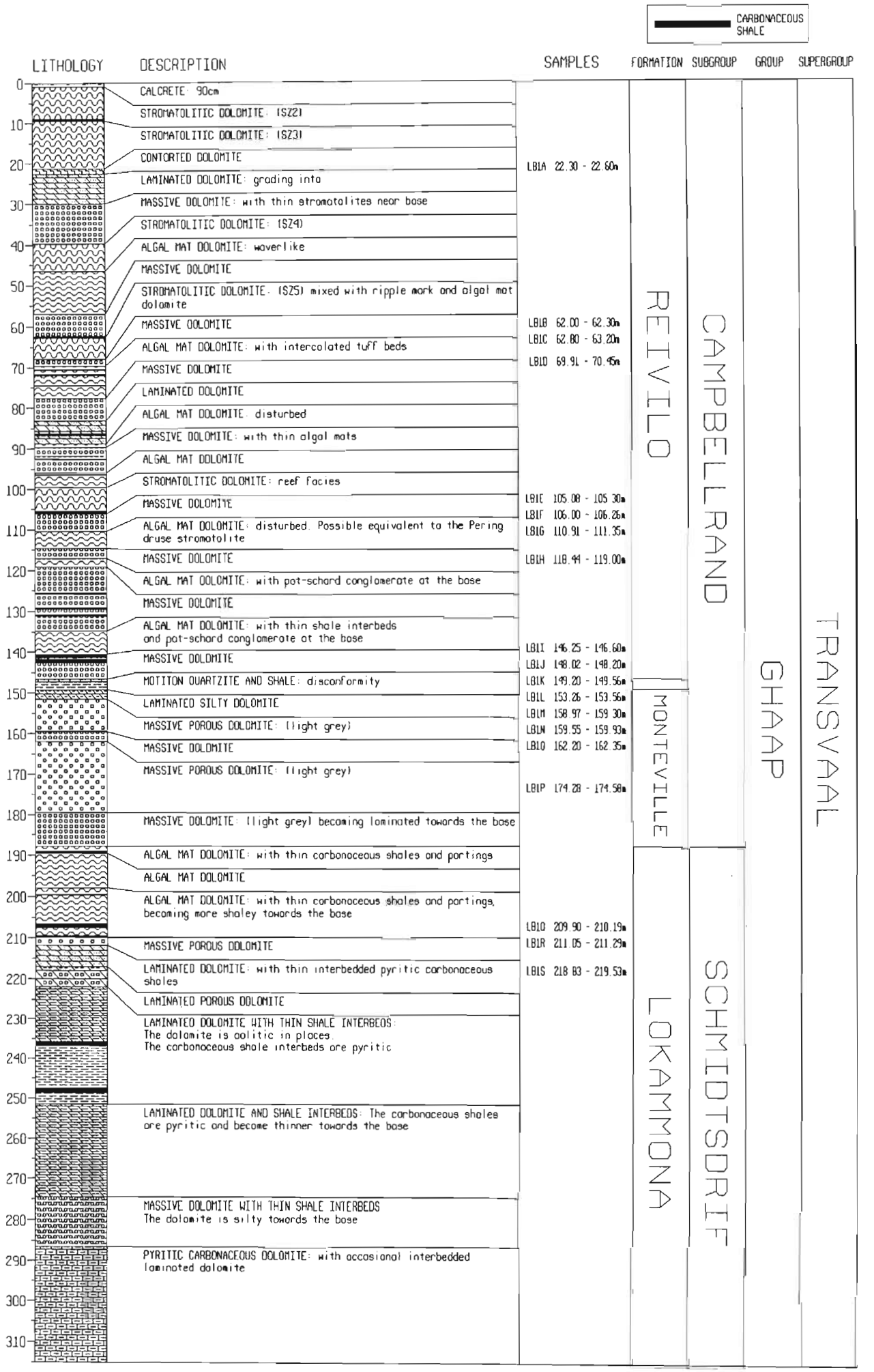

Figure 8. Detailed lithology and sample locations of borehole LB1.

2.3 Cathodoluminescence Microscopy

Cathodoluminescence microscopy was undertaken at the Rand Afrikaans University in Johannesburg, using a Cambridge Image Technology Cold Luminescence Model 8200 MK II connected to a Nikon transmitted-light microscope. An accelerating voltage of 9-20kV and gun current of 208-500μA was used.

Luminescence is the emission of light from a solid which is "excited" by some form of energy (Kopp, 1981). Cathodoluminescence results from excitation by electrons. Carbonate minerals can exhibit intense cathodoluminescence which is attributed to the presence of Mn^{2+} as an activator ion. Fe^{2+} is believed to be the most important quencher ion, that is, high Fe^{2+} concentrations reduce luminescence even if Mn^{2+} is present in the crystal lattice (Fairchild, 1983). To produce cathodoluminescence Mn^{2+} ions must be present in the mineral in concentrations ranging from 10ppm to around 1% (Walker *et al.*, 1989). Fe^{2+} concentrations in excess of about 1% has the effect of drastically reducing any such luminescence. Ten Have and Heijnen (1985) have shown that the Mn^{2+} emission in calcite is visible at concentrations as low as 15-30ppm, provided the Fe^{2+} concentration is less than 200ppm. Calcite luminesces bright yellow or orange, whereas most dolomite luminesces red or reddish purple (Kopp, 1981).

In the vugs examined three phases of carbonate were identified. The carbonate phases have been numbered from the oldest phase (C1) deposited on the dolomite, to the youngest phase (C3) in the centre of the vug. Phase C1 (Plates 2 and 3) luminesces bright reddish-orange. The crystals of phase C2 exhibit fine oscillatory growth zones, indicating varying trace element concentrations (Plates 4 and 5). These zones luminesce either a bright reddish-orange or dull red. Phase C3 luminesces a bright orange-yellow (Plates 6 and 7). The sphalerite is associated with phases C1 and C2, the first two phases of carbonate deposited within the vugs. The sphalerite is found:

(1) between the dolomite and C1;
(2) within phase C1;
(3) between phases C1 and C2; and
(4) within phase C2 (Plate 8 and 9).

Organic matter was deposited with phase C2 and phase C3 (Plates 10 and 11).

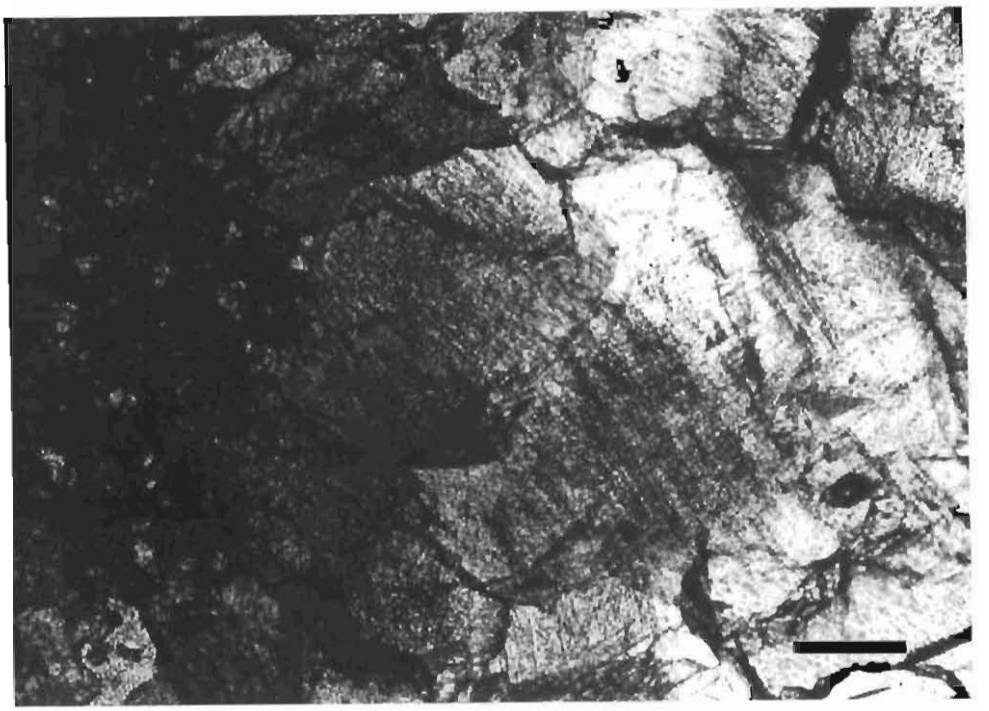

Plate 2. Dolomite, phase C1 and phase C2 shown under transmitted light. Scale = 200μm.

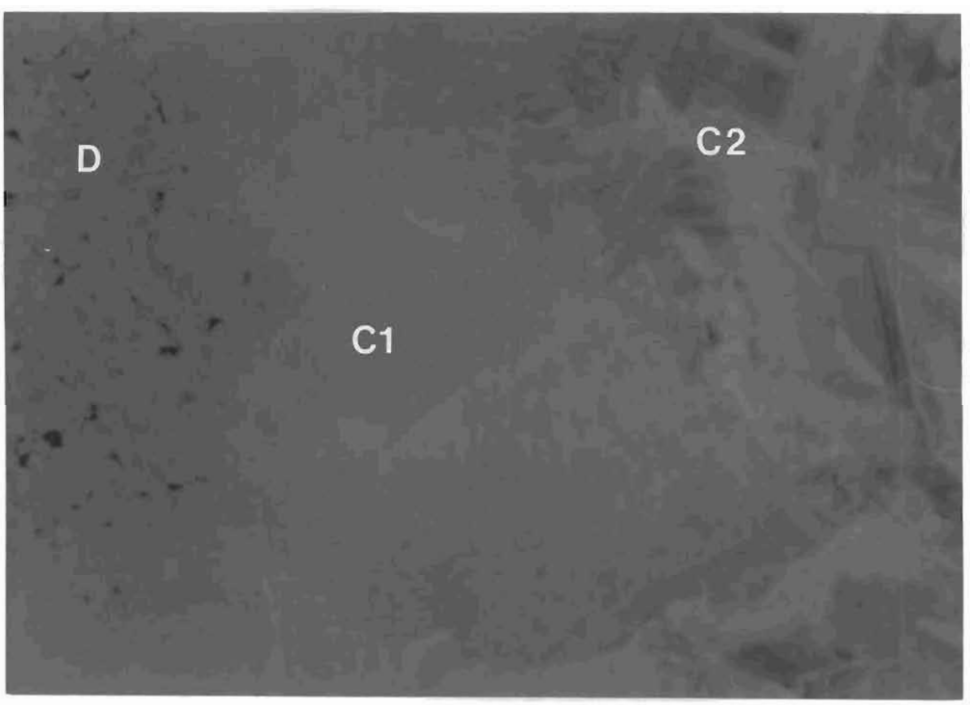

Plate 3. Cathodoluminescent photomicrograph of dolomite, phase C1 and phase C2. Scale = 200μm.

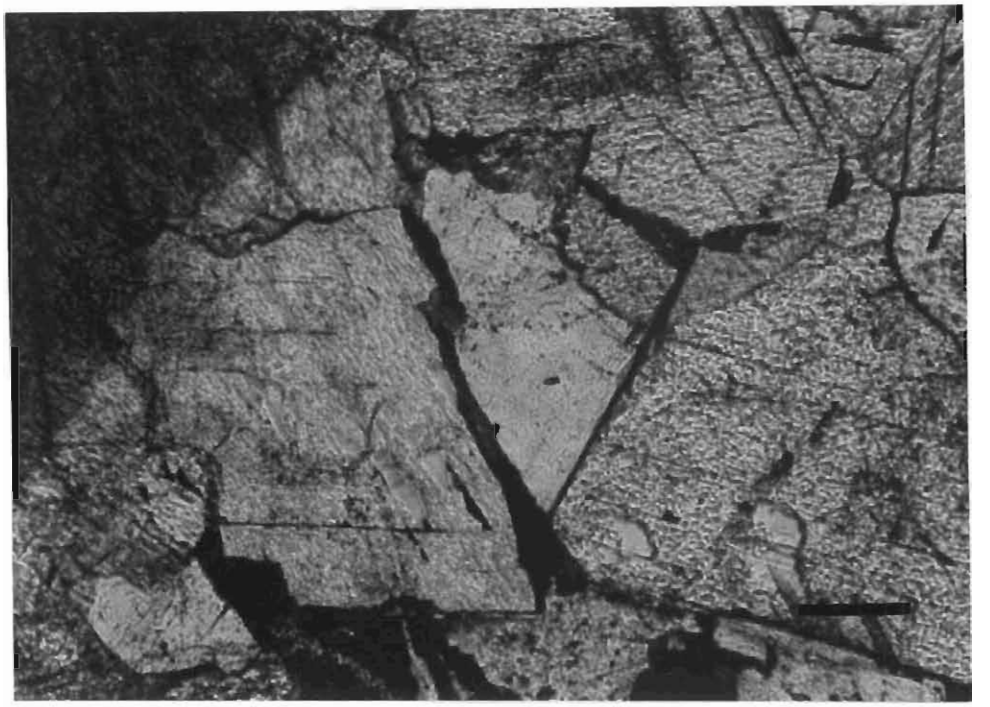

Plate 4. Phases C1, C2 and C3 shown under transmitted light. Scale = 200μm.

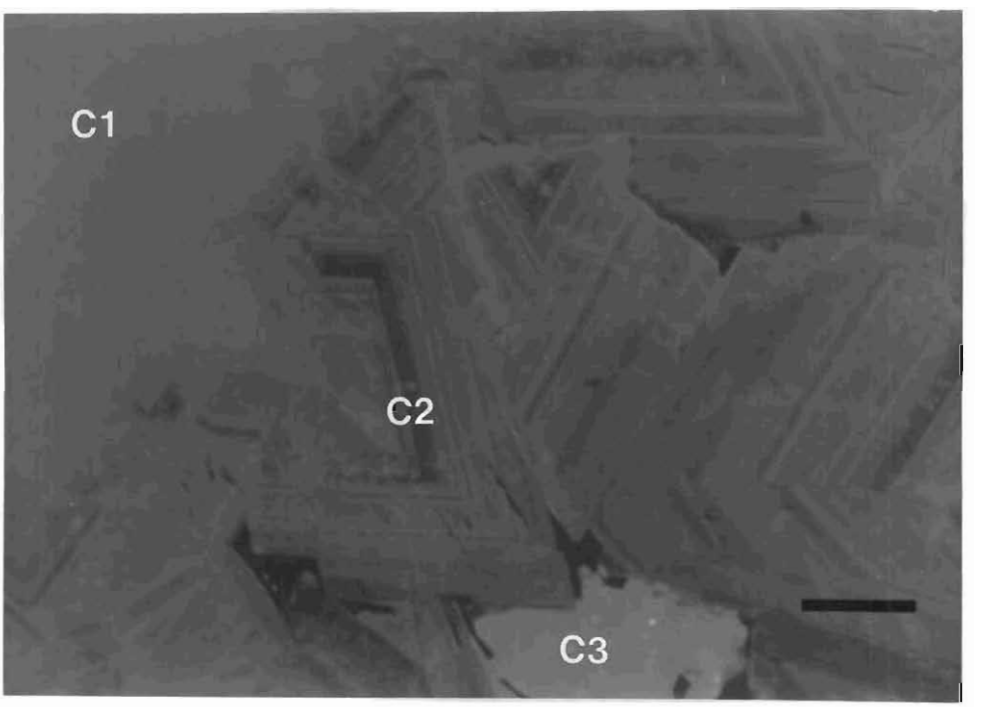

Plate 5. Cathodoluminescent photomicrograph of phases C1, C2 and C3. Scale = 200μm.

Plate 6. Phases C1, C2 and C3 shown under transmitted light. Scale = 200μm.

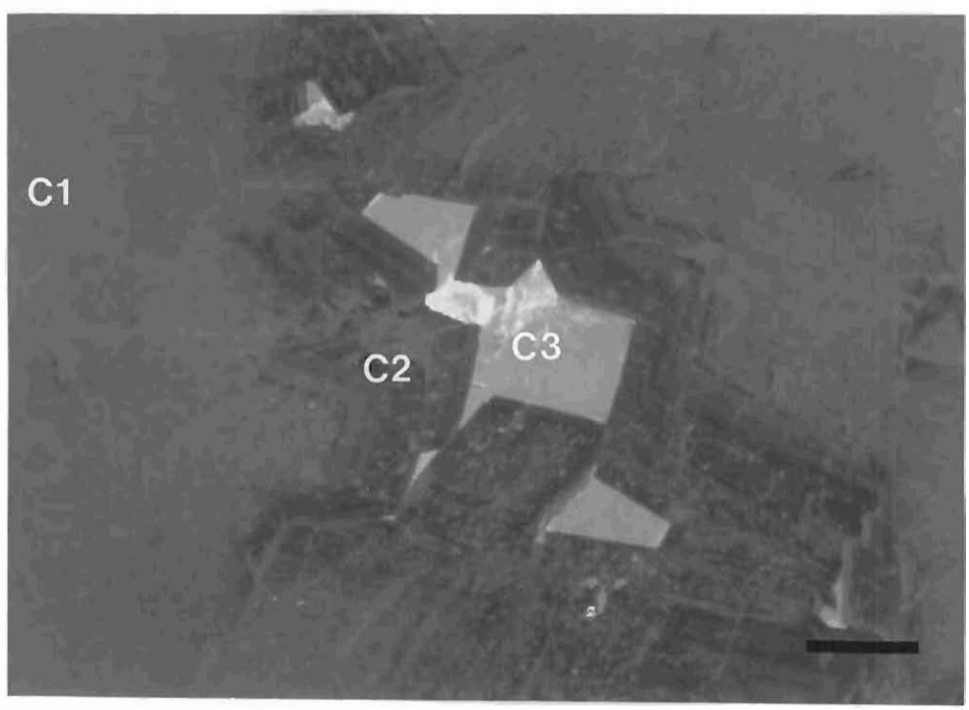

Plate 7. Cathodoluminescent photomicrograph of phases C1, C2 and C3. Scale = 200μm.

Plate 8. Sphalerite deposited with phase C2 shown under transmitted light. Scale = 200μm.

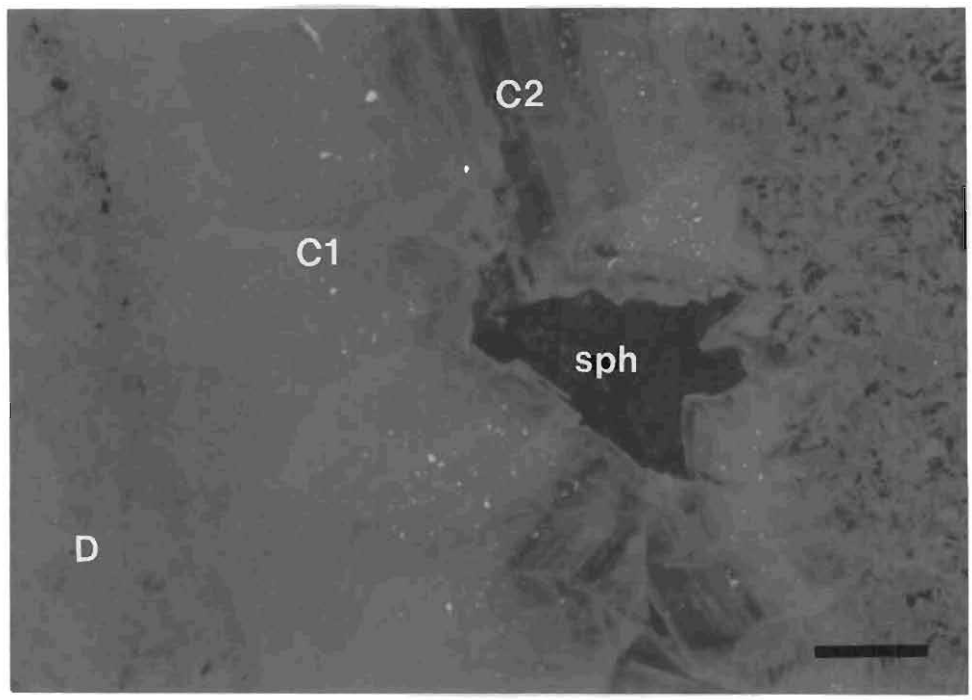

Plate 9. Cathodoluminescent photomicrograph showing sphalerite deposited with phase C2. Scale = 200μm.

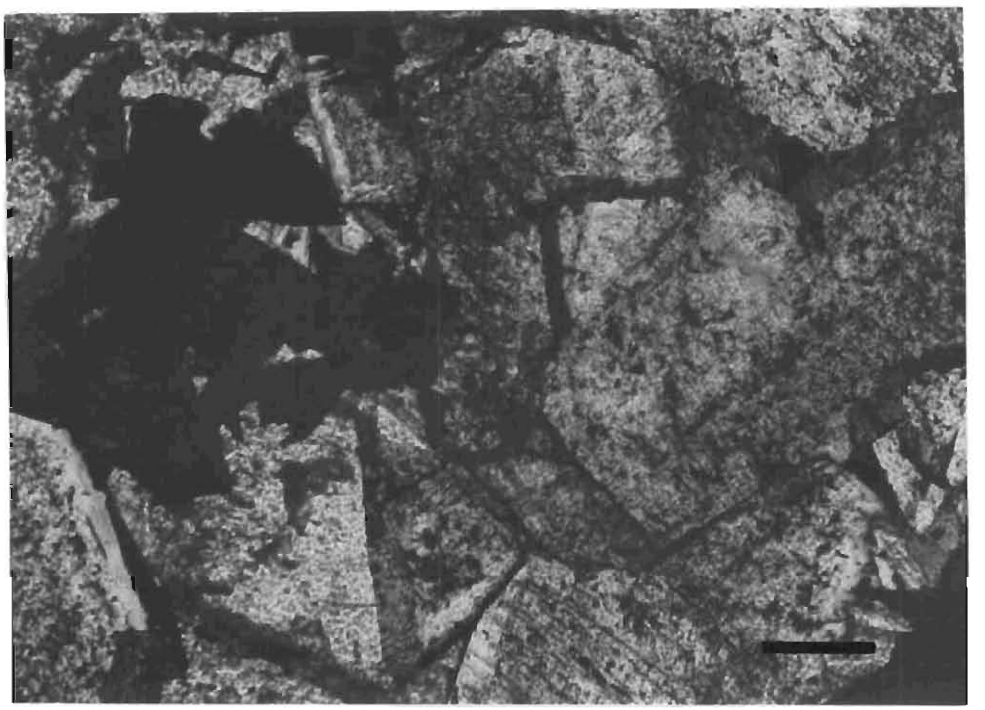

Plate 10. Organic matter deposited with phase C3 shown under transmitted light. Scale = 200μm.

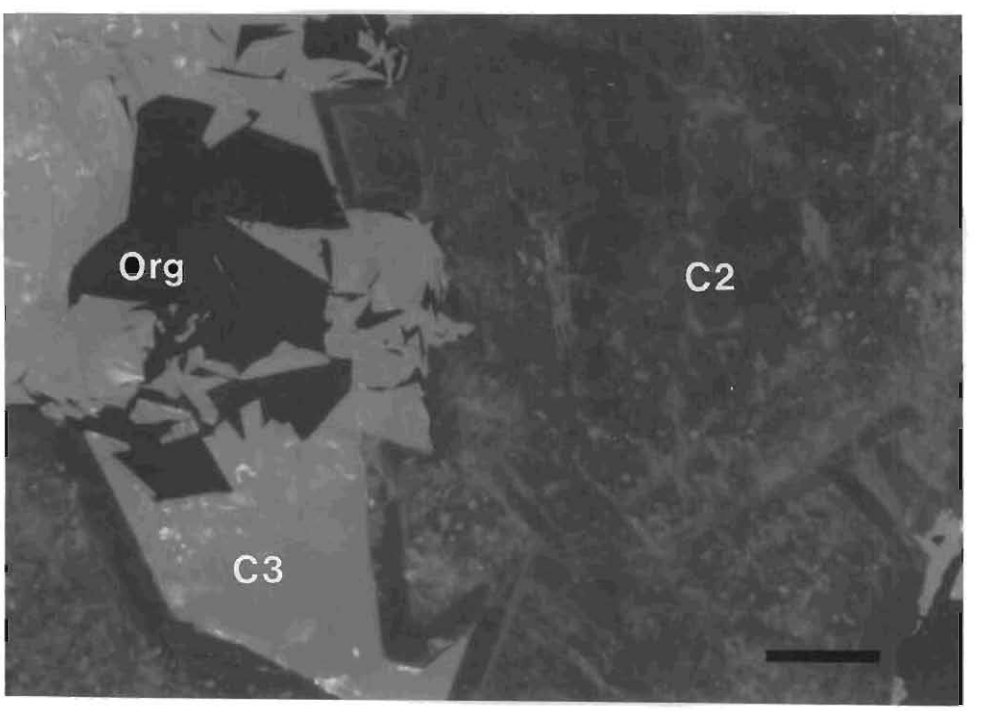

Plate 11. Cathodoluminescent photomicrograph showing organic matter deposited with phase C3. Scale = 200μm.

2.4 Initial Sample Preparation

Cathodoluminescence photographs were used to select suitable borehole core samples for isotopic analysis. The carbonate phases were not drilled out of the polished thin sections, as the amount of sample needed for isotopic analysis was greater than that obtainable from the polished thin sections. Samples were chosen which had:

(1) large vugs which facilitated easier hand-picking of each carbonate phase; and

(2) where possible, sphalerite associated with the carbonate phases in the vugs (Plate 12).

Each core sample selected for isotopic work was sliced into 1mm thick slices perpendicular to the long edge of the core, using a microtome diamond saw. These slices were placed on strips of masking tape for staining and hand-picking.

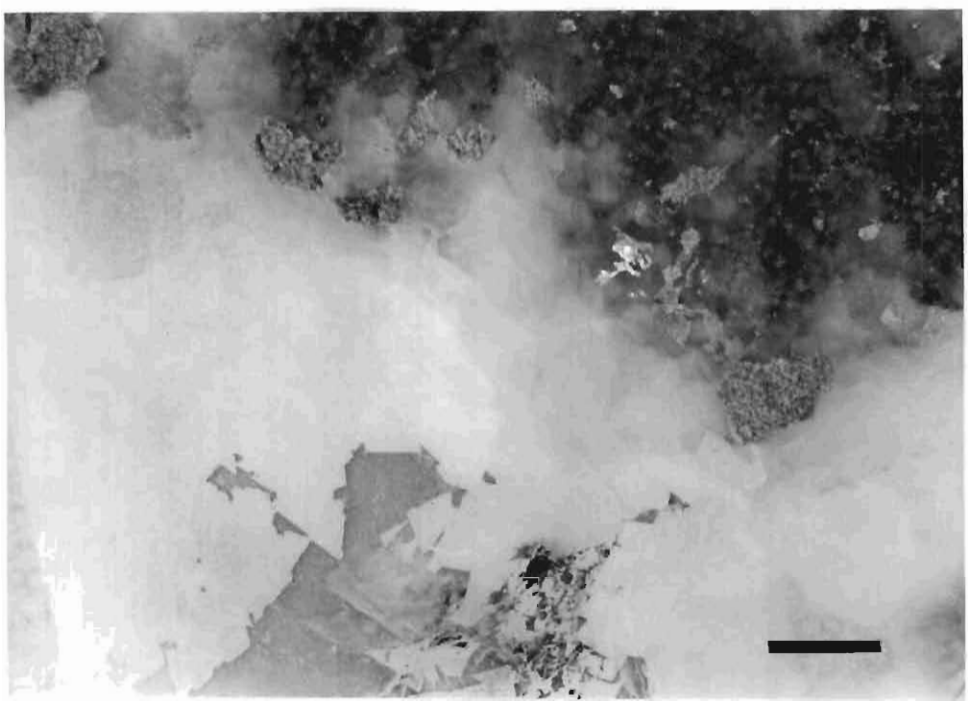

Plate 12. Sphalerite deposited within phases C1 and C2. Scale = 2mm.

Due to the difficulty in distinguishing the carbonate phases in the core slices when compared with the cathodoluminescence photographs, a solution of Alizarin Red S was used to stain and differentiate the carbonate phases. The third carbonate phase (C3) stained bright pink within one minute of applying the Alizarin Red S (Plate 13). The third phase was thus easily distinguishable from the first and second phases. It was difficult to distinguish between the first and second phases, as the first phase forms a very thin "reaction rim" between the dolomite host rock and phase C2. Only after being immersed in Alizarin Red S for three-quarters of an hour did the oscillatory zones in phase C2 become visible. From this staining experiment it became evident that only phase C3 is pure calcite; the first and second phases may be a form of recrystallized dolomite.

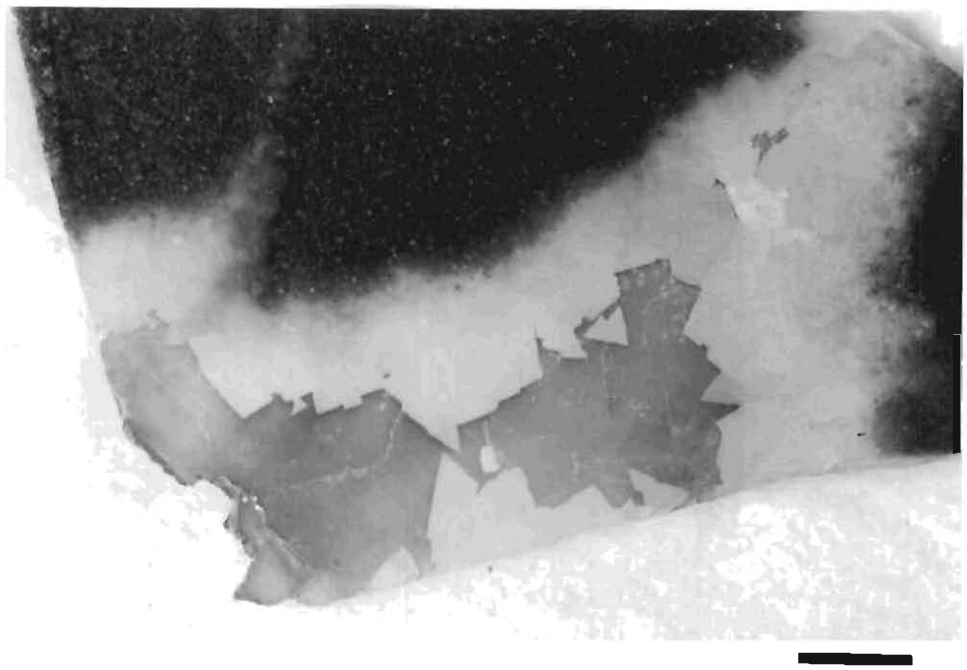

Plate 13. Distinct staining of phase C3 (pink), compared to phases C1 and C2, using Alizarine Red-S. Scale = 2mm.

Using a binocular microscope the individual dolomite and vug-filling carbonate phases were hand-picked from the core slices. Extreme care was taken to prevent contamination of the carbonate phases with the sphalerite, and contamination between individual carbonate phases. The samples were washed in dilute (0.2%) HCl to remove the Alizarin Red S stain, and then washed in an ultrasonic bath, dried, and weighed. Approximately 0.1g of each carbonate phase was used for Pb and Rb/Sr isotopic analysis, and duplicate samples of 0.01-0.02g were collected for C and O isotopic analysis. Quartz, found in the vugs of two samples, was collected for O isotopic analysis. The samples selected, and the various phases analysed from each sample are listed in Table 1. Sphalerite was found in samples S26A, S26B and S26N2.

TABLE 1: Carbonate and silicate phases analysed from each sample.

SAMPLE NUMBER	DOLOMITE	PHASE C1	PHASE C2	PHASE C3	QUARTZ
S26A	X	X	X		
S26B	X		X	X	
S26Gb	X		X		
S26L	X		X		
S26M	X	X	X	X	
$S26N_1$	X	X	X		
$S26N_2$	X	X	X		
S26X	X		X	X	
LB1N	X		X	X	
LB1P	X		X		
LB1R	X		X		X
LB1S	X		X	X	X

2.5 Chemical Sample Preparation

Chemical preparation for the analysis of the Pb, Rb and Sr isotopes was carried out in ultra-clean pressurised laboratories at the Bernard Price Institute of Geophysics, University of the Witwatersrand, Johannesburg. The Rb and Sr concentrations were determined by isotope dilution mass spectrometry, and the $^{87}Sr/^{86}Sr$ values were determined on spiked samples. Pb was extracted from the same solutions. The analytical procedures used to prepare the samples for Pb, Rb and Sr isotopic analysis are recorded in Appendix 2.

Chemical preparation for the analysis of the C and O isotopes was carried out at the Schonland Centre, University of the Witwatersrand. Duplicate samples were finely ground and dissolved in 100% pure phosphoric acid, in glass ampoules under vacuum. The two quartz samples were analysed for O isotopes by Dr C. Harris, in the Geochemistry Department at the University of Cape Town.

2.6 Analytical Techniques

The Pb samples were loaded onto single outgassed Re filaments with silica gel and phosphoric acid (H_3PO_4), and analysed on a fully automatic VG-354, extended geometry, mass spectrometer. The instrument uses a technique that automatically increases the filament current up to 2A in 10 seconds, and then the beam is found and focused. Due to the very small sample size, and the low Pb concentrations in the carbonates, the Daly detector was initially used to focus and collect some data, before the filament current was increased and the Faraday Cup used. The beam was not always sufficiently large to allow Faraday collection, despite high filament currents up to 3A. All the Pb collected from each sample was loaded onto the filaments which allowed only one run on each sample to be performed. Various runs failed which accounts for the deficiency of data for several samples. The analyses were normalised to those run with the Faraday Cup, and corrected for mass fractionation (Appendix 3a). The Daly and Faraday values for each sample are tabulated in Appendix 3b, and the ratios obtained after mass-fractionation corrections and normalisation are shown in Appendix 3c. A difference of less than five percent between the Daly and Faraday values was used as a basis for determining acceptable ratios (Appendix 3d). The dolomite samples S26A, S26M and S26X were not used as they show a variation between the Daly and Faraday data of more than 20%. In addition to the carbonate analyses, galena associated with a hydrocarbon sample collected near the Pering deposit was analysed for Pb. This analysis is included in Appendix 3e together with galena Pb data and Rb-Sr carbonate analyses obtained by Duane *et al.* (1991) around Pering Mine.

The Rb samples were loaded directly from the centrifuge tube as a chloride onto double outgassed Ta filaments, and analysed on a VG Aldermaston Micromass 30, which has a 30cm radius, 90° mass spectrometer fitted with a Keithley Electrometer. The instrument was run using computerised peak switching and an 8kV accelerating potential. Two blank samples contained 180pg and 160pg total Rb. Although this only affects the analyses in the fourth decimal place, the average of these two values (170pg) has been subtracted from all Rb analyses. Each Sr sample was converted to a nitrate, and loaded onto single outgassed Ta filaments with phosphoric acid (H_3PO_4). The Sr isotopic compositions and concentrations have been determined using the VG-354 mass spectrometer. Spiked and unspiked replicates of the SRM-987 Sr standard are routinely run in the BPI Geophysics laboratories, and an average of 19 duplicates gave a $^{87}Sr/^{86}Sr$ value of 0.71022±6. The average Sr blank is less than 2μg which is not significant for the Sr results obtained (pers. comm. Dr F.J. Kruger, B.P.I. Geophysics). The Rb and Sr results are tabulated in Appendix 4.

C and O isotopic compositions of the dolomite and carbonate phases were determined by analysing the liberated CO_2 from each sample on a VG Micromass 602C fitted with a double-inlet, double-collecting isotope ratio unit. The instrument was run using a 2.4-2.5kV accelerating potential. Based on duplicate analyses of most samples, the analytical uncertainty (σ) is no greater than ± 0.05‰ for $\delta^{13}C$, and no greater than ± 0.12‰ for $\delta^{18}O$. The analytical uncertainty for the two quartz samples is ±0.15‰ (2σ) based on 20 standard (NBS-28) determinations. The quartz data have been normalised such that the standard value is 9.64‰ on the SMOW (Standard Mean Ocean Water) scale (pers. comm. Dr C. Harris, Department of Geochemistry, U.C.T.). The C and O isotope results, and temperature calculations for the carbonate and quartz phases, are tabulated in Appendix 5a and 5b respectively.

CHAPTER 3
ISOTOPE SYSTEMATICS

3.1 The U-Th-Pb Isotope System

Natural Pb contains the following four isotopes (average abundances): ^{204}Pb (1.4%), ^{206}Pb (24.1%), ^{207}Pb (22.1%), and ^{208}Pb (52.4%) (Faure, 1986). Only ^{204}Pb has no radiogenic component. ^{206}Pb is produced by the radioactive decay of ^{238}U, ^{207}Pb by the decay of ^{235}U, and ^{208}Pb by the decay of ^{232}Th (Faure, 1986).

Two distinct categories of Pb, ordinary Pb and anomalous Pb, have been recognised. Ordinary Pb has isotope ratios that can be related to:

(1) the age of the Earth;

(2) proportions of U, Th and Pb in the source rocks in which the Pb occurred prior to mineralization; and

(3) the time of mineral deposition.

Anomalous Pb isotope ratios are quite different from ordinary Pb. For example, Pb in galena from classic Mississippi Valley-type deposits are found to be notably enriched in the radiogenic isotopes (^{206}Pb/^{204}Pb values of 20 or greater) compared to ordinary Pb (Heyl *et al.*, 1974).

Representation of the ^{207}Pb-^{206}Pb data includes comparing the plotted ^{207}Pb/^{204}Pb and ^{206}Pb/^{204}Pb values of the samples with a simple hypothetical case or model. The model states that the sample was isolated at time t from a region in which the U/Pb ratio has been constant since an initial time t_i (Figure 9). Growth curves which arise from this hypothesis each describe the isotopic development with time of Pb in an isolated source with different but constant ^{238}U/^{204}Pb values (μ). The straight lines which intersect these growth curves are known as primary isochrons. They describe, for any t (the "model age") the range of possible Pb isotope ratios, each of which changed due to radioactive decay in a different μ value environment which stayed unaltered since the initial t_i. Using the two-stage Pb evolution model of Stacey and Kramers (1975), the common origin of both growth curves and isochrons represents the single value for the isotopic composition of all Pb at t_i, the age of geochemical differentiation in the Earth's history (3.70Ga). In this model, Pb evolved from a primordial Pb isotope ratio from 4.57Ga (the age of the Earth, t_o) to 3.70Ga, in a reservoir with a μ value of 7.19 (Faure, 1986). This initial stage is not plotted on the graphs used to display the Pb isotope results of this study.

The model age t only has meaning if the model is something like reality. This model is therefore used tentatively as many published model ages are much younger or older than the true age of the deposit. This suggests that the true situation is more complicated than allowed for by this simple model. The two stage model can only be an approximation, as large differentiation events in the upper parts of the Earth may have started shortly after its origin. Pb isotope data, as interpreted by the two-stage model,

reflect a fairly constant μ value (9.74) since about 2.5Ga. These differentiation events were probably completed by that time (Stacey and Kramers, 1975).

The ^{208}Pb-^{206}Pb data is compared with the second stage (>3.7Ga) growth curve for average modern Pb (Stacey and Kramers, 1975). The $^{232}Th/^{204}Pb$ value or ω value for this growth curve is 37.19.

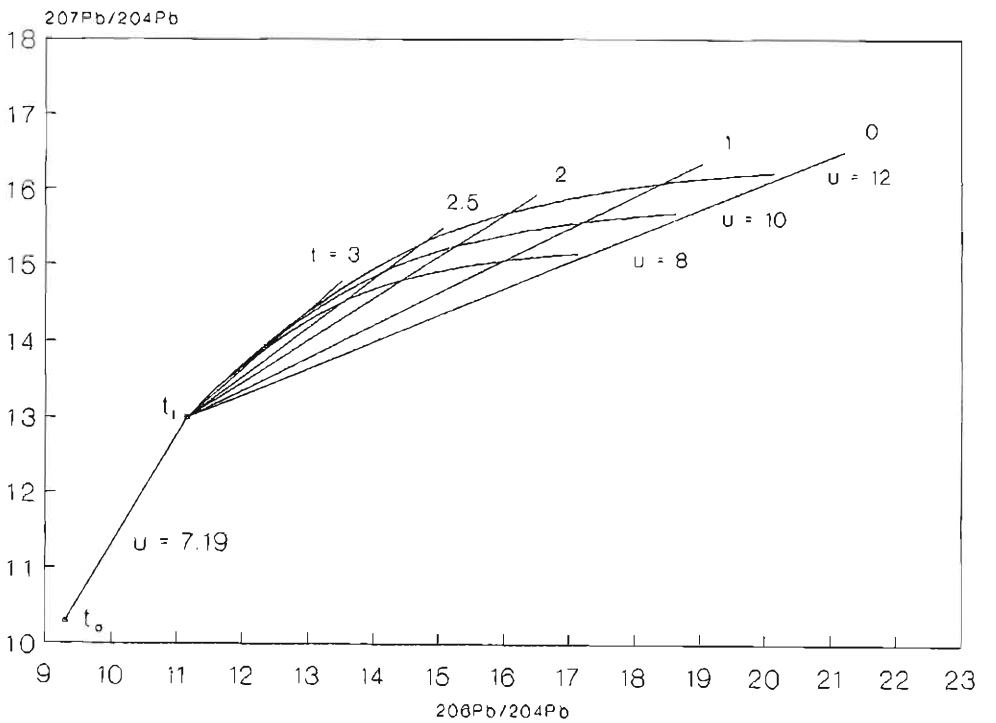

Figure 9. Pb isotope evolution by a two-stage model with primary isochrons of 0, 1, 2, 2.5 and 3 Ga superimposed on growth curves with μ values ($^{238}U/^{204}Pb$) of 8, 10 and 12. The first stage from 4.57 (t_o) to 3.7 Ga (t_1) has a μ value of 7.19 (From Stacey and Kramers, 1975).

3.2 The Rb-Sr Isotope System

Sr has four stable isotopes: ^{88}Sr, ^{87}Sr, ^{86}Sr and ^{84}Sr. The isotopic abundances are 82.53%, 7.04%, 9.87% and 0.56% respectively (Faure, 1986). The isotopic abundances of Sr are variable because of the formation of radiogenic ^{87}Sr from the β-decay of naturally occurring ^{87}Rb. Because the concentration of ^{87}Sr may vary significantly, it is by convention expressed relative to the abundance of stable ^{86}Sr (Elderfield, 1986). The $^{87}Sr/^{86}Sr$ ratio is therefore a measure of the enrichment of radiogenic ^{87}Sr relative to ^{86}Sr.

During the early separation of the crust and mantle, significant elemental fractionation took place. Incompatible elements were excluded from basaltic melts and became more enriched in the more silicic products. Thus, the continental crust developed with a higher Rb/Sr value than the upper mantle. Therefore, evolution of these two geochemical reservoirs with time lead to distinctly different isotopic compositions: higher $^{87}Sr/^{86}Sr$ values in the continental crust than in the upper mantle (Elderfield, 1986). ^{87}Sr was present when the Earth formed and the primordial $^{87}Sr/^{86}Sr$ value was about 0.699. The Earth's mantle must have a Rb/Sr value of approximately 0.025 because modern mantle-derived rocks have $^{87}Sr/^{86}Sr$ values near 0.703. Crustal rocks, however, have a Rb/Sr value about an order of magnitude higher than the mantle value, and the $^{87}Sr/^{86}Sr$ value in crustal rocks therefore increases at an appreciable rate relative to the mantle value. Average Precambrian continental crust has an average $^{87}Sr/^{86}Sr$ value in the range of 0.720 to 0.750. These values will vary considerably depending on the local type and age of the rock. Phanerozoic sedimentary rocks have lower $^{87}Sr/^{86}Sr$ values, than Precambrian continental crust, between 0.708 and 0.720 (Hedge, 1974).

3.3 The Stable Isotope System

Changes in the isotopic abundances for the lighter elements (below about 40 atomic mass units), which include C and O, arise not from radioactive decay but from mass dependent fractionation during geological processes. Carbon has two stable isotopes: ^{12}C (98.89%) and ^{13}C (1.11%) (Nier, 1950). Oxygen has three stable isotopes: ^{16}O (99.763%), ^{17}O (0.0375%) and ^{18}O (0.1995%) (Garlick, 1969). Because of the higher abundance and greater mass difference between ^{16}O and ^{18}O, these two isotopes are used when expressing the O isotopic concentration of a substance. The carbonate C and O isotope results are reported as the variation per mil relative to the PDB standard. The PDB standard is based on CO_2 produced from Cretaceous belemnites of the Peedee Formation in South Carolina (Faure, 1986). The two quartz samples analysed are reported as the variation per mil relative to the Vienna SMOW standard (Faure, 1986). The C and O isotopic concentrations is expressed in terms of the delta notation:

$$\delta^{13}C=\frac{(^{13}C/^{12}C)_{spl}-(^{13}C/^{12}C)_{std}}{(^{13}C/^{12}C)_{std}}x10^{3} \quad \text{... (1)}$$

$$\delta^{18}O=\frac{(^{18}O/^{16}O)_{spl}-(^{18}O/^{16}O)_{std}}{(^{18}O/^{16}O)_{std})}x10^{3} \quad \text{... (2)}$$

where the "spl" and "std" represent sample and standard respectively.

Positive values of $\delta^{13}C$ and $\delta^{18}O$ indicate enrichment of a sample in ^{13}C and ^{18}O relative to the PDB standard, whereas negative values indicate a depletion of these isotopes in the sample relative to the standard.

According to Friedman and O'Neil (1977) the conversion between SMOW and PDB $\delta^{18}O$ values can be achieved using the following equation:

$$\delta^{18}O_{SMOW}=1.03086\delta^{18}O_{PDB}+30.86 \quad \text{... (3)}$$

This equation was used to convert $\delta^{18}O$ values of the carbonate samples of phases C2 and C3, that have crystallised with quartz, to SMOW. The temperature at which these two minerals may have equilibrated was then determined using the following equation from Faure (1986) (Appendix 5b).

$$T=\sqrt{\frac{10^{6}x0.60}{\delta_{quartz}-\delta_{calcite}}} \quad \text{... (4)}$$

Mass dependent fractionation during geological processes results from equilibrium or kinetic effects.

(1) Equilibrium effects include the isotopic exchange of an element between molecules, due to the greater stability of a molecule containing the heavier as opposed to the lighter isotope.

(2) Kinetic effects result from rapid, incomplete or unidirectional processes such as evaporation, condensation, melting, crystallization, adsorption-desorption or diffusion (Smith, 1991).

The two stable isotopes of carbon, ^{12}C and ^{13}C, are fractionated by a variety of natural processes, including photosynthesis and isotopic exchange reactions among carbon compounds.

(1) Photosynthesis leads to an enrichment of ^{12}C in biologically synthesised organic compounds.

(2) Isotopic exchange reactions between CO_2 gas and aqueous carbonate species tend to enrich carbonates in ^{13}C (Faure, 1986).

The equilibrium carbon isotopic fractionation effects between precipitating carbonate and surrounding bicarbonate are relatively small and temperature effects are relatively minor (Marshall, 1992). Precipitated aragonite has a higher $\delta^{13}C$ than ambient dissolved inorganic C but the fractionation seems to decrease with increasing temperature (Grossman and Ku, 1986). The relatively minor temperature dependency of the fractionation effects, and uncertainties over the magnitude of variation, negate the use of C isotope values for temperature determination, but stratigraphic changes in carbonate C values are extremely useful as indicators of changes in the composition of the marine bicarbonate reservoir (Marshall, 1992).

The O isotopic composition of a carbonate mineral which is precipitated in equilibrium with its environment is determined by the O isotopic composition of the fluid from which the mineral precipitated and the temperature of precipitation. The O isotopic fractionation between water and calcite is highly temperature-dependent, with the $\delta^{18}O_{calcite}$ becoming increasingly lower with increasing temperature (Friedman and O'Niel, 1977). Palaeotemperature equations imply that $\delta^{18}O_{calcite}$ decreases by approximately 1‰ for every 4°C increase in temperature. Additional controlling factors are the mineralogical form of the $CaCO_3$ phase and its Mg content. Aragonites and Mg-calcites tend to preferentially concentrate the heavier ^{18}O isotope compared to calcites. Palaeotemperature equations derived for aragonite (Grossmann & Ku, 1986) and for magnesium calcite (Tarutani *et al.*, 1969), indicate that aragonite will have $\delta^{18}O$ approximately 1‰ greater than calcite precipitated under the same conditions. As $\delta^{18}O_{calcite}$ increases by approximately 0.06‰ for each mol.% $MgCO_3$, biogenic high-magnesium calcites with 12 mol.% $MgCO_3$ will have $\delta^{18}O$ 0.7‰ greater than calcite precipitated from the same water at the same temperature.

Evaporation processes strongly affect the isotopic composition, since they cause a preferential depletion in the lighter isotopes, which become enriched in the vapour phase. Consequently, the remaining water will be heavier, i.e., highly saline waters generally have the highest ^{18}O-content (Marshall, 1992).

CHAPTER 4

THE ISOTOPIC SIGNATURES OF SYNGENETIC AND EPIGENETIC PROCESSES

4.1 Introduction

The present-day chemistry of carbonate rocks reflect a combination of properties inherited from the original carbonate sediments and post-depositional alteration phenomena. Dolomites have undergone one or several additional dissolution/reprecipitation stages overprinting the already complex diagenetic histories of the $CaCO_3$ precursors (Veizer *et al.*, 1990). Because carbonate minerals formed as a result of syngenetic or epigenetic processes have distinctive isotopic signatures, the two types of processes can be easily distinguished. The isotopic composition of carbonate phases associated with epigenetic ore deposition will record the isotopic signature of the ore-forming fluid, whereas diagenetic carbonates record the isotopic composition of the diagenetic or dolomitizing fluid. In this chapter, the distinctive isotopic signatures of syngenetic processes such as carbonate diagenesis, and epigenetic carbonate-hosted Zn-Pb mineralization will be discussed in detail.

4.2 Syngenetic Carbonate Diagenesis

4.2.1 Introduction

In carbonate sediments diagenesis is essentially the transformation into stable limestones or dolomites. This includes the dissolution, neomorphism, and replacement of unstable minerals, the compaction of grains, and the lithification by the precipitation of void-filling cements (Scoffin, 1987). During carbonate diagenesis the unstable carbonate minerals such as aragonite and high-Mg calcite are converted to stable low-Mg calcite (Moore, 1989).

Dolomite commonly originates as a metastable phase (protodolomite) that is susceptible to recrystallization and hence isotopic re-equilibrium during burial and diagenesis (Land, 1980; 1985). The isotopic composition of the dolomites therefore reflects the nature of the recrystallizing or dolomitizing solution.

4.2.2 The U-Th-Pb isotope system

The concentration of U, Th and Pb in carbonate minerals is very low. Swart (1988) has suggested that the U concentration of dolomites is inherited from the original sedimentary and diagenetically altered components. Carbonates with higher concentrations of U, and in which the original fabrics are largely preserved, were dolomitized directly from the aragonite and high-Mg calcite precursors. There is a general decrease in the U concentration of carbonate rocks during freshwater diagenesis as metastable

aragonite and high-Mg calcite are dissolved and/or replaced by low-Mg calcite (Lahoud *et al.*, 1966; Haglund *et al.*, 1969; Gvirtzman *et al.*, 1973). Dolomites with lower U concentrations therefore formed from a low-Mg calcite precursor which presumably lost U during stabilization by meteoric waters (Swart, 1988). The type of diagenetic environment therefore influences the U and Pb concentration of a carbonate mineral.

4.2.3 The Rb-Sr isotope system

According to Milliman (1974) aragonite precipitated from average seawater contains ~7000ppm Sr, high-Mg calcite ~2500ppm Sr and diagenetic low-Mg calcite ~500ppm Sr. Geochemical profiles from deep-sea sediment pore-waters (Baker *et al.*, 1982; Wetzel, 1989) suggest that the stabilization of high-Mg calcite and aragonite skeletal calcites begins in the first few metres of burial, being accompanied by a loss of Mg and Sr from the sediment by diffusion to the overlying water column. Vehrenkamp and Swart (1988) have shown that high Sr carbonates such as aragonite, may introduce a significant precursor memory into an otherwise seawater-dominated Sr-isotopic signature if small quantities of seawater per unit volume of precursor carbonate are involved. The dolomitization of low Sr carbonates (i.e. low Mg-calcite) is shown to create an isotopic signature indistinguishable from that of the seawater involved in the reaction.

Because Sr is not measurably mass fractionated, carbonate cements will have the same Sr isotope ratio as the pore water at the time they precipitated, and if progressive cementation occurs, the Sr isotope ratios of the cements will record both the evolution of the pore water and the extent of diagenesis with time (Schultz *et al.*, 1989).

The dolomitization of limestone requires the addition of large quantities of Mg^{2+} to the rock system. According to Veizer (1978) the majority of the so-called late diagenetic dolomites were formed relatively soon ($\leq 10^7$ years) after the deposition of the original sediments. The dolomitization of a pure carbonate sequence in an epicontinental oceanic setting, for example the Transvaal epeiric sea, can realistically only have two important sources of Sr:

(1) the precursor rock or sediment being replaced; and

(2) the seawater involved in the dolomitization process (Vehrenkamp and Swart, 1988).

The average Sr isotopic composition of Proterozoic seawater is 0.703 (Veizer *et al.*, 1992). In addition, the $^{87}Sr/^{86}Sr$ value of precursor carbonate minerals is also very low. The $^{87}Sr/^{86}Sr$ value of diagenetic carbonates is therefore very low, when compared with the gangue carbonate minerals discussed in the following section.

4.2.4 The stable isotope system

C and O isotopic fractionation in carbonate rocks continues during diagenesis. In general, open systems and high water-rock ratios lead to loss of primary environmental isotopic signals whilst closed systems and low water-rock ratios favour partial or even total retention of the original composition (Marshall, 1992).

In shallow meteoric zones, open-system recrystallization and high water-rock ratios will lead to the precipitation of cements and replacements with a very negative C isotopic composition due to the incorporation of isotopically negative CO_2 (Marshall, 1992). The $\delta^{18}O$ value of a carbonate mineral deposited in this zone approaches -4‰ because of the large O reservoir available in meteoric water (Scoffin, 1987).

Cements precipitated in the relatively closed system of the deep burial environment would reflect the isotopic composition of the original marine sediments, with the higher temperature at depth influencing the O isotopic fractionation (Scoffin, 1987). Progressive cementation with burial often leads to decreasing $\delta^{18}O$ in later zones within cement crystals as temperature effects dominate (Dickson and Coleman, 1980).

The C and O isotope values for carbonates of various origins are shown in Table 2.

TABLE 2: Representative $\delta^{13}C$ and $\delta^{18}O$ values for carbonates of different environmental origins (modified from Scoffin, 1987).

	$\delta^{13}C$	$\delta^{18}O$
Marine carbonates	0 to +4‰	-0.5‰
Meteoric groundwater	-20‰	-4‰
Exposure surface calcite	-8‰	-2‰
Deep burial calcite	+1‰	-8‰

4.3 Isotopic Signatures Related To Zn-Pb Mineralization

4.3.1 Introduction

Zn-Pb mineralization is classified according to the environment of ore deposition and the geological process responsible for the concentration of the ore minerals. These include:

(1) Mississippi Valley-type deposits;

(2) sedimentary exalative deposits (Sedex); and

(3) metasomatic processes eg. skarn deposits.

The Pering deposit is believed to be a Mississippi Valley-type deposit. This is according to the descriptions of the Pering deposit by Wheatley *et al.* (1986) and the model of Duane *et al.* (1991). Furthermore, the mineralization and structural setting of the deposit fulfils the 8 requirements, listed below for Mississippi Valley-type deposits, given by Guilbert and Park (1986).

(1) Their formation is not related to igneous activity

(2) The major ore minerals include only low-silver galena, low-iron sphalerite, barite and fluorite.

(3) Gangue minerals include dolomite, calcite, jasperoid and silica.

(4) Pyrite and marcasite are present but normally sparse.

(5) The ore minerals contain negligible silver and gold.

(6) They occur as bedded stratabound replacement sheets in dolomitic host rocks, veinform fluorite-calcite ores, fold-related joint fillings or solution-collapse breccia fillings.

(7) They occur towards the margins of many major sedimentary basins of the world where sediments onlap cratonic shelves.

(8) They are most commonly found at shallow depths in structurally passive, anorogenic areas.

Base metal sulphides are relatively insoluble which poses a "transport problem", in that large quantities of solution and/or long periods of time and/or large rates of flow are required to move ore-quantities of Pb and Zn (Anderson, 1983). Roedder (1960) showed that metal concentrations must exceed about 1ppm ($\sim 10^{-5}$ molal), and should preferably be several hundreds of ppm ($\sim 10^{-4}$ to 10^{-3} molal) before a fluid becomes a reasonable candidate as an ore-forming solution.

Goodfellow and Jonasson (1986) have summarized some of the work done on Mississippi Valley-type deposits. Chemical analyses of fluid inclusions from Mississippi Valley-type deposits show that these ore-forming fluids are most commonly Na-Ca-Cl brines having salinities between 100‰ and 300‰ (Hall and Friedman, 1963; Roedder *et al.*, 1963; Roedder, 1971). These fluids are similar in composition to basinal sedimentary brines (Carpenter *et al.*, 1974; White, 1965), except that they are characterised by higher K/Cl ratios (Hanor, 1979). Fluid inclusion homogenisation and freezing temperature measured for minerals from Mississippi Valley-type deposits (Sawkins, 1968; Roedder, 1971) and summarised by Hanor (1979) show distinctive ranges for each mineral district. Hanor (1979) concluded that there is no unique composition for ore-forming fluids, although they all fall into a broad class of Na-Ca-Cl brines.

The basinal brine theory of Mississippi Valley-type genesis suggested by White (1958) states that warm sedimentary brines from nearby basins carry dissolved metals and possibly S from depth to basin margins, forming ore deposits. Bethke (1986) outlines the three variants of this theory. These include:

(1) compaction-driven flow where deep fluids move toward basin margins as a result of sediment compaction during basin evolution (Noble, 1963; Jackson and Beales, 1967; Dozy, 1970);

(2) episodic dewatering where sediment compaction in basins causes high excess pore pressures, which drive sudden bursts of deep brines toward basin margins (Sharp, 1978; Cathles and Smith, 1983); and

(3) gravity-driven flow suggested over a century ago (Daubree, 1887; Cox, 1911; Siebenthal, 1915) and recently revised by Garven and Freeze (1984a,b) and Garven (1985), states that gravity-driven ground water flow caused by topographic differences across basins, carries warm fluids from deep strata into shallow sediments.

Modelling of the compaction-driven ground-water flow shows that the fluids move slowly and cool by conduction long before reaching host rocks at the basin margin (Bethke, 1983; Cathles and Smith, 1983). Episodic dewatering events are unlikely to occur in basins where slow burial, low shale contents occur as the sediments are not overpressurised during diagenesis (Bethke, 1986). In the Griqualand West sub-basin, episodic dewatering events are however possible due to the high shale content within the sub-basin. Garven and Freeze (1984a,b) and Hanor (1979) have emphasised that episodic basin dewatering is probably most important in the relatively early stages of the development of a deep sedimentary basin, whereas basin-wide gravity-driven fluid migration may predominate in more mature sedimentary basins with regional topographic gradients resulting from tectonic uplift and erosion (Sverjensky, 1981). Bethke (1986) believes that gravity-driven ground-water flow, possibly resulting from tectonic events in the southern Basin, was capable of introducing warm fluids to the Upper Mississippi Valley district in the U.S.A.

Models for the genesis of Mississippi Valley-type deposits fall into three groups (Sverjensky, 1986):

(1) mixing of separate metal-bearing and sulphur-bearing (H_2S) solutions at the site of deposition (two-fluid mixing model);

(2) transport of metals together with sulphate which is reduced by organic matter or ferrous iron at the site of mineralization (sulphate reduction model);

(3) transport of metals and reduced S together, with precipitation of sulphide caused by dilution, a pH increase, or a temperature decrease (reduced-sulphur model).

The oxidation state of the mineralizing fluid and the environment of deposition is a controversial subject. According to Anderson (1983) metals are transported in an oxidizing fluid and deposited when a reducing agent such as organic matter is encountered. Barnes (1983) however advocates that the metals and sulphides are transported in an organic-rich reducing fluid with deposition of the metal sulphides in an oxidising environment.

From a compilation of pore fluid compositions world-wide, White (1981) concluded that low temperature brines (<200°C) have little reduced S within the limits of detection. Only at temperatures greater than 200°C can significant amounts of reduced S coexist with base metals in solution. Low temperature fluids must therefore rely on alternate sources of sulphides to precipitate their metals. Ore-forming fluids rich in both base metals and reduced S species probably require high salinities, high temperatures and rock-water reactions buffered at low pH (White, 1981).

The pH and H_2S concentrations of a fluid are important factors influencing the deposition of galena and sphalerite. Sulphide precipitation (with H_2S as the source of reduced sulphur) is an acid-generating process (Anderson, 1983). The acid-generating reaction is as follows:

$$Zn^{2+} + H_2S \rightarrow ZnS + 2H^{2+} \quad \ldots (5)$$

where Zn is used to represent any of a number of metals (Anderson, 1983).

In carbonate host rocks this process must inevitably cause dissolution and probably solution collapse brecciation of the carbonate and/or sulphides. The only way that acid-generation could be avoided would be in extremely alkaline solutions, with reduced S present predominantly as alkali sulphide such as Na_2S, or by a process of sulphide replacement.

The processes described in the two-stage mixing model and reduced-sulphur model are both acid-generating (Sangster, 1990). As a consequence carbonate minerals are deposited with the sulphides. The sulphate reduction model describes a process in which acid is not generated and carbonate is not generated.

Sverjensky (1984) has suggested an association between the lithology of the aquifer unit and the metal ratios of the associated ores. These relationships are shown in Table 3.

TABLE 3: Relationships between aquifer lithologies, state of saturation of the migrating fluids, and metal abundances in resultant ores (After Sverjensky, 1981).

	AQUIFER LITHOLOGY		
	Carbonate	Quartz sandstone	Red-bed
Migrating Fluid[1] undersaturated saturated	 – sp, gn, cp, py	 sp gn, cp, py	 sp, gn cp, py
Metal abundances in resultant ores	Zn > Pb >> Cu	Pb > Zn >> Cu	Cu > Pb, Zn
Stratabound ore examples	Most Mississippi Valley-type ores	Sandstone Pb; southeast Missouri	Red-bed coppers

[1] State of saturation of fluid with respect to sphalerite (sp), galena (gn), chalcopyrite (cp), and pyrite (py).

4.3.2 The U-Th-Pb isotope system

Excluding carbonate-hosted Pb-Zn ore deposits genetically related to igneous activity, there is a continuum in $^{206}Pb/^{204}Pb$ and $^{208}Pb/^{204}Pb$ values of the remaining deposits which runs from (Doe and Zartman, 1979):

(1) deposits with Pb isotope ratios that approximate those of orogeny or single-stage model Pb (Pine Point, Bleiberg);

(2) through those that have Pb isotope ratios only slightly radiogenic for their ages (Phoenixville, Um Gheig);

(3) to those that are highly radiogenic for their ages, such as the deposits of the Mississippi Valley in the U.S.A. (East and Central Tennessee, Illinois-Kentucky, Wisconsin-Illinois-Iowa, Southeast Missouri, and Tri-State districts) and the Bou Grine deposit in Tunisia (Calvez and Orgeval, 1989).

The highly radiogenic Pb ratios of the Mississippi Valley deposits are known as J-type Pb ($^{206}Pb/^{204}Pb$ = 21-23; $^{207}Pb/^{204}Pb$ = 16.0-16.2; $^{208}Pb/^{204}Pb$ = 40-42) (Doe and Zartman, 1979). The large diversity of Pb isotope ratios within ore deposits has resulted from local and regional effects of fluid migration. The Pb isotope ratios of the gangue and sulphide minerals indicate the type of rock through which fluid migration has occurred, and the migration routes of the mineralizing fluid. Before depositing sulphide minerals this fluid can interact with the interstitial fluid of the carbonate host rock. Organic matter can be highly enriched in U (Taylor, 1979). Organic matter, associated with carbonates or carried by the mineralizing fluid, may therefore alter the U concentration of a fluid, and subsequently the Pb isotope ratios of carbonates minerals deposited from this fluid. This depends on the U/Pb value of the depositing fluid, and whether U is deposited with Pb in the carbonates. Pb substitutes for K in feldspar and micas and could be released during burial diagenesis or hydrothermal alteration of these phases (Hanor, 1979). Pb acquired from these phases during ore fluid migration, will be incorporated into the ore and gangue minerals that are deposited from this fluid.

4.3.3 The Rb-Sr isotope system

Studies of Mississippi Valley-type deposits indicate that where mineralization is sparse, Sr isotope ratios of calcite, barite and fluorite are similar to those of the host carbonates. In districts of major economic mineralization, the ratios are anomalous and increase as mineralization progresses (Kessen *et al.*, 1981). The $^{87}Sr/^{86}Sr$ value in ore-forming brines reflects the superposition of Sr arising in the original marine source and of Sr from marine and/or continental origin contributed by interaction of the mineralizing fluid with aquifer rocks prior to or during ore deposition. The $^{87}Sr/^{86}Sr$ value of carbonate gangue minerals can therefore be used to identify the sources of the ore fluids (Ghazban *et al.*, 1991).

Determining the $^{87}Sr/^{86}Sr$ values of the vug-filling carbonates was therefore undertaken to determine whether these phases were associated with the main episode of mineralization and the regional fluid flow of the ore-forming fluid at Pering Mine.

4.3.4 The stable isotope system

Hydrothermal carbonates associated with ore deposition indicate the conditions of ore formation. The isotopic composition of C in hydrothermal carbonates depends on the:

(1) $\delta^{13}C$ of the ore-forming fluid;
(2) fO_2;
(3) pH;
(4) temperature;
(5) ionic strength of the fluid; and
(6) total concentration of C in the ore forming fluid (Ohmoto, 1972; Rye & Ohmoto, 1974).

The $\delta^{13}C$ values of carbonate gangue minerals from a number of hydrothermal ore deposits show an enrichment in ^{13}C from the early to late phases (Rye and Ohmoto, 1974). Most early carbonates have $\delta^{13}C$ values between -5‰ and -7‰ which may indicate a deep-seated origin of the C or the mixing between carbonate-derived and organically derived CO_2. According to Hoefs (1980) the late stage carbonates may show an enrichment in the heavy isotope due to:

(1) cooling of the ore fluid;
(2) decreasing CO_2/CH_4 ratios in the fluid; and/or
(3) increasing contribution of CO_2 from another source.

The major isotopic character of hydrothermal fluids is that there is commonly a wide range in $\delta^{18}O$ (Hoefs, 1980). The O isotopic composition of hydrothermal carbonates can be used to determine the temperature of formation or the O isotopic composition of the parent hydrothermal fluid (Robinson, 1975). The chemical evolution and migration history of oil-field waters have been successfully reconstructed from their chemical and stable isotope data (e.g. Sulin, 1947; White, 1965; Collins, 1975; Carpenter, 1978).

CHAPTER 5
RESULTS

5.1 The U-Th-Pb Isotope System

Model age curves with μ values ($^{238}U/^{204}Pb$) of 8, 10 and 12, superimposed on primary isochrons of 0, 1, 2, 2.5 and 3 Ga, have been used as a basis to plot the ^{207}Pb-^{206}Pb data. Because of the limited data available, where possible, both Daly and Faraday values have been plotted for each sample. Figure 10 shows the $^{207}Pb/^{204}Pb$ and $^{206}Pb/^{204}Pb$ values for S26. The main group of samples have model ages between 2 and 2.7Ga, with μ values between 7 and 10. A second group of values plots around 1Ga with μ values between 10 and 11. This second group of values are exclusively from the vugs $S26N_1$ and $S26N_2$. Sphalerite was deposited within vug $S26N_2$ and organic matter was deposited on phase C2 in both vugs. The radiogenic $^{206}Pb/^{204}Pb$ values of these samples may have been acquired from the potentially uranium-rich organic matter deposited with phase C2, or from the source region through which the mineralizing fluids migrated. A galena analysed from around Pering Mine and three galena samples reported by Duane *et al.* (1991) are plotted for comparison. These galena samples plot in the same area as most of the vug-filling carbonates from S26, indicating that the Pb in the vug-filling carbonates, and in the galena from the Pering orebody was acquired from a similar source. Figure 11 is an enlargement of the area where the main group of samples plot, showing that most of the samples plot on the growth curve where $\mu = 8$.

The determination of the Pb isotopic composition of the carbonate samples posed numerous problems due to the low Pb concentrations. As mentioned in Section 2.6, the dolomite samples S26A, S26M and S26X are not plotted on the graphs as they show a variation between the Daly and Faraday data of more than 20%. In addition, sample $S26N_1$-C2 is not plotted. The Daly and Faraday $^{207}Pb/^{204}Pb$ values of this sample are very radiogenic (~ 21), whereas the $^{206}Pb/^{204}Pb$ values (~ 15) plot within the same range as the data plotted on the graph. This indicates that the radiogenic values may be the result of instrumental fractionation and drift, due to the very low concentrations of Pb in the carbonate samples. The Pb isotope data obtained from the samples of LB1 have very radiogenic $^{207}Pb/^{204}Pb$ values (up to 41) indicating that either the fluids depositing these carbonates were relatively enriched in U, or the low Pb concentrations of the samples have produced instrumental error and drift during analysis. The latter explanation is more probable as the $^{206}Pb/^{204}Pb$ values for these samples seem feasible.

Figure 13 shows the variation in the $^{208}Pb/^{204}Pb$ and $^{206}Pb/^{204}Pb$ values of the samples from S26. This is compared with the second stage growth curve (<3.7Ga) with a ω value of 37.19 (Stacey and Kramers, 1975). This graph shows that the U-Th ratio may have been affected by a regional geological event. It is more likely that the U ratio, rather than the Th ratio, has been disturbed as the uranyl ion (UO_2^{2+}) is more soluble in water, and therefore more mobile than Th, which only exists in the tetravalent state. The U-Th ratio of the samples from LB1 are highly variable indicating either, that the ratio has been affected by a regional geological event, or that the variation is due to instrumental fractionation and drift. Because the $^{207}Pb/^{204}Pb$ values show a similar variation the latter explanation is preferred.

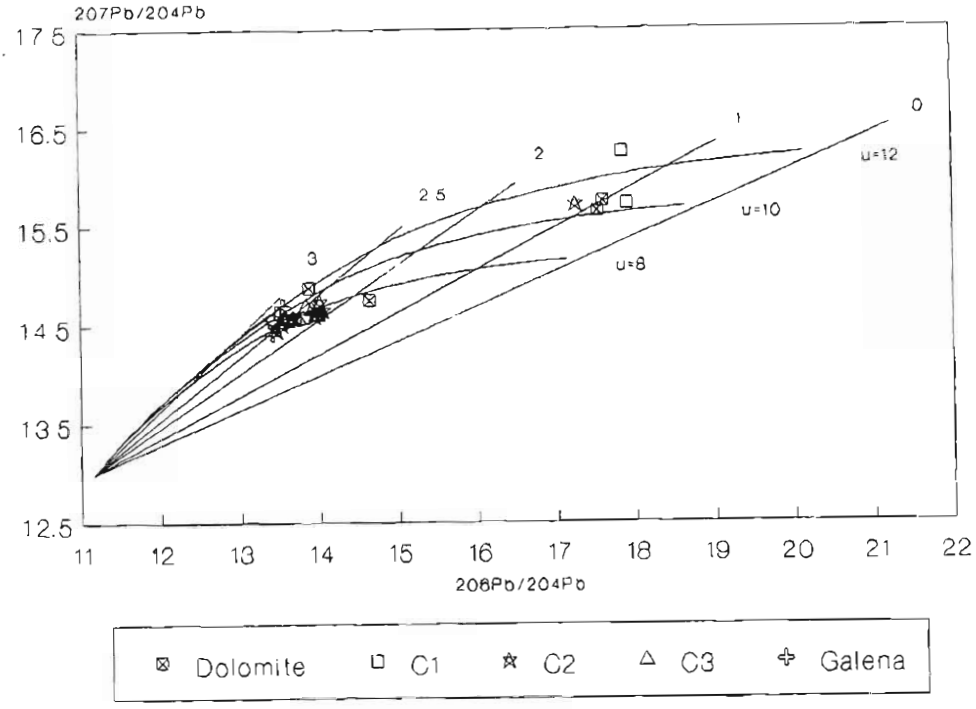

Figure 10. ^{207}Pb-^{206}Pb data for S26, with primary isochrons of 0, 1, 2, 2.5 and 3 Ga superimposed on growth curves with μ values ($^{238}U/^{204}Pb$) of 8, 10 and 12.

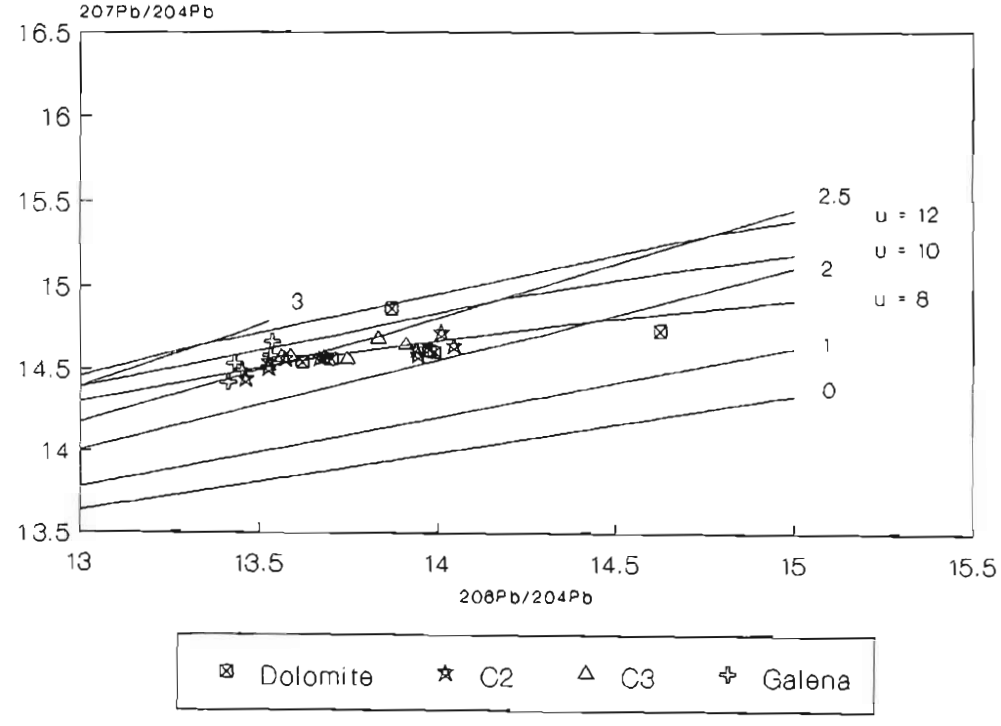

Figure 11. Enlargement of the area on Figure 10 between $^{206}Pb/^{204}Pb$ values of 13 and 15.

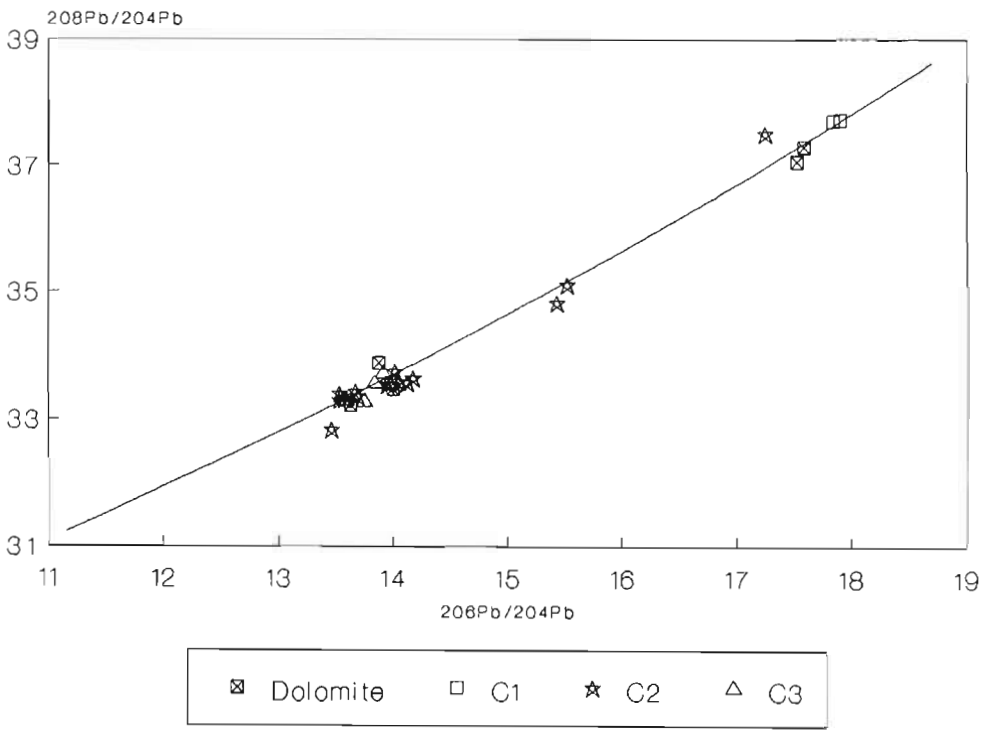

Figure 12. ^{208}Pb-^{206}Pb data for S26, compared with the growth curve from Stacey and Kramers (1975) with a ω value ($^{232}Th/^{204}Pb$) of 37.19.

5.2 The Rb-Sr Isotope System

From Figure 13 it can be seen that within S26 the dolomites have a relatively low $^{87}Sr/^{86}Sr$ initial ratio (~0.70-0.72) whereas most of the vug-filling carbonates have very radiogenic Sr isotopic signatures (~0.72-0.765). In addition, the Sr concentration of the vug-filling carbonates (excluding three samples) is higher than the associated dolomites. These results are comparable with those of the gangue carbonates and dolomitic host rock within the Pering deposit, which have an initial ratio of 0.7305 and 0.7092, respectively (Duane *et al.*, 1991). In LB1 the vug-filling carbonates are also more radiogenic and have a higher Sr concentration than the dolomites (Figure 14). The $^{87}Sr/^{86}Sr$ values of the dolomites and particularly the vug-filling carbonates are higher than the average Sr isotopic composition (0.703) of Proterozoic seawater (Veizer *et al.*, 1992). The ^{87}Sr enrichment of the minerals suggests that at least some of the Sr in the mineralizing fluids was derived from a Rb-rich source.

Figures 15 and 16 show the $^{87}Sr/^{86}Sr$ versus 1/Sr relationship of the vuggy carbonate minerals and their host dolomites for S26 and LB1, respectively. The observed relationships indicate that there may have been mixing of a fluid, or the dolomitic host rock, which has a low initial ratio (0.70-0.71) and low Sr concentration (10ppm) with a radiogenic fluid (0.75-0.76) with a high Sr concentration (100ppm). This cannot be proved with any certainty due to the scatter of the data. The processes involved seem to be more complex than can be explained by a simple two-component mixing model. The scatter of the data may indicate that two or more extraformational fluids, with variable Sr isotope ratios may have been involved in the mineralizing process. The mineralizing fluids may have picked up Sr from the numerous source rocks through which they migrated, finally interacting with each other and the carbonate host rock.

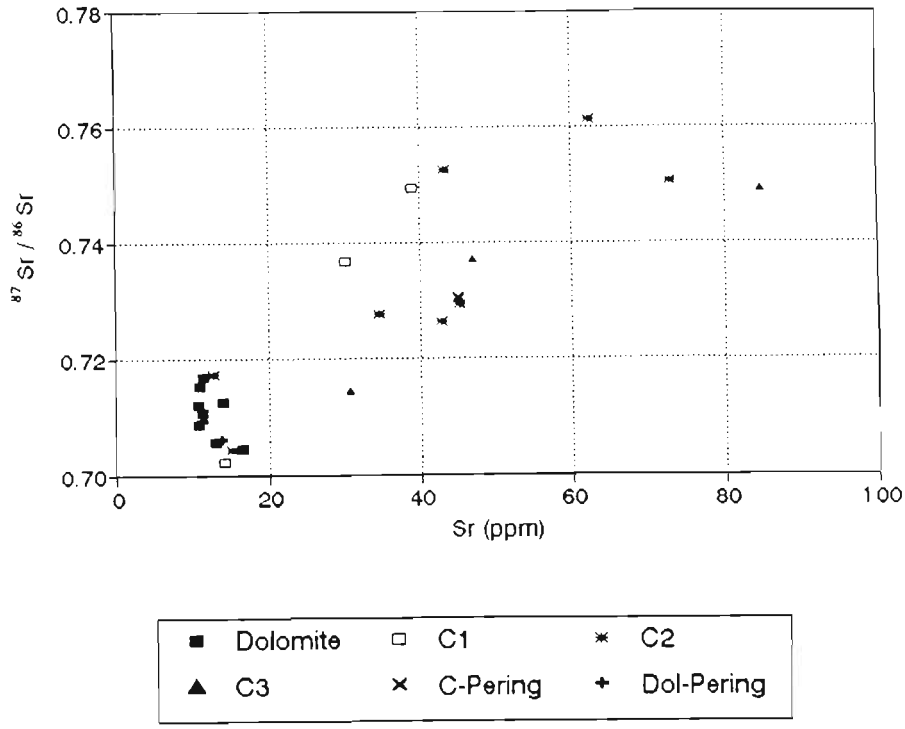

Figure 13. Correlation between the $^{87}Sr/^{86}Sr$ (initial ratio) and Sr concentration (ppm) of the host dolomite and vug-filling carbonate phases of S26. Pering mine carbonates are used for comparison.

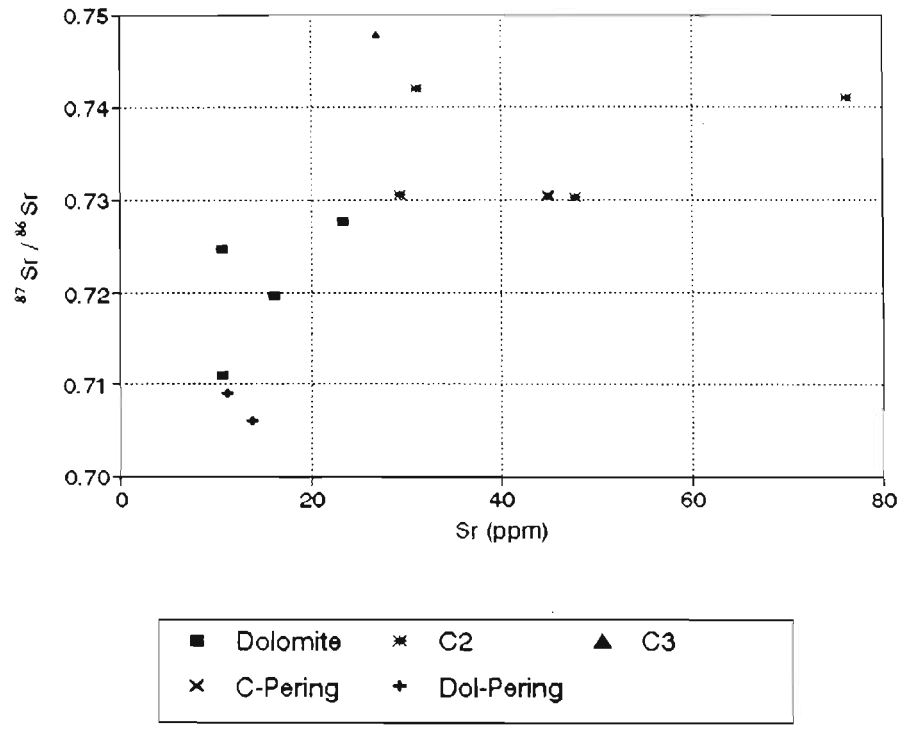

Figure 14. Correlation between the $^{87}Sr/^{86}Sr$ (initial ratio) and Sr concentration (ppm) of the host dolomite and vug-filling carbonate phases of LB1.

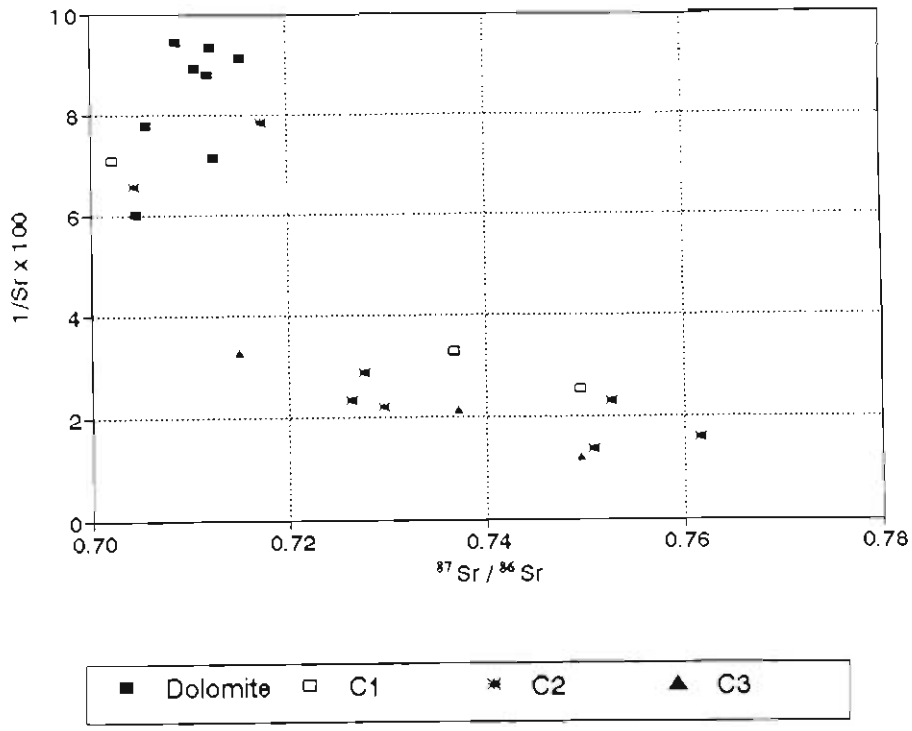

Figure 15. Correlation between the $^{87}Sr/^{86}Sr$ (initial ratio) and 1/Sr x 100 of the host dolomite and vug-filling carbonate phases of S26.

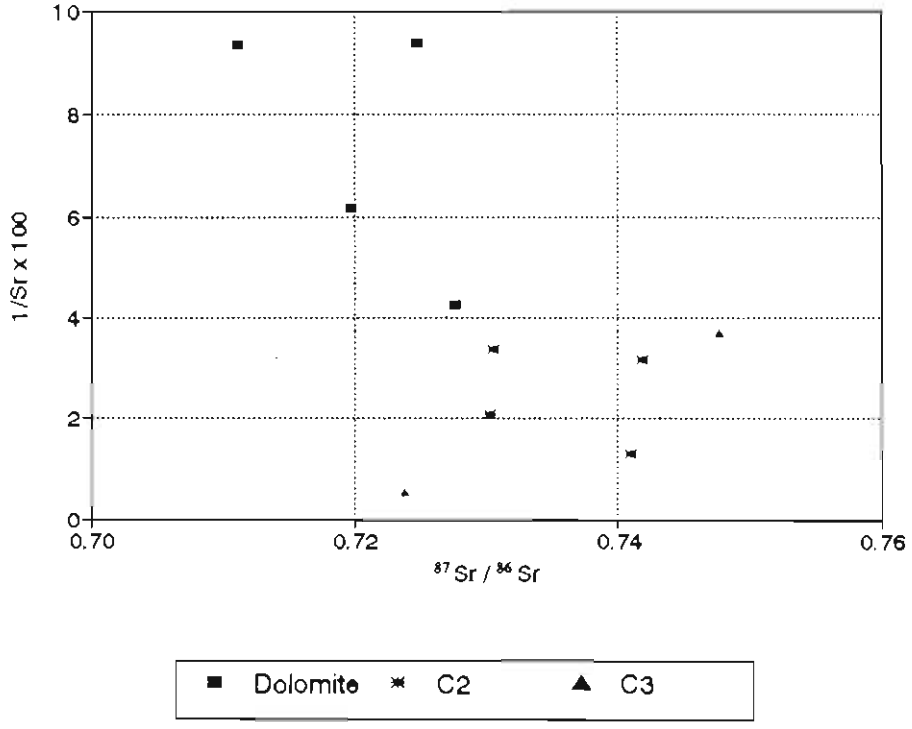

Figure 16. Correlation between the $^{87}Sr/^{86}Sr$ (initial ratio) and 1/Sr x 100 of the host dolomite and vug-filling carbonate phases of LB1.

5.3 The Stable Isotope System

Figure 17 is a comparison of the $\delta^{13}C$ and $\delta^{18}O$ values from LB1 and S26. The $\delta^{18}O$ values of the dolomites in both LB1 and S26 are similar (between -11.3‰ and -9.8‰, with an outlier at -13.5‰ [$S26Gb_4$]), whereas the samples from LB1 have higher $\delta^{13}C$ values. The lower $\delta^{13}C$ values of the dolomites in S26 may be due to inherent lithological differences, as the samples of S26 are mainly from the Reivilo Formation, which contains abundant stromatolites, whereas the samples from LB1 are from the Monteville and Lokammona Formations. Phase C2 from LB1 have higher $\delta^{13}C$ values than S26, and three of the four samples have a slightly higher $\delta^{18}O$ value than those from S26. The two samples of phase C3, from LB1, have similar $\delta^{13}C$ values but different $\delta^{18}O$ values, whereas both values shown for S26 are similar. An outlier ($S26X_1$-C3: $\delta^{13}C$ = -6.5‰, $\delta^{18}O$ = -8.9‰) has not been included on the graph as the minimum value on the y-axis becomes -7 and the distribution of the remaining data cannot be clearly illustrated. The $\delta^{13}C$ values of phase C3 are higher in LB1, and the $\delta^{18}O$ values are higher in S26.

In S26 the $\delta^{13}C$ and $\delta^{18}O$ values of the dolomite and phase C1 overlap, indicating that phase C1 may be a reaction rim formed when phase C2 was deposited. Phase C2 has a similar $\delta^{13}C$ range to the dolomite and phase C1. The $\delta^{18}O$ values for phase C2 are lower than the dolomite and phase C1. The calcite phase (C3) has similar $\delta^{18}O$ values, but distinctly lower $\delta^{13}C$ values than the other carbonate phases. In LB1 the dolomite has the highest $\delta^{13}C$ and $\delta^{18}O$ values with a progressive decrease in each set of values towards phase C3. There is some overlap between the values of the dolomite and phase C2, providing further evidence that phase C2 may be recrystallized dolomite. The absence of phase C1 in LB1 may indicate that the fluids, which deposited phase C2, were much cooler in the area surrounding LB1. This is indicated by the slightly higher $\delta^{18}O$ values of phase C2 in LB1, when compared with S26. The pure calcite phase (C3) has distinctive values by comparison with the other carbonate phases from each drillcore.

The $^{87}Sr/^{86}Sr$ values of each the samples from each borehole have been plotted against $\delta^{13}C$ and $\delta^{18}O$, to determine the relationship between these isotopes during the deposition of the various carbonate phases. The vug-filling carbonates of S26 have a similar $\delta^{13}C$ value (Figure 18) and lower $\delta^{18}O$ value (Figure 19) in comparison to the host dolomites. There is therefore no clear correlation between $\delta^{13}C$ and the $^{87}Sr/^{86}Sr$ value, and a small, but variable, correlation between $\delta^{18}O$ and ^{87}Sr in S26. LB1 shows a systematic decrease in $\delta^{13}C$ (Figure 20) and $\delta^{18}O$ (Figure 21) with a progressive enrichment in ^{87}Sr from the host dolomites into the vugs (C2 and C3). There is however some overlap in the C and O values between the dolomites and phase C2, and the $^{87}Sr/^{86}Sr$ value one of the phase C3 samples and the host dolomites.

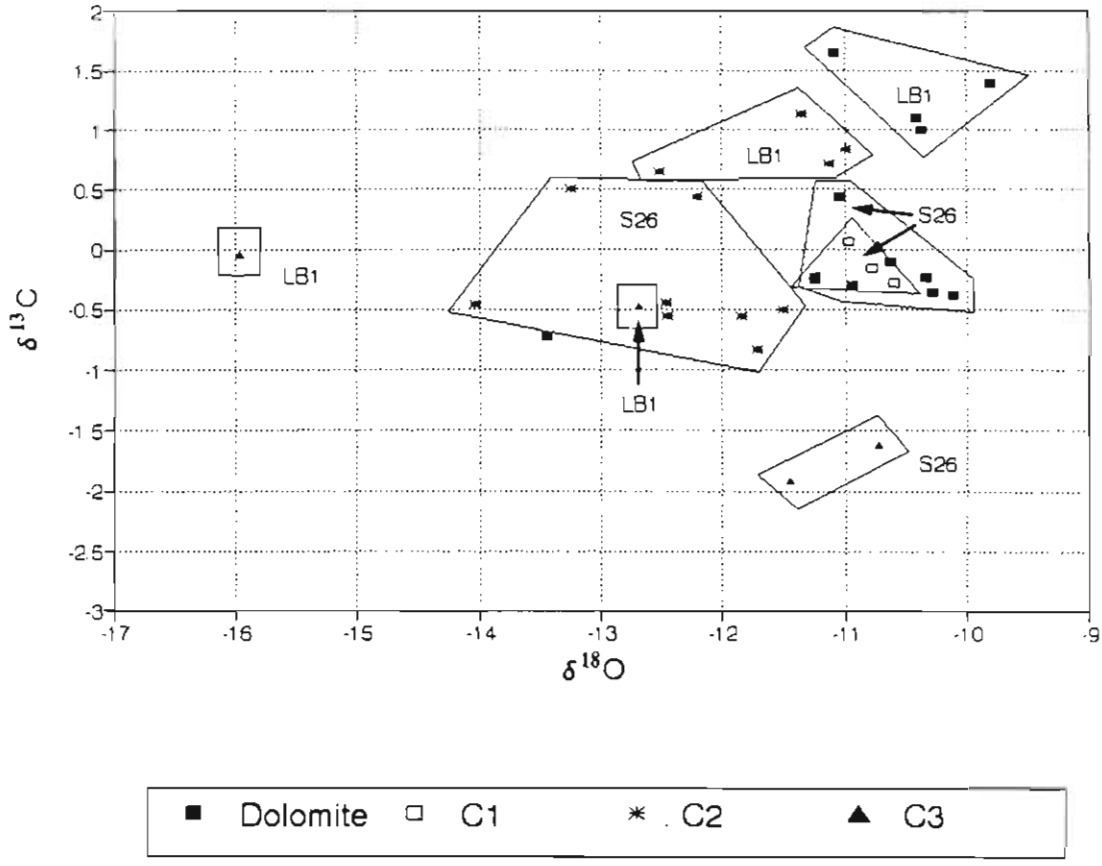

Figure 17. Carbon and oxygen isotopes ($\delta^{13}C$ vs $\delta^{18}O$) of the carbonate phases from S26 and LB1.

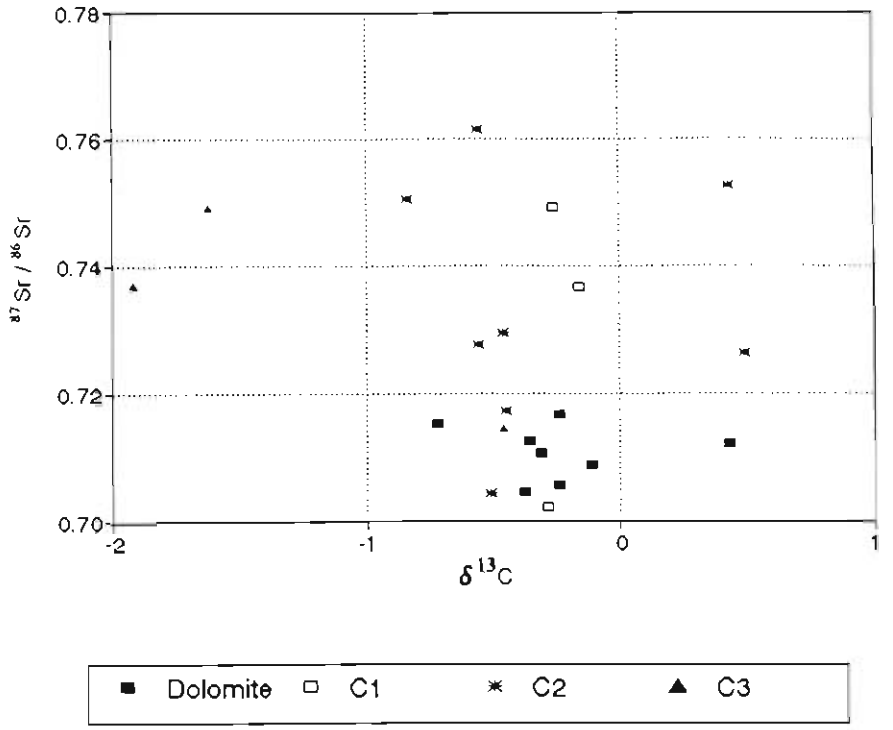

Figure 18. Correlation between the $\delta^{13}C$ and $^{87}Sr/^{86}Sr$ (initial ratio) of the host dolomite and vug-filling carbonate phases of S26.

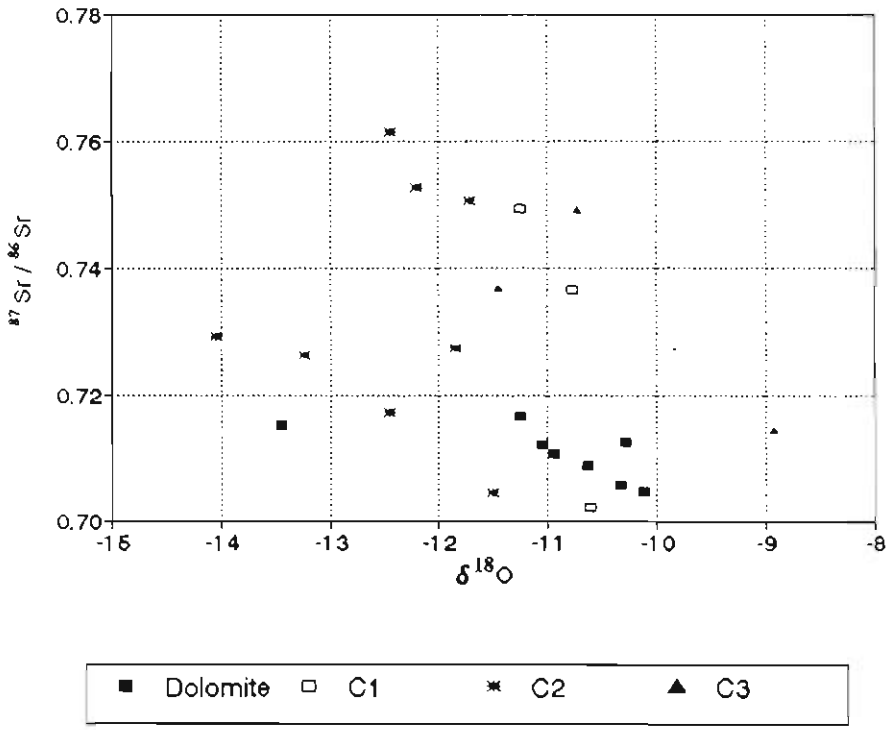

Figure 19. Correlation between the $\delta^{18}O$ and $^{87}Sr/^{86}Sr$ (initial ratio) of the host dolomite and vug-filling carbonate phases of S26.

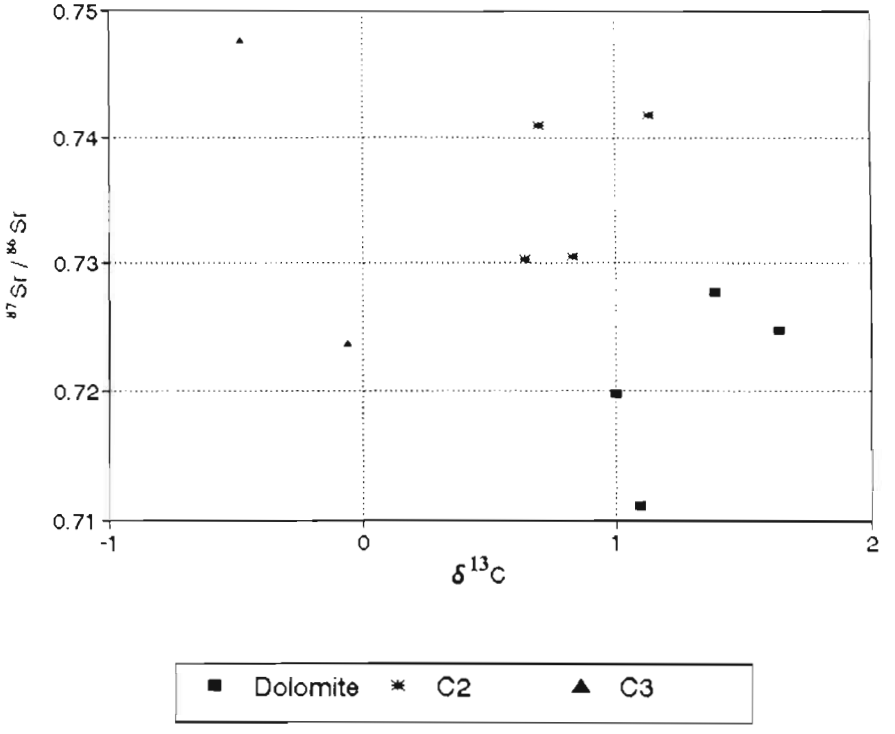

Figure 20. Correlation between the $\delta^{13}C$ and $^{87}Sr/^{86}Sr$ (initial ratio) of the host dolomite and vug-filling carbonate phases of LB1.

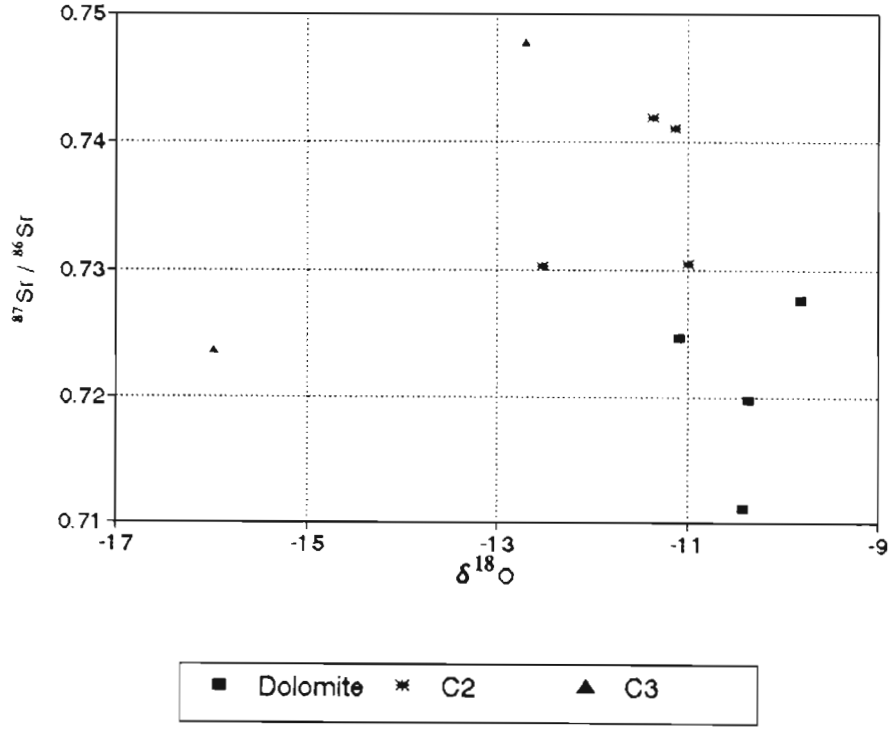

Figure 21. Correlation between the $\delta^{18}O$ and $^{87}Sr/^{86}Sr$ (initial ratio) of the host dolomite and vug-filling carbonate phases of LB1.

5.4 Integrated Isotope Data

Figure 22 is a composite plot of the $\delta^{13}C$, $\delta^{18}O$, $^{87}Sr/^{86}Sr$ (initial ratio), $^{206}Pb/^{204}Pb$ and $^{207}Pb/^{204}Pb$ of the dolomite and vug-filling carbonate samples from S26. The $\delta^{13}C$ values decrease progressively from the dolomite to phase C3, with the exception of samples $S26L_4$, $S26Gb_4$, and S26X where there is an increase in value from the dolomite to phase C2. Phase C3 of sample S26X has a $\delta^{13}C$ value of -6.5‰. Phase C1 has a higher $\delta^{13}C$ than the corresponding dolomite and C2 phase from each sample. The $\delta^{18}O$ values decrease systematically from the dolomite to phase C1 (which is similar to the value of the dolomite) and finally to phase C2. The exception is sample $S26Gb_4$ where the dolomite value is lower than phase C2. Phase C3 has a higher $\delta^{18}O$ value than the corresponding C2 phase in each vug which may indicate a decrease in the temperature of deposition. The $^{87}Sr/^{86}Sr$ values are very low for vug S26A. The other vugs show a systematic increase in the initial ratio from the host dolomites into the vugs with the exception of S26X where the ratio decreases from C2 to C3. The Pb isotope data is highly variable. Because of the low concentrations of Pb in the samples, and the difficulty experienced when analysing the carbonate samples for Pb, caution should be exercised when studying the variation between the Pb isotope ratios of the carbonate phases within each vug. Various observations can however be made from the data. The $^{206}Pb/^{204}Pb$ values of the dolomites are very similar to those of the respective vug-filling carbonates. There is an overall enrichment in the carbonate phases of samples $S26N_1$ and $S26N_2$. The dolomites and vug carbonates have very similar $^{207}Pb/^{204}Pb$ values in S26A to S26N2, with the exception of $S26N_1$, whereas there is a decrease in the ratio from the dolomite to phase C3 in sample S26X.

The data from LB1 are plotted in Figure 23. There is a systematic decrease in both the $\delta^{13}C$ and $\delta^{18}O$ values from the dolomite to phase C2 and C3. This contrasts with S26 where there is an increase in the $\delta^{18}O$ values from phase C2 to phase C3. There is an enrichment in ^{87}Sr from the dolomites to phase C2 in vugs LB1N, LB1P and LB1R and a decrease in LB1S. Phase C3 shows a decrease towards C3 in LB1N, and an enrichment in ^{87}Sr in LB1S. Although the $^{206}Pb/^{204}Pb$ values are variable the $^{207}Pb/^{204}Pb$ values increase from the dolomite host rocks into the vugs. No Pb data is available for sample LB1R and LB1S-Dol. The $^{207}Pb/^{204}Pb$ values are however very radiogenic and may simply be due to analytical error as a result of instrumental drift and fractionation.

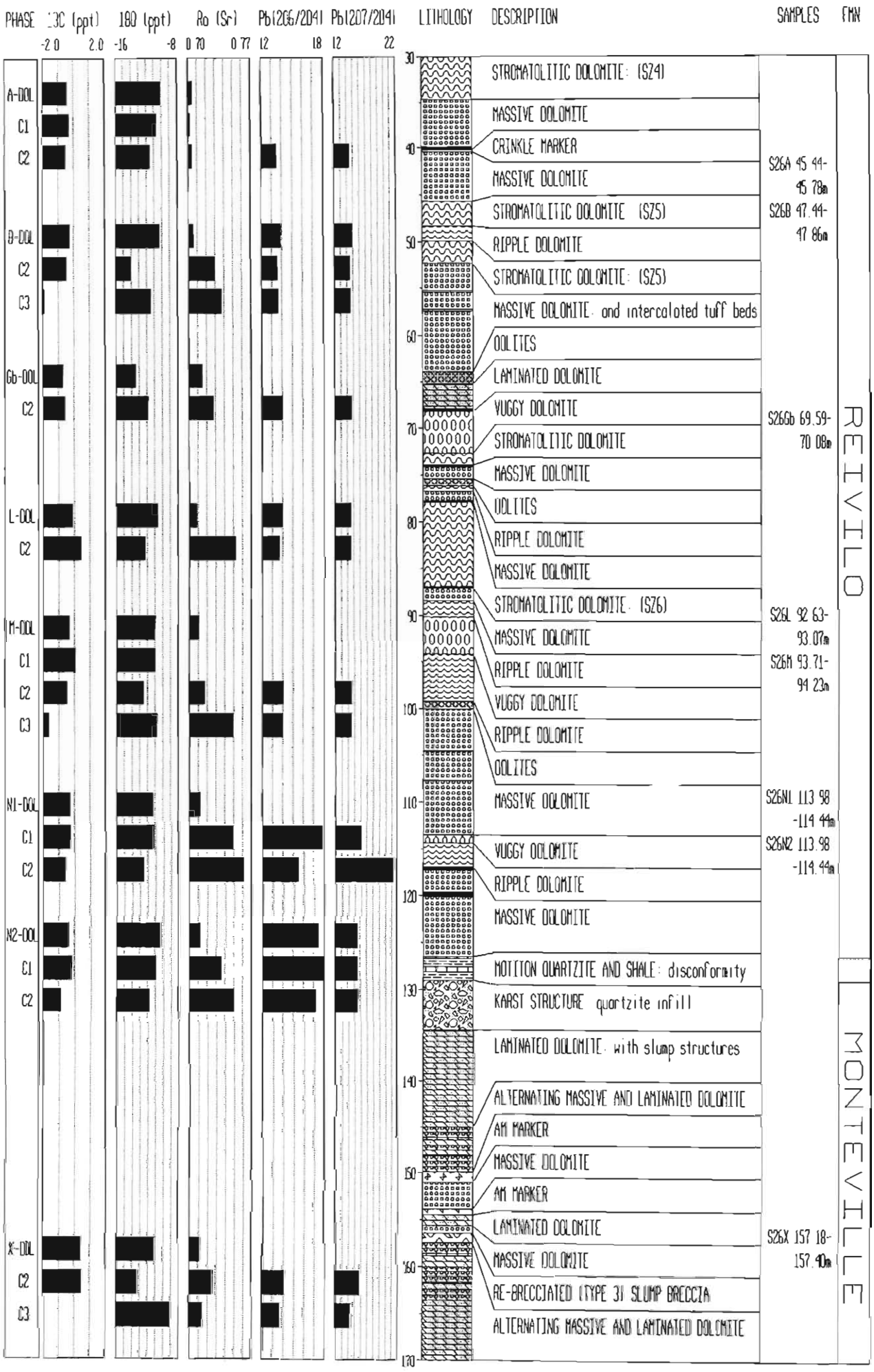

Figure 22. Correlation between the $\delta^{13}C$, $\delta^{18}O$, $^{87}Sr/^{86}Sr$ (initial ratio), $^{206}Pb/^{204}Pb$ and $^{207}Pb/^{204}Pb$ of the host

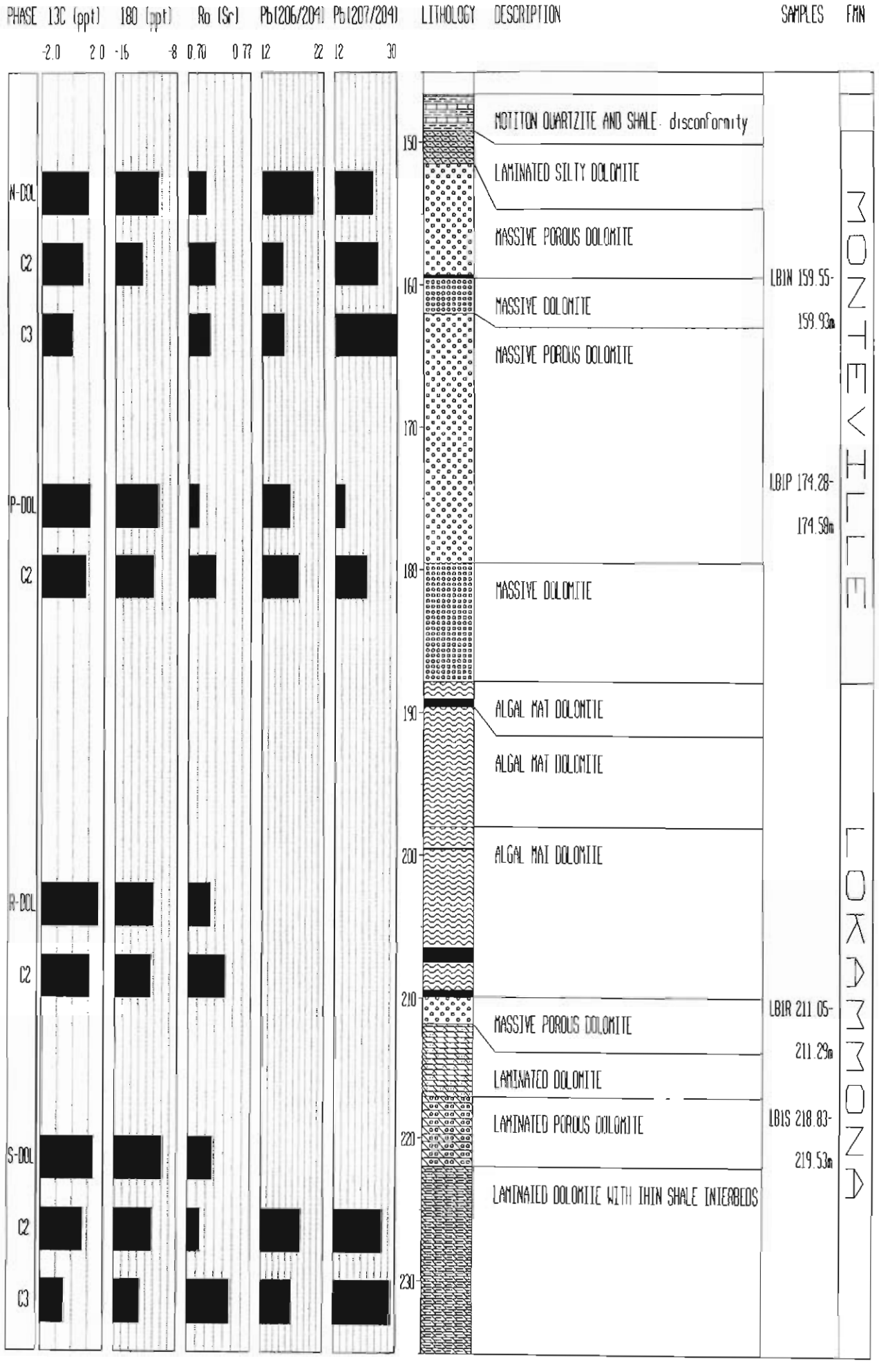

Figure 23. Correlation between the $\delta^{13}C$, $\delta^{18}O$, $^{87}Sr/^{86}Sr$ (initial ratio), $^{206}Pb/^{204}Pb$ and $^{207}Pb/^{204}Pb$ of the host

CHAPTER 6
DISCUSSION

6.1 Introduction

The concentration of trace elements in the vug-filling carbonates was controlled by various factors such as crystallography, temperature, fO_2, pH, and the total concentration of the each element in the depositing fluid. The isotopic composition of the gangue minerals have been used to determine the lateral extent of the mineralizing fluid around Pering Mine, the potential source areas through which these fluids passed, and the depositional environment of the sphalerite.

6.2 Evidence For Epigenetic Mineralization

Common carbonate cements have very low Rb/Sr values and faithfully record the Sr isotopic composition of the fluid from which they were deposited (Smalley *et al.*, 1987). Mineralizing fluids can acquire Sr with a high $^{87}Sr/^{86}Sr$ value, as a result of interaction with various rock types encountered on its way to the site of deposition. Carbonate minerals deposited with ore minerals may therefore be enriched in ^{87}Sr, relative to the pre-existing carbonate minerals that were deposited from contemporaneous sea water. The vug-filling carbonates in the boreholes, and in the main Pering orebody, have similar high $^{87}Sr/^{86}Sr$ values. These carbonate minerals are radiogenic relative to the dolomite host rock. The vug-filling carbonates are therefore directly related to the mineralizing event that formed the Pering orebody, and the vugs may therefore have formed part of the aquifer system of the mineralizing Zn-Pb fluids. The $^{87}Sr/^{86}Sr$ values of the dolomite host rock and carbonate gangue minerals, from various deposits, are compared to those of the Pering deposit in Table 4.

TABLE 4: The $^{87}Sr/^{86}Sr$ values of the dolomite and gangue minerals from various Mississippi Valley-type Zn-Pb deposits.

Locality	Host dolomite	Ore-stage gangue	Post-ore stage gangue	Reference
Bushy Creek Pb-Zn Mine, Viburnum Trend, S.E. Missouri, U.S.A. (Phanerozoic)	0.70839-0.70891	0.70929-0.71020 vuggy-dolomite 0.71061-0.71227 vuggy-calcite	-	Chaudhuri et al. (1983)
Gays River Zn-Pb deposit, Canada. (Phanerozoic)	0.7083	0.7117	0.708-0.709	Ravenhurst et al. (1987)
Bou Grine Zn-Pb deposit, Tunisia. (Phanerozoic)	0.7075	0.7083-0.8087	-	Calvez and Orgeval (1989)
Pering Zn-Pb Mine, S.A. (Proterozoic)	0.705-0.728 (0.7092)	0.704-0.762 (0.7305)	0.715-0.749	Present Study (Duane et al., 1991)

The difference in the ratios between the various carbonate phases from the U.S.A. and Canada is not as large, and the ratios of the ore-stage and post-ore stage carbonates not as radiogenic, as those found around Pering Mine. The dolomites and gangue carbonates from the Bushy Creek and Gays River deposits fall within the same field as the Pering dolomites. The gangue minerals of the Pering and Bou Grine deposits have very radiogenic Sr isotope ratios when compared with the host rocks. This indicates that the mineralizing fluids that affected the Pering and Bou Grine areas either migrated through very radiogenic source rocks, or altered the rocks through which they migrated to a greater degree, before depositing the ore minerals. In addition, the ratios of the Pering dolomites analysed are high relative to the other Phanerozoic deposits, indicating that the mineralizing fluids may have affected the host dolomites close to the vugs. The $^{87}Sr/^{86}Sr$ values of the dolomites analysed in this study are higher than that determined by Duane *et al.* (1991).

6.3 Fluid Mixing Model

The Pering brines do not yield a linear relationship in a plot of $^{87}Sr/^{86}Sr$ versus 1/Sr. The following reasons advocated by Stueber *et al.* (1984) for this non-linearity in the brine samples from the Smackover Formation, in southern Arkansas, can also be applied to the Pering brines.

(1) This trend could not have been caused simply by the mixing of two different component solutions each having a specific $^{87}Sr/^{86}Sr$ value and Sr concentration (Faure, 1977).

(2) The fluids were undoubtedly heterogeneous in $^{87}Sr/^{86}Sr$ and Sr content due to different degrees of interaction with different minerals as a function of specific migration routes.

(3) This Sr heterogeneity of fluids has apparently combined with variable mixing with interstitial waters to produce the presently observed $^{87}Sr/^{86}Sr$ distribution in brines.

Two models are proposed for the genesis of the main Pering deposit, and the occurrence of sphalerite in the vug-filling carbonate surrounding the deposit (Figure 24).

(1) Mixing Model

Two separate fluids each having different sources of Sr, as a result of interaction with one or more source rocks, mixed with one another and the host rock and/or interstitial pore fluid.

(2) Single Fluid Model

The interaction of a single fluid with highly variable but radiogenic Sr isotope values (due to the interaction with various source rocks as a function of specific migration routes) with the carbonate host rock and/or interstitial pore fluid.

The mineralizing fluid(s) that carried the metals in solution to the Pering deposit must have been pervasive as similar carbonate phases with the same range of radiogenic $^{87}Sr/^{86}Sr$ values are seen in both boreholes. The lateral fluid movement extended over a minimum area of 20km (between boreholes S26 and LB1), and vertically the fluids passed through the Reivilo, Monteville, and Lokammona Formations. Similar high $^{87}Sr/^{86}Sr$ values were recognised in the vugs of all three formations.

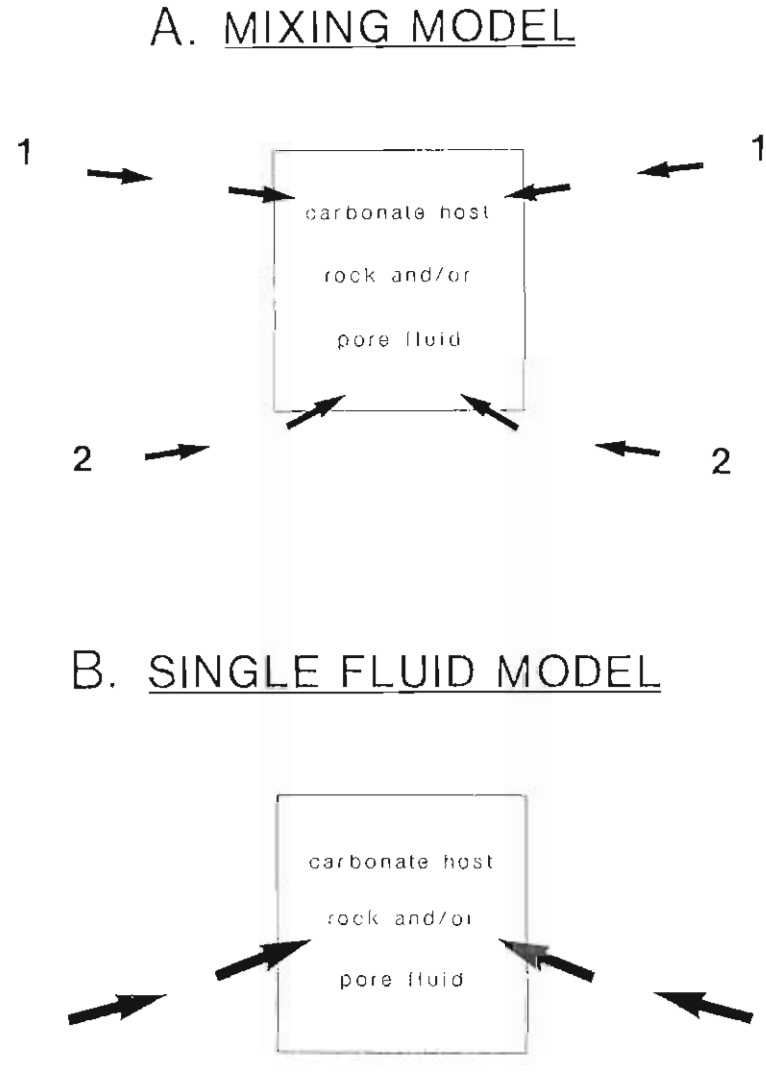

Figure 24. Schematic diagram of the (A) Mixing Model, and (B) Single Fluid Model.

Swennen (1986) has suggested that the main mineralizing event occurred during the early to late diagenesis of the Reivilo Formation. However, field evidence suggests that the mineralization around Pering Mine was epigenetic, and occurred subsequent to dolomitization of the host rock. Following dolomitization the host rock was affected by a major mineralizing event, that caused brecciation of the dolomites, with mineralization occurring around the dolomite fragments. Wheatley *et al.* (1986) have suggested that dewatering of the shales within the Lokammona Formation, which are anomalously high in Pb and Zn, provided metal-rich fluids which migrated upwards through vug-filled algal dolomites into the Reivilo Formation. Meteoric waters were envisaged to mix with these hypersaline basinal fluids forming cyclical plume zones, causing solution and hydraulic fracture brecciation. As the breccia fragments became cemented, mineralization spread outwards along the stromatolite zones where sulphate reduction and precipitation was facilitated by the carbonaceous algal material (Wheatley *et al.*, 1986). The vug-filling carbonates in the present study, however, indicate that the fluids were not influenced by meteoric waters. The $\delta^{13}C$ and $\delta^{18}O$ values are much higher than the meteoric values of -20 and -4 respectively. The $\delta^{13}C$ values of the vug-filling carbonates range between -1.9 and 1.1, and the $\delta^{18}O$ values fall within the range of -16 to -8.9. These values indicate that the fluids are related to an environment of deep burial. Sphalerite and galena may therefore have been deposited due to the mixing of a fluid that had acquired its isotopic signatures from migration through the lithologies below the Reivilo Formation, and an extra-formational fluid rich in radiogenic Sr, but not of meteoric origin. These fluids would then have reacted with interstitial waters within the carbonates and the carbonates themselves, before deposition occurred (Mixing Model). If the extra-formational fluid was driven by a tectonic event then the mineralization formed much later than the deposition of the Ghaap Group. On the south western margin of the Kaapvaal Craton two major orogenic belts have been identified:

(1) the Kheis Tectonic Province (Stowe, 1986); and

(2) the Namaqua Mobile Belt (Vajner, 1974).

Duane *et al.* (1991) suggested that the Kheis orogeny was instrumental in driving hydrothermal fluids along highly permeable thrust planes and along significant regional structures such as the Black reef décollement (Fletcher and Reimold, 1989). Local fluid migration in the Pering area may also have been driven by the re-activation of major syndepositional faults, in particular the lower Monteville Formation fault striking approximately east-west, 400m south of the Pering Mine (Swennen, 1986). No previous correlation between the Pering mineralization and the Namaqua Tectonic event has been made.

The Single Fluid Model suggests that only one main fluid rich in radiogenic Sr was responsible for the mineralization. This may have been driven laterally by tectonic activity in the region, migrated upwards locally and laterally through porous structures such as breccias and vuggy horizons, and mixed with the carbonate host rock and/or interstitial pore waters within the carbonate succession, before depositing the ore minerals.

The vugs analysed in this study did form part of the aquifer system of the mineralizing fluid, prior and subsequent to entering the main zone of deposition. If the mineralizing fluids were driven laterally

by an orogenic event they may have been concentrated within the area of the Pering deposit by the regional flexure, which is expressed as possibly domal by Swennen (1986).

The Pering deposit has a high Zn/Pb+Cu ratio. According to Sverjensky (1984) this indicates that the aquifer structure of the mineralizing fluid was mainly carbonate material. Areas of net permeability in the carbonate succession include brecciated zones and vuggy horizons. The carbonates are more permeable than the surrounding shales. This allowed the fluids to move laterally through the carbonates.

If the H_2S and metals were carried together (>200° C solution), or if the metal-bearing fluids encountered a large H_2S reservoir at the deposition site, Anderson and Garven (1987) and Anderson (1983) show that acid would be generated leading to extensive dissolution of the carbonate host rocks and probably solution collapse brecciation of host rocks and/or sulphides. The evidence of solution collapse brecciation and carbonate minerals deposited with the sulphides within the main Pering orebody indicates that the acid-generating processes described in the two-stage mixing model and reduced-sulphur model are both applicable. The reduced-sulphur model of ore transport is preferred in the Pering area. This implies that the temperature of the mineralizing fluids was relatively high, as only at temperatures greater than 200° C can significant amounts of reduced S coexist with base metals in solution. In addition, this type of ore fluid requires high salinities, and rock-water reactions buffered at low pH (White, 1981). The metals and reduced S were transported together in the same fluid, with precipitation of sulphide caused by dilution, a pH increase, or a temperature decrease. The metals were probably transported as chloride complexes in a reduced fluid. According to Sverjensky (1986) neither the metal-bisulphide (Barnes, 1967; Barnes and Czamanske, 1967; Barnes, 1979) nor the organometallic complexing (Barnes, 1979; Giordano and Barnes, 1981; Barnes, 1983; Giordano, 1985) theories appear to be viable alternatives to the metal-chloride complexing for Mississippi Valley-type ore forming fluids that transport both metals and reduced sulphur. Model 2 is therefore preferred for the deposition of the Pering ore deposit and the sphalerite in surrounding vug-filling carbonates. Using this model it is not necessary to envisage that the reduced fluid mixed with oxidising groundwaters before the metals were deposited as in the model of Duane *et al.* (1991).

6.4 Potential Source Rocks

The isotopic character of the vug-filling carbonates, that were derived from the Pering mineralizing fluid, can be used to estimate the composition of the rocks with which the mineralizing fluid interacted, and hence the local or regional nature of the mineralizing fluid migration. According to Banner *et al.* (1989), high $^{87}Sr/^{86}Sr$ values in mineralizing fluids can be ascribed to two processes:

(1) the albitisation or dissolution of K-feldspar in either granitic basement or detrital clastic components (Land and Milliken, 1981; Chaudhuri *et al.*, 1987; Land, 1987; McNutt, 1987); and

(2) cation exchange with clay minerals (Stueber *et al*, 1984; Chaudhuri *et al.*, 1987).

The very radiogenic $^{87}Sr/^{86}Sr$ values of the gangue carbonates in the Pering area indicate that similar reactions may have occurred between the mineralizing fluid and source rocks in this area. The isotopic composition of various source rocks are shown in Table 5.

TABLE 5: Possible source rocks of the Pering Zn-Pb brines.

Lithologies	$^{86}Sr/^{87}Sr$
Carbonate	0.70 - 0.727[1]
Vryburg Formation - lava	0.7092[2]
Ventersdorp Supergroup - Makwassie Quartz Porphyry	0.7366 ± 34[3]
Ventersdorp Supergroup - mafic lavas	0.7043[2]
Kaapvaal Craton (Basement)	0.7295[4]

(1) Present Study; (2) Armstrong (1987);
(3) Walraven et al. (1990b); (4) Cawthorn et al. (1985).

The $^{87}Sr/^{86}Sr$ values of the host dolomites are too low to have contributed to the very radiogenic $^{87}Sr/^{86}Sr$ values of the later vug-filling carbonates. Dolomitizing fluids, although rich in Sr, could not have been the source of the very radiogenic values observed in the Pering gangue minerals. In addition, because carbonates contain very low concentrations of Pb and Zn, it is more likely that in the Pering Mine area the hydrothermal fluids attained their isotopic and chemical composition through exchange with the surrounding lithologies.

From Table 5 the most probable sources of the radiogenic Sr, in rocks of known composition, is the Makwassie Quartz Porphyry of the Ventersdorp Supergroup, and the basement granites forming the Kaapvaal Craton. Although the $^{87}Sr/^{86}Sr$ value quoted for the Kaapvaal Craton is for basement rocks to the dolomites in the northern and eastern Transvaal sub-basin, the mineralizing fluid could have interacted with basement rocks with a similar ratio closer to the Pering deposit. The essential minerals in both felsic rock types are quartz, plagioclase, K-feldspar, and biotite. The interaction of groundwaters with plagioclase results in low $^{87}Sr/^{86}Sr$ values with increasing Sr concentration in the fluid (Franklyn *et al.* 1991). Franklyn *et al.* (1991) showed that the Sr signatures of groundwaters (0.706-0.707, average 0.7064) in and near a felsic pluton were derived from groundwater-plagioclase (0.703-0.715, average 0.7065) interaction, and not from K-feldspar (0.707-0.729, average 0.720), biotite (0.783-0.894, average 0.839), or whole rock (0.706-0.717, average 0.710) interactions. The mineralizing fluids at Pering have the opposite trend to that described by Franklyn *et al.* (1991), with high $^{87}Sr/^{86}Sr$ values and increasing Sr concentrations. The Sr isotope ratios of the carbonates within the Pering deposit, and in the vug-filling carbonates, show that the source of Sr is unlikely to be plagioclase. Interaction with minerals such as K-

feldspar or biotite would however increase the $^{87}Sr/^{86}Sr$ value of the mineralizing fluid. Feldspar and biotite are major constituents of the Makwassie Quartz Porphyry and granitic rocks of the Kaapvaal Craton, further implicating these rocks as potential source material through which the Pering fluids migrated.

Chaudhuri *et al.* (1987) considered the alteration or dissolution of K-feldspar and clay minerals to be potential sources of radiogenic Sr. The alteration of K-feldspar will be discussed first. Albitisation involves the alteration of K-feldspar and release of K^+ (and Rb^+) into the mineralizing fluid. The reaction is as follows:

$$KAlSi_3O_8 + Na^+ = NaAlSi_3O_8 + K^+ \quad \text{... (6)}$$

Cathles (1992) proposed a model, involving K-feldspar alteration, with two separate fluid-rock interactions, depending on the vertical direction of fluid flow. Firstly, he envisaged that an upward migrating fluid would result in epidote and K-feldspar alteration below 1750m (See Cathles (1992) for parameters) and muscovite, quartz and calcite alteration above 1750 m. Secondly, he envisaged that a downward migrating fluid would show a reversed trend to the above alteration trend. Plagioclase and biotite are altered to very small degrees in both domains. Therefore K-feldspar is preferentially altered at depth during metamorphic fluid expulsion, and near the surface where meteoric fluids are migrating downward. The incorporation of $^{87}Sr/^{86}Sr$ signatures from the alteration of K-feldspar may occur by two separate mechanisms during orogenesis: rehydration or dehydration. It is difficult to define a deep or shallow source for the mineralizing fluids from the Sr isotope values of the gangue minerals around Pering Mine. However, the $\delta^{18}O$ values of the vug-filling carbonates indicate that fluids were derived from a deep source. The alteration of K-feldspar occurs at depth and could therefore be the source of the very radiogenic Sr values in the gangue minerals.

The data of McCaig *et al.* (1990) show that the upward expulsion of fluids in shear zones, in the Pyrenees, has resulted in retrograde metamorphic alterations in the surrounding gneisses, with the release of elements such as Sr, Rb, Zn and Pb. Albitisation of the wall rocks resulted in reductions of Sr by 29%, Rb by 53%, Zn by 38% and Pb by 64%. Muscovitation resulted in the loss of Sr by 90%, Zn by 60% and Pb by 94%, with a gain of Rb of 14%. The reactions involved in the alteration are:

$$3microcline + 2HCl(aq) = muscovite + 2KCl(aq) + 6SiO_2 \quad \text{... (7)}$$

$$3albite + 2HCl(aq) + KCl(aq) = muscovite + 3NaCl(aq) + 6SiO_2 \quad \text{... (8)}$$

$$microcline + NaCl(aq) = albite + KCl(aq) \quad \text{... (9)}$$

These reactions show that large quantities of SiO_2 are released into solution which may be an explanation for the high quartz contents found in the Pering deposit.

According to Goodfellow and Jonasson (1986), Pb (Pb^{2+} 1.20Å, Pb^{4+} 0.84Å) and Ba^{2+} (1.35Å) are probably derived from K-feldspar since they substitute isomorphously for K (1.33Å) in the crystal structure. Equivalent gneisses and granulites are present within the Kheis Tectonic Province and may therefore be source areas for Pb, Zn and Sr.

The second mechanism proposed by Chaudhuri *et al.* (1987) to increase the radiogenic Sr content of the mineralizing fluid involves the reaction between the mineralizing fluid and Ca-bearing clay. This would produce an increase in the concentration of Ca^{2+} (and Sr^{2+}) in the mineralizing fluid. The ion-exchange reaction is as follows:

$$Ca\text{-}ClayMineral + 2Na^{+} = Na\text{-}ClayMineral + Ca^{2+} \quad \text{... (10)}$$

The expulsion of fluids from the shale-rich Lokammona Formation, proposed by Wheatley *et al.* (1986), may have affected the composition of the mineralizing fluid. Shales are derived from clay-rich muddy sediments enriched in detrital micas and can display a wide range of Sr isotope ratios, due to their variable but high Rb and Sr contents (Ghazban *et al.*, 1991). Sedimentary rocks such as shale are rich in ^{87}Sr (Perry and Turekian, 1974) and relatively enriched in Pb and Zn, and could have served as one of the sources of these metals in the ore deposit. In a study of oil-field brines from central Mississippi, Carpenter *et al.* (1974) indicated that movement of K-rich brines through metal-rich marine shales may be an important mechanism for the origin of metal-rich brines in sedimentary basins. The conversion of smectite to illite, caused by the introduction of the K-rich brines, might be accompanied by the release of adsorbed and/or interlayered base-metal ions associated with the original clay minerals. The penetration of the shales by the mineralizing fluids is regarded as unlikely, when other rocks, such as the dolomites, are of greater net permeability.

According to Goodfellow and Jonasson (1986) elements such as Zn, Cu, Ni, Co, As, Cd, etc. are more likely derived from the dissolution of sulphides such as pyrite that commonly occur finely dispersed throughout intercalated fine-grained carbonaceous clastic sediments. If the shales in the Lokommona

Formation were penetrated by fluids or were dewatered, the S component of the galenas and sphalerites in the Pering area may be partially derived from the dissolution of diagenetic iron sulphides, such as pyrite, which are commonly found within the carbonaceous shale horizons.

6.5 Pb Isotope Data

Galena samples from Pering Mine contain the least radiogenic Pb of the deposits analysed in the Transvaal and Griqualand West sub-basins (Duane *et al.*, 1991). The Pb in these galenas has apparently evolved for a significant period of time in an environment with low U/Pb and Th/Pb values. According to Duane *et al.* (1991), the source of the Pb in the galenas at Pering Mine may be the underlying altered Ventersdorp lavas since they are known to have non-radiogenic Pb isotopic compositions (Armstrong, 1987; Walraven *et al.*, 1990b). The model age for the galenas (2.6-2.8Ga) is similar to the ca. 2.7Ga age of the Ventersdorp lavas as recorded by Walraven *et al.* (1990a). A galena from around Pering Mine, analysed in the present study, has comparable Pb ratios to three galena samples reported by Duane *et al.* (1991) ($^{206}Pb/^{204}Pb$ = 13.41-13.53; $^{207}Pb/^{204}Pb$ = 14.42-14.68; $^{208}Pb/^{204}Pb$ = 32.88-33.63). The model age for this galena is 2.45Ga, which is close to the age of the host dolomites. The Pb isotope ratios of the galenas in the Pering deposit cannot be classified as J-type Pb, as in the classic Mississippi Valley-type deposits.

Most of the samples from S26 give a model age from 2.0-2.7Ga. Various samples from S26, and most of the samples from LB1, have very radiogenic $^{207}Pb/^{204}Pb$ values relative to their normal $^{206}Pb/^{204}Pb$ values. Although a geological explanation is given for these values, analytical error involving instrumental fractionation and drift should not be discounted. However, very radiogenic samples may have acquired U from the interaction of the fluids with minerals during migration, the organic matter deposited with the fluids in the carbonate vugs, or from fluids expelled from the shale-rich Lokammona Formation. The samples analysed from LB1 were taken from the Monteville and Lokammona Formations, which contain more carbonaceous material than the Reivilo Formation. The very radiogenic Pb isotope ratios of the vugs in LB1 may therefore be a result of interaction with these carbonaceous-rich and possibly U-rich lithologies. Organic matter was deposited on phase C2 of samples S26N1 and S26N2. This may have been due to the reaction of the fluids locally with the Motiton shales. These samples give model ages of around 1Ga which may be a result of acquired U into the carbonate lattice, or may indicate a local effect of the Namaqua tectonogenesis (1300-1100Ma; Barton and Burger, 1983). However, more proof is needed to substantiate either of these hypotheses.

6.6 Crystallographic Considerations

6.6.1 Sr concentration

The increase in the Sr concentration from the dolomites into the vug-filling carbonates may be related to the crystal structure of each phase. According to Kretz (1982), the carbonate minerals are somewhat unique in the sense that their structure and behaviour can be largely understood in terms of the size of the principal cations which make up the calcite, aragonite and dolomite-type structures (Goldsmith, 1959). It is conceivable therefore that the distribution of trace elements between associated calcite and dolomite may also be understood in relation to ionic size. Thus Jacobson and Usdowski (1976) suggested that the large Sr ion is confined to the Ca positions of both calcite and dolomite, leading to twice as much Sr in the calcite as in associated dolomite, in good agreement with their experimental results.

Theoretical considerations predict that an increasing degree of post-depositional alteration leads to Sr depletion and Mn enrichment (Veizer *et al.*, 1992). According to crystallochemical considerations (Kretz, 1982), the calcite structure accommodates about twice as much Sr and considerably less Mn than the dolomite one.

6.6.2 Oscillatory zoning

Oscillatory banding, seen under cathodoluminescence in phase C2, can be used as an exploration tool. This phase was deposited with the main phase of sphalerite mineralization at Pering Mine. Oscillatory zoning is commonly attributed to fluctuations in redox conditions in the pore waters, leading to changes in the activities of Fe and Mn in solution (Mason, 1987). However, the concentrations of trace elements co-precipitating from solution depends on distribution coefficients as well as solution composition. Distribution coefficients may depend on crystal growth rate (Lorens, 1981) as well as, in general, pressure, temperature and composition of the growing crystal structure (McIntyre, 1963). Wang and Merino (1992) have proposed a positive feedback model to explain oscillatory zoning in calcites. The calcites crystallized from an aqueous solution containing growth-inhibiting cations such as Mn^{2+}. According to Marshall (1992) Mn and Fe can be incorporated in calcite only in reducing conditions; such conditions occur rarely in depositional environments but are common to many diagenetic settings and areas of sulphide mineralization.

6.7 Stable Isotope Data

In Table 6 the $\delta^{13}C$ and $\delta^{18}O$ values of the Pering dolomites and vug-filling carbonates are compared with various results obtained by other workers for the Transvaal Supergroup.

TABLE 6: The $\delta^{13}C$ and $\delta^{18}O$ values of carbonates of the Transvaal Supergroup (PDB).

Lithology	$\delta^{13}C$	$\delta^{18}O$	Reference
Malmani dolomite, Transvaal	-0.9 ± 0.7 ‰	-8 ± 2.5 ‰	Veizer et al. (1992)
Transition zone, Campbellrand area, Northern Cape	-1.2 ± 1.1 ‰	-6.6 ± 2.7 ‰	Beukes et al. (1990)
Campbellrand Subgroup	-5 to 0.5 ‰	-14 to -7 ‰ (-8 = average dolomite -10 = average calcite)	Dirr et al. (1990)
Ghaap Group, Pering area	-0.7 to 1.6 (Dol) -1.9 to 1.1 (C1-C3)	-11.3 to -9.8 (Dol) -16.0 to -8.9 (C1-C3)	Present Study

The $\delta^{13}C$ and $\delta^{18}O$ values of the Pering dolomites and vug-filling carbonates have a similar range to carbonate phases of the Transvaal Supergroup analysed by various other workers (Table 5). Beukes *et al.* (1990) has suggested that the $\delta^{18}O$ values of -5‰ and -7‰ for the early Precambrian dolomites and calcites, respectively, represent reasonable estimates for carbonate phases formed in approximate equilibrium with coeval seawater. The Pering dolomites have a much lower $\delta^{18}O$ value than -5. This lower value may indicate the mixing of the original marine signature with the later dolomitizing fluid. In addition, the mineralizing fluid in the Pering area may have affected the dolomites close to the vugs. The vug-filling carbonates have a lower $\delta^{18}O$ value than the dolomites indicating that they were not formed by direct precipitation from coeval seawater. The Sr isotopic analyses of the vug-filling carbonates indicate that they were deposited from the main mineralizing fluid in the Pering area. The lower $\delta^{18}O$ value in phase C2 when compared with the host dolomites may indicate an increase in temperature of deposition. The fluid which deposited phase C3 around S26 may have had a similar temperature to the dolomites, whereas the fluid depositing the same phase around LB1 had a higher temperature than any of the other carbonate phases. Alternatively, the variation in $\delta^{18}O$ values between the different phases could be caused by a variation of the $\delta^{18}O$ of the fluids (Fritz, 1969).

Rye and Ohmoto (1974) present $\delta^{13}C$ values of carbonate gangue minerals from a number of hydrothermal ore deposits. The several generations of carbonate gangue minerals in each deposit define a definite paragenetic sequence. The earliest generation is invariably rhombohedral carbonate, which is followed by other crystal varieties. The carbonate minerals in these deposits show an increase in the $\delta^{13}C$ values from the earliest to the latest phase. This trend is observed, in S26, from the dolomites into phase C1 where this phase is present, and in some of the vugs from the dolomite into the vug where no C1 is present. According to Hoefs (1980) this is a result of:

(1) cooling of the ore fluid;

(2) decreasing CO_2/CH_4 ratios in the fluid; and or

(3) increasing contribution of CO_2 from another source.

Ravenhurst *et al.* (1987) have determined the C and O isotopic composition of four distinct paragenetic stages of carbonates at the Gays River Zn-Pb deposit, Canada. A trend towards more negative $\delta^{13}C$ values in the paragenetic sequence is explained not by changes in oxidation state but by localised changes in the total C isotopic composition. Organic material which is typically depleted in ^{13}C is relatively common in the Gays River, and hydrocarbons have been noted in fluid inclusions in fluorite. The incorporation of organic material into post ore fluids could provide the required decrease in $\delta^{13}C$. This process has also been used by Ghazban *et al.* (1991) to explain the observed depletion in ^{13}C from the host rock into the carbonate gangue minerals in the Nanisivik Zn-Pb deposit, Canada. A decrease in ^{13}C from the ore-stage calcite to post ore calcite is also seen in the analysed vugs of S26. In LB1 there is depletion in ^{13}C from the dolomites into the vugs.

The $\delta^{18}O$ values of two quartz samples deposited with phase C2 in vugs LB1R and LB1S were used to determine the temperature of deposition of these phases using equation 4. The temperatures were 370°C and 609°C for vugs LB1R and LB1S respectively. These temperatures are very high and indicate that these phases may not have been in equilibrium when they were deposited, thus giving erroneous temperatures. Fluid inclusion data for Pering gangue carbonates indicate that salinities and crystallization temperatures increase downwards through the rock sequence, from ± 100°C at 50 m depth to ± 175°C at 180 m depth (Wheatley *et al.*, 1986). These temperatures are much lower than those obtained in this study and appear more realistic temperatures.

The $\delta^{13}C$ and $\delta^{18}O$ values of the carbonate phases in the Pering area yield new insights into the nature of the mineralizing fluid.

(1) The $\delta^{13}C$ and $\delta^{18}O$ values of the vug-filling carbonates indicate that the depositing fluids were derived from a deep burial environment. The introduction of a fluid enriched in isotopically light organic C, as suggested by Hall and Friedman (1963) would account for the small drop in $\delta^{13}C$ from the host dolomite into the vugs. Alternatively, if the mineralizing system became at least locally closed to fluid migration, preferential concentration of the heavier isotope in earlier formed carbonates would eventually deplete the residual fluid in $\delta^{13}C$. There may also have been a decrease in the contribution of C from limestone/dolomite sources as deposition of successive phases into the vugs occurred (Rye and Ohmoto, 1974). The depositional environment within the vugs changed from one in which the depositing fluid was initially influenced by the dissolution of the host dolomite to one in which the fluid became less enriched in dissolved dolomite. The later phases were insulated from the host dolomite by former phases deposited within the vugs.

(2) The very low $\delta^{18}O$ values of the dolomites and carbonates analysed are similar to those found in carbonates from a deep burial environment. The progressive decrease in $\delta^{18}O$ from the dolomite host rock to phase C2 in both boreholes indicates an increase in the temperature of the fluid depositing these carbonate phases. Local controls have influenced the $\delta^{18}O$ value phase C3 to produce an increase from phase C2 to C3 in S26 and a decrease in LB1. An additional

controlling factor is that dolomite and early carbonate phases have a higher Mg concentration and therefore preferentially concentrate ^{18}O compared to ^{16}O. A trend towards a less saline fluid can be seen towards the centre of the vugs, however further evidence is needed to substantiate this observation.

(3) Variations in the trends observed within the vugs can be explained by a change in one or all of the environmental controls affecting the fluids depositing the carbonate phases.

CHAPTER 7
CONCLUSION

* Zn-Pb mineralization in and around Pering Mine occurred after diagenesis and dolomitization of the host carbonates, and is therefore epigenetic. Open spaces, such as vugs, formed during late-stage diagenesis and dolomitization, acted as part of the conduit system that channelised the later mineralizing fluids.

* The vug-filling carbonates in the drillcores analysed are related to the gangue minerals of the Pering deposit. Both have similar, very radiogenic $^{87}Sr/^{86}Sr$ values compared to the relatively non-radiogenic host dolomites. The $^{87}Sr/^{86}Sr$ values of the vug-filling carbonates are more radiogenic than gangue minerals associated with classic Mississippi Valley-type deposits in the U.S.A. and Canada.

* Large scale fluid migration must be invoked to explain the very radiogenic $^{87}Sr/^{86}Sr$ values in the gangue minerals associated with Zn-Pb mineralization. In addition, the combined $\delta^{13}C$ and $\delta^{18}O$ values of the dolomite host rock and vug-filling carbonates indicate that the mineralizing fluid was derived from a deep burial environment.

* The Single Fluid Model is preferred for the genesis of the main Pering deposit and the occurrence of sphalerite in the vug-filling carbonate surrounding the deposit. One main fluid, rich in radiogenic Sr, was responsible for the mineralization, which may have been driven laterally by tectonic compression in the region. Upward migration and lateral migration locally was controlled by porous structures and flexural doming. The fluid interacted with the carbonate host rock and/or interstitial pore waters within the carbonate succession, before depositing the ore minerals.

* The driving mechanism of the fluids may have been a combination of episodic dewatering events during compaction of the sediments and tectonic compression and uplift on the margin of the sub-basin.

* The metal chloride complexes were transported simultaneously with the reduced S at a temperature greater than 200°C, with precipitation of sulphide caused by dilution, pH increase, or a decrease in temperature.

* Phase C1 is probably a reaction rim associated with the deposition of phase C2, indicate that only one pulse of Fe-poor sphalerite deposition occurred. Calcite (phase C3) was the final carbonate phase deposited within the vugs, and is believed to be post-sphalerite mineralization.

* The various rock units through which the mineralizing fluids migrated and interacted include the Makwassie Quartz Porphyry of the Ventersdorp Supergroup, basement rocks of the Kaapvaal Craton, and the granulites and amphibolites related to the tectonic events which may have driven the mineralizing fluids.

* The decrease in $\delta^{13}C$ from the dolomites into the vugs indicates that in later carbonate phases there was an increase in the organic-derived C component of the fluid.

* The O isotopic work indicates that the temperature of the fluids may have increased as phase C2 was deposited, with minor exceptions close to Pering Mine (S26). There was a decrease in temperature of the phase C3 relative to C2, after sphalerite deposition, close to Pering Mine (S26), and a relative increase in temperature during the deposition of this phase further east of the Pering deposit (LB1). This may represent an influx of cooler fluid in the Reivilo Formation following mineralization. However, these variations in $\delta^{18}O$ may be related to the mineralogy of the various carbonate phases, with the dolomite and earlier vug-filling carbonates preferentially concentrating ^{18}O relative to ^{16}O compared to the late calcite phase.

* Galena samples from Pering Mine contain the least radiogenic Pb of several deposits investigated by other authors in the Transvaal and Griqualand West sub-basins. The Pb isotopic ratios are not characterised as J-type Pb as in the younger classic Mississippi Valley-type deposits.

* Most of the carbonate samples from S26 give a model age from 2.0-2.7Ga. The galena analysed in this study gives a model age of 2.45Ga. These model ages may not indicate the age of galena deposition, but the age of older rocks through which the mineralizing fluid passed prior to ore deposition. Very radiogenic samples may have initially interacted with U source rocks through which the mineralizing fluids migrated.

* The isotopic composition, cathodoluminescence and carbonate staining of the gangue minerals associated with sphalerite deposition has yielded a better understanding of the local fluid flow and source areas of the mineralizing fluids in the Pering area. This type of exploration method should be extended into the rest of the Griqualand West sub-basin to enable the paths of mineralizing fluids to be determined. The application of cathdoluminescence and staining methods basin-wide will be a cost-effective and useful exploration tool that would provide

information concerning fluid flow and point to potential areas of mineralisation. Isotopic analysis, if applied, should be confined to the Sr-isotope system, which may act as a proximity indicator of mineralization. These method may assist in the discovery of additional Zn-Pb deposits within the Griqualand West sub-basin.

CHAPTER 8

REFERENCES

Anderson, G.M. (1983). Some geochemical aspects of sulphide precipitation in carbonate rocks. *In*: Kisvarsanyi, G.; Grant, S.K.; Pratt, W.P. and Koenig, J.W. (Eds.), *Int. Conf. on Mississippi Valley Type Lead-Zinc Deposits. Preceedings volume. University of Missouri-Rolla. Missouri*, 61-76.

Anderson, G.M. and Garven, G. (1987). Sulphate-sulphide-carbonate associations in Mississippi Valley-type lead-zinc deposits. *Econ.Geol.*, **82**, 482-488.

Armstrong, R.A. (1987). *Geochronological Studies on Archaean and Proterozoic Formations of the Foreland of the Namaqua Front and Possible Correlates on the Kaapvaal Craton.* (Unpub. Ph.D.). University of the Witwatersrand, Johannesburg, 274pp.

Baker, P.A.; Gieskes, J.M. and Elderfield, H. (1982). Diagenesis of carbonates in deep-sea sediments - evidence from Sr/Ca ratios and interstitial dissolved Sr^{++} data. *J. Sed. Petrol.*, **52**, 71-82.

Banner, J.L.; Wasserburg, G.J.; Dobson, P.F.; Carpenter, A.B. and Moore, C.H. (1989). Isotopic and trace element constraints on the origin and evolution of saline groundwaters from central Missouri. *Geochim. Cosmochim. Acta*, **53**, 383-398.

Barnes, H.L. (1967). Sphalerite solubility in ore solutions of the Illinois-Wisconsin district. *In*: Brown, J.S. (Ed.), *Genesis of Stratiform Lead-Zinc-Barite-Fluorite Deposits, Monograph 3*. Econ. Geol. Publ. Co., Lancaster Press, Lancaster, 443pp.

Barnes, H.L. (1979). Solubilities of ore minerals. *In*: Barnes, H.L. (Ed.), *Geochemistry of Hydrothermal Ore Deposits (2nd Edition)*. Wiley-Interscience, New York, 787pp.

Barnes, H.L. (1983). Ore depositing reactions in Mississippi Valley-type deposits. *In*: Kisvarsanyi, G.; Grant, S.K.; Pratt, W.P. and Koenig, J.W. (Eds.), *Int. Conf. on Mississippi Valley Type Lead-Zinc Deposits. Preceedings volume. University of Missouri-Rolla. Missouri*, 77-85.

Barnes, H.L. and Czamanske, G.K. (1967). Solubilities and transport of ore minerals. *In*: Barnes, H.L. (Ed.), *Geochemistry of Hydrothermal Ore Deposits (1st Edition)*. Holt, Rinehart and Winston, New York, 670pp.

Barton, E.S. and Burger, A.J. (1983). Reconnaissance isotopic investigations in the Namaqua mobile belt and implications for Proterozoic crustal evolution - Upington geotraverse. *In*: Botha, B.J.V. (Ed.), *Namaqualand Metamorphic Province*. Geol. Soc. S. Afr., Johannesburg, 173-191.

Bethke, C.M. (1983). Fluid flow and heat transport in compacting sedimentary basins. *Geol. Soc. Amer. Abstr. with Programs*, **15**, 526pp.

Bethke, C.M. (1986). Hydrologic constraints on the genesis of Upper Mississippi Valley mineral district from Illinois basin brines. *Econ. Geol.*, **81(2)**, 233-249.

Beukes, N.J. (1978). *Die Karbonaatgesteentes en Ysterformasies van die Ghaap-groep van die Transvaal-Supergroup in noord-Kaapland*. (Unpub. Ph.D.). Rand Afrikaans University, Johannesburg, 580pp.

Beukes, N.J. (1983a). Palaeoenvironmental setting of iron formations in the depositional basin of the Transvaal Supergroup, South Africa. *In*: Trendall, A.F. and Morris, R.C. (Eds.), *Iron-Formation: Facts and Problems*. Elsevier Science Publishers B.V., Amsterdam, 131-209.

Beukes, N.J. (1983b). Ooids and oolites of the Proterophytic Boomplaas Formation, Transvaal Supergroup, Griqualand West, South Africa. *In*: Peryt, T.M. (Ed.), *Coated Grains*. Springer-Verlag, Heidelberg, 199-214.

Beukes, N.J. (1986). The Transvaal Sequence in Griqualand West. *In*: Anhaeusser, C.R. and Maske, S. (Eds.), *Mineral Deposits of Southern Africa*. Geol. Soc. S. Afr., Johannesburg, 819-828.

Beukes, N.J. (1987). Facies relations, depositional environments and diagenesis in a major early Proterozoic stromatolitic carbonate platform to basinal sequence, Campbellrand Subgroup, Transvaal Supergroup, Southern Africa. *Sed. Geol.*, **54**, 1-46.

Beukes, N.J. and Smit, C.A. (1987). New evidence for thrust faulting in Griqualand West, South Africa: implications for stratigraphy and the age of red beds. *S. Afr. J. Geol.*, **90(4)**, 378-394.

Beukes, N.J.; Klein, C.; Kaufman, A.J. and Hayes, J.M. (1990). Carbonate petrography, kerogen distribution, and carbon and oxygen isotope variations in an Early Proterozoic transition from limestone to iron formation deposition, Transvaal Supergroup, South Africa. *Econ. Geol.*, **85**, 663-690.

Button, A. (1973). The stratigraphic history of the Malmani dolomite in the eastern and north-eastern Transvaal. *Trans. Geol. Soc. S. Afr.*, **76**, 229-247.

Calvez, J.Y. and Orgeval, J.J. (1989). Pb and Sr isotopic studies of the carbonate-hosted Zn-Pb deposit of Bou Grine (Tunisia) and its environment, genetic implications and possible use in exploration [abs.]. *Chem. Geol.*, **70(1-2)**, 133.

Carpenter, A.B.; Trout, M.L. and Pickett, E.E. (1974). Preliminary report on the origin and chemical evolution of lead- and zinc-rich oil field brines in central Mississippi. *Econ. Geol.*, **69**, 1191-1206.

Carpenter, A.B. (1978). Origin and chemical evolution of brines in sedimentary basins. *Okla. Geol. Surv. Circ*, **79**, 60-77.

Cathles, L.M. (1992). Some simple models for chemical alteration caused by the movement of metamorphic fluids in the deeper parts of the crust. *Earth-Sci Rev.*, **32**, 133-135.

Cathles, L.M. and Smith, A.T. (1983). Thermal constraints on the formation of Mississippi Valley-type lead-zinc deposits and their implications for basin dewatering and deposit genesis. *Econ. Geol.*, **78**, 983-1002.

Cawthorn, R.G.; Barton, J.M. and Viljoen, M.J. (1985). Interaction of floor rocks with the platreef on Overysel, Potgietersrus, northern Transvaal. *Econ. Geol.*, **80**, 988-1006.

Clendenin, C.W.; Charlesworth, E.G. and Maske, S. (1988). An early Proterozoic three-stage rift system, Kaapvaal craton, South Africa. *Tectonophysics*, **145**, 73-96.

Clendenin, C.W. (1989). *Tectonic Influence on the Early Proterozoic Transvaal Sea, Southern Africa.* (Unpub. Ph.D.). University of the Witwatersrand, Johannesburg, 367pp.

Chaudhuri, S.; Broedel, V. and Clauer, N. (1987). Strontium isotope evolution of oilfield waters from carbonate reservoir rocks in Bindley field, central Kansas, USA. *Geochim. Cosmochim. Acta*, **51**, 45-53.

Chaudhuri, S.; Clauer, N.; and Ramakrishnan. (1983). Strontium isotopic composition of gangue carbonate minerals in the lead-zinc sulphide deposits at the Bushy Creek mine, Viburnum Trend, southeast Missouri. *In*: Kisvarsanyi, G.; Grant, S.K.; Pratt, W.P. and Koenig, J.W. (Eds.), *Int. Conf. on Mississippi Valley Type Lead-Zinc Deposits. Preceedings volume. University of Missouri-Rolla. Missouri*, 140-144.

Collins, A.G. (1975). *Geochemistry of Oil Field Brines*. Elsevier Science Publishers B.V., Amsterdam, 496pp.

Coward, M.P. and Potgieter, R. (1983). Trust zones and shear zones of the margin of the Namaqua and Kheis mobile belts, southern Africa. *Precamb. Res.*, **21**, 39-54.

Cox, G.H. (1911). The origin of lead and zinc ores of the Upper Mississippi Valley district. *Econ. Geol.*, **6**, 427-448, 582-603.

Daubree, A. (1887). *Les eaux souterraines, au époques anciennes et à l'époque actuelle.* Paris, Dunod, 3 vols.

Dickson, J.A.D. and Coleman, M.L. (1980). Changes in carbon and oxygen isotope composition during limestone diagenesis. *Sedimentology*, **27**, 107-118.

Dirr, H.V.; Danielson, A. and Beukes, N.J. (1990). Oxygen isotopes in the carbonates of the Campbellrand Subgroup, Northern Cape, South Africa [abs.]. *Int. Archaean Symposium, Perth, Australia*, 311.

Doe, B.R. and Zartman, R.E. (1979). Plumbotectonics 1, the Phanerozoic. *In*: Barnes, H.L. (Ed.), *Geochemistry of Hydrothermal Ore Deposits (2nd Edition)*. Wiley-Interscience, New York, 787pp.

Dozy, J.J. (1970). A geologic model for the genesis of the lead-zinc ores of the Mississippi Valley, U.S.A. *Inst. Mining Metall. Trans.*, **79(B)**, 163-170.

Duane, M.J., Kruger, F.J., Roberts, P.J., Smith, C.B. and Maske, S. (1991). Pb and Sr isotopic and origin of Proterozoic base metal (fluorite) and gold deposits, Transvaal Sequence, South Africa. *Econ.*

Geol., **86**, 1491-1505.

Elderfield, H. (1986). Strontium isotope stratigraphy. *Palaeogeography, palaeoclimatology, palaeoecology*, **57**, 71-90.

Fairchild, I.J. (1983). Chemical controls of cathodoluminescence of natural dolomites and calcites: new data and review. *Sedimentology*, **30**, 579-583.

Faure, G. (1977). *Principles of Isotope Geology*. John Wiley & Sons, Inc., U.S.A., 464pp.

Faure, G. (1986). *Principles of Isotope Geology (2nd Edition)*. John Wiley & Sons, Inc., U.S.A., 589pp.

Fletcher, P. and Reimold, W.U. (1989). Some notes and speculations on the pseudotachylites in the Witwatersrand basin and Vredefort dome, South Africa. *S. Afr. J. Geol.*, **92**, 223-234.

Franklyn, M.T.; McNutt, R.H.; Kamineni, D.C.; Gascoyne, M. and Frape, S.K. (1991). Groundwater $^{87}Sr/^{86}Sr$ values in the Eye-Dashwa Lakes pluton, Canada: Evidence for plagioclase-water reaction. *Chem. Geol.*, **86**, 111-122.

Friedman, I and O'Niel, J.R. (1977). Compilation of stable isotope factors of geochemical interest. *In*: Fleischer, M. (Ed.), *Data of Geochemistry*. U. S. Geol. Surv. Prof. Paper 440-KK.

Fritz, P. (1969). The oxygen and carbon isotpic composition of carbonates from the Pine Point lead-zinc ore deposits. *Econ. Geol.*, **64**, 733-742.

Garlick, G.D. (1969). The stable isotopes of oxygen. *In*: Wedepohl, K.H. (Ed.), *Handbook of Geochemistry*. Springer-Verlag, Berlin, pp.

Garven G. and Freeze, R.A. (1984a). Theoretical analysis of the role of groundwater flow in the genesis of stratabound ore deposits 1. Mathematical and numerical model. *Am. J. Sci.*, **284**, 1085-1124.

Garven G. and Freeze, R.A. (1984b). Theoretical analysis of the role of groundwater flow in the genesis of stratabound ore deposits 2. Quantitative results. *Am. J. Sci.*, **284**, 1125-1174.

Garven, G. (1985). The role of regional fluid flow in the genesis of the Pine Point deposit, Western Canada sedimentary basin. *Econ. Geol.*, **80**, 307-324.

Ghazban, F.; Schwarcz, H.P. and Ford, D.C. (1991). Correlated strontium, carbon and oxygen isotopes in carbonate gangue at the Nanisivik zinc-lead deposits, northern Baffin Island, N.W.T. Canada. *Chem. Geol.*, **87**, 137-146.

Giordano, T.H. (1985). A preliminary evaluation of organic ligands and metal-organic complexing in Mississippi Valley-type ore solutions. *Econ. Geol.*, **80**, 96-106.

Giordano, T.H. and Barnes, H.L. (1981). Lead transport in Mississippi Valley-type ore solutions. *Econ. Geol.*, **76**, 2200-2211.

Goldsmith, J.R. (1959). Some aspects of the geochemistry of carbonates. *In*: Abelson, P.H. (Ed.), *Researches in Geochemistry*. J. Wiley, New York.

Goodfellow, W.D. and Jonasson, I.R. (1986). Environment of formation of the Howard Pass (XY) Zn-Pb deposit, Selwyn Basin, Yukon. *In*: Morin, B.W. (Ed), *Mineral Deposits of Northern Cordillera, CIMM Special Vol. 37*, 19-50.

Grossmann, E.L. & Ku, T.L. (1986). Oxygen and carbon isotope fractionation in biogenic aragonite: temperature effects. *Chem. Geol.*, **59**, 59-74.

Guilbert, J.M. and Park, C.F. (1986). *The Geology of Ore Deposits*. W.H. Freeman and Company, New York, 985pp.

Gvirtzman, G.; Friedman, G.M. and Miller, D.S. (1973). Control and distribution of uranium in coral reefs during diagenesis. *J. Sed. Petrol.*, **43**, 983-997.

Haglund, D.S.; Friedman, G.M. and Miller, D.S. (1969). The effect of fresh water on the redistribution of uranium in fresh water sediments. *J. Sed. Petrol.*, **39**, 1283-1296.

Hall, W.E. and Friedman, I. (1963). Oxygen and carbon isotope composition of ore and host rock of selected Mississippi Valley deposits. *U.S. Geol. Survey Prof.*, Paper **650-C** C140-C148.

Hanor, J.S. (1979). The sedimentary genesis of hydrothermal fluids. *In*: Barnes, H.L. (Ed.), *Geochemistry of Hydrothermal Ore Deposits (2nd Edition)*. Wiley-Interscience, New York, 787pp.

Hedge, C.E. (1974). Strontium isotopes in economic geology. *Econ. Geol.*, **69**, 823-825.

Heyl, A.V.; Landis, G.P. and Zartman, R.E. (1974). Isotopic evidence for the origin of Mississippi Valley-type mineral deposits: A review. *Econ. Geol.*, **69**, 992-1006.

Hoefs, J. (1980). *Stable Isotope Geochemistry*. Springer-Verlag, Berlin, 208pp.

Jackson, S.A. and Beales, F.W. (1967). An aspect of sedimentary basin evolution, the concentration of Mississippi Valley-type ore during the stages of diagenesis. *Can. Petrol. Geol. Bull.*, **15**, 393-433.

Jacobson, R.L. and Usdowski, H.E. (1976). Partitioning of strontium between calcite, dolomite and liquids. *Contrib. Min. Petrol.*, **59**, 171-185.

Jahn, B; Bertrand-Sarfati, J.; Morin, N. and Macé, J. (1990). Direct dating of stromatolitic carbonates from the Schmidtsdrif Formation (Transvaal Dolomite), South Africa, with implications on the age of the Ventersdorp Supergroup. *Geology*, **18**, 1211-1214.

Kessen, K.M.; Woodruff, M.S. and Grant, N.K. (1981). Gangue mineral $^{87}Sr/^{86}Sr$ ratios and the origin of Mississippi Valley-type mineralization. *Econ. Geol.*, **76**, 913-920.

Kopp, O.C. (1981). Cathodoluminescence petrography: A valuable tool for teaching and research. *J. Geol. Educ.*, **29**, 108-113.

Kretz, R. (1982). A model for the distribution of trace elements between calcite and dolomite. *Geochim. Cosmochim. Acta*, **46**, 1979-1981.

Lahoud, J.A.; Miller, D.S. and Friedman, G.M. (1966). Relationship between depositional environment and uranium concentration of molluscan shells. *J. Sed. Petrol.*, **36**, 541-547.

Land, L.S. (1980). The isotopic and trace element geochemistry of dolomite: the state of the art. *In*: Ethington, D.H.; Dunham, J.B.; & Zenger, R.L. (Eds.), *Concepts and Models of Dolomitization*. Soc. Econ. Paleo. and Min. Spec. Pub. No. 28, 87-110.

Land, L.S. (1985). The origin of massive dolomite. *J. Geol. Educ.*, **33**, 112-125.

Land, L.S. (1987). The major ion chemistry of saline brines in sedimentary basins. *In*: Banavar, J.R.; Koplik, J. and Winkler, K.W. (Eds.), *Physics and Chemistry of Porous Media II, Amer. Inst. Phys. Conf. Proc. 154, Rigdefield, CT*, 160-179.

Land, L.S. and Milliken, K.L. (1981). Feldspar diagenesis in the Frio Formation, Brazoria County, Texas Gulf Coast. *Geology*, **9**, 314-318.

Lorens, R.B. (1981). Sr, Cd, Mn, and Co distribution coefficients in calcite as a function of calcite precipitation rate. *Geochim. Cosmochim. Acta*, **45**, 553-561.

Marshall, J.D. (1992). Climatic and oceanographic isotopic signals from the carbonate rock record and their preservation. *Geol. Mag.*, **129(2)**, 143-160.

Mason, R.A. (1987). Ion microprobe analysis of trace elements in calcite with an application to the cathodoluminescence zonation of limestone cements from the Lower Carboniferous of South Wales, U.K. *Chem. Geol.*, **64**, 209-224.

McCaig, A.M.; Wickham, S.M. and Taylor, H.P. (1990). Deep fluid circulation in alpine shear zones, Pyrenees, France: field and oxygen isotope studies. *Contrib. Min. Petrol.*, **106**, 41-60.

McIntyre, W.L. (1963). Trace element partition coefficients - a review of theory and application to geology. *Geochim. Cosmochim. Acta*, **27**, 1209-1264.

McNutt, R.H. (1987). $^{87}Sr/^{86}Sr$ ratios as indicators for water-rock interactions: applications to brines found in Precambrian age rocks from Canada. *In*: Fritz, P. and Frape, S.K. (Eds.), *Saline Waters and Gases in Crystalline Rocks*. Geol. Assoc. Can. Spec. Pap. 33, 81-88.

Milliman, J.D. (1974). *Marine Carbonates*. Springer-Verlag, 375pp.

Moore, C.H. (1989). *Carbonate Diagenesis and Porosity*. Elsevier Science Publishers B.V., Amsterdam, 338pp.

Nier, A.O. (1950). A redetermination of the relative abundances of the isotopes of carbon, nitrogen, oxygen, argon, and potassium. *Phys. Rev.*, **77**, 789.

Noble, E.A. (1963). Formation of ore deposits by water of compaction. *Econ. Geol.*, **58**, 1145-1156.

Ohmoto, H. (1972). Systematics of sulphur and carbon isotopes in hydrothermal ore deposits. *Econ. Geol.* **67**, 551-578.

Perry, E.A. and Turekian, K.K. (1974). The effect of diagenesis on the distribution of strontium isotopes in shales. *Geochim. Cosmochim. Acta*, **38**, 929-935.

Ravenhurst, C.E., Reynolds, P.H., Zentilli, M. and Akande, S.O. (1987). Isotopic constraints on the genesis of Zn-Pb mineralisation at Gays River, Nova Scotia, Canada. *Econ. Geol.*, **82**, 1294-1308.

Robinson, B.W. (1975). Carbon and oxygen isotopic equilibrium in hydrothermal calcites. *Geochem.*, **9**, 43.

Roedder, E. (1960). Fluid inclusions as samples of ore-forming fluids. *Int. Geol. Congr., Copenhagen*, **16**, 218-229.

Roedder, E.; Ingram, B. and Hall, W.E. (1963). Studies of fluid inclusions, III: Extraction and quantitative analysis of inclusions in the milligram range. *Econ. Geol.*, **58**, 353-374.

Roedder, E. (1971). Fluid inclusion evidence of the environment of formation of mineral deposits in the Southern Appalachian Valley. *Econ. Geol.*, **66**, 777-791.

Rye, R.O. and Ohmoto, H. (1974). Sulphur and carbon isotopes and ore genesis. A review. *Econ. Geol.*, **69**, 826-842.

SACS - South African Committee for Stratigraphy. (1980). *Stratigraphy of South Africa (Part 1), Lithostratigraphy of the Republic of South Africa, South West Africa/Namibia and the Republics of Bophuthatswana, Transkei and Venda.* (Comp. L.E. Kent). Handbook Geol. Surv. S. Afr., **8**, 690pp.

Sangster, D.F. (1990). Mississippi Valley-type and sedex lead-zinc deposits: a comparative examination. *Inst. Mining Metall. Trans.*, **99(B)**, 21-42.

Sawkins, F.J. (1968). The significance of Na/K and Cl/SO_4 ratios in fluid inclusions and surface waters, with respect to the genesis of Mississippi Valley-type ore deposits. *Econ. Geol.*, **63**, 935-942.

Schultz, J.L.; Boles, J.R. and Tilton, G.R. (1989). Tracking calcium in the San Joaquin basin, California: A strontium isotope study of carbonate cements at North Coles Levee. *Geochim. Cosmochim. Acta*, **53**, 1991-1999.

Scoffin, T.P. (1987). *An Introduction to Carbonate Sediments and Rocks*. Blackie and Son Ltd, Glascow and London, 274pp.

Sharp, J.M. (1978). Energy and momentum transport model of the Ouachita basin and its possible impact on formation of economic mineral deposits. *Econ. Geol.*, **73**, 1057-1068.

Siebenthal, C.E. (1915). Origin of the zinc and lead deposits of the Joplin region. *U.S. Geol. Sur. Bull.*, **606**, 283pp.

Smalley, P.C., Forsberg, A. and Råheim, A. (1987). Rb-Sr dating of fluid migration in hydrocarbon source rocks. *Chem. Geol.*, **65**, 223-233.

Smith, C.B. (1991). *Isotope Geochemistry and Geochronology (Lecture notes)*. Bernard Price Institute for Geophysical Research, University of the Witwatersrand, Johannesburg.

Stacey, J.S. and Kramers, J.D. (1975). Approximation of terrestrial lead isotope evolution by a two stage model. *Earth Planet. Sci. Let.*, **26**, 207-221.

Stowe, C.W. (1986). Synthesis and interpretation of structures along the north eastern boundary of the Namaqua Tectonic Province, South Africa. *Trans. Geol. Soc. S. Afr.*, **89**, 185-198.

Stueber, A.M.; Pushkar, P. and Hetherington, E.A. (1984). A strontium isotopic study of Smackover brines and associated solids, southern Arkansas. *Geochim. Cosmochim. Acta*, **48**, 1637-1649.

Sulin, V.A. (1947). Waters of petrolium formations in the system of natural waters. *Moscow. Gostopekhizdat*, 35-96.

Sverjensky, D.A. (1981). The origin of a Mississippi Valley-type deposit in the Viburnum Trend, southeast Missouri. *Econ. Geol.*, **76**, 1848-1872.

Sverjensky, D.A. (1984). Oil-field brines as ore-forming solutions. *Econ. Geol.*, **79**, 23-37.

Sverjensky, D.A. (1986). Genesis of Mississippi Valley-type lead-zinc deposits. *Ann. Rev. Earth Planet. Sci.*, **14**, 177-199.

Swart, P.K. (1988). The elucidation of dolomitization events using nuclear-track mapping. *In*: Shukla, V. and Baker, P. (Eds). *Sedimentology and Geochemistry of Dolostones*. Soc. Econ. Paleontologists and Mineralogists, Spec. Publ. 43, 266pp.

Swennen, R.A.J. (1986). Lithostratigraphy and sedimentology of the Lokamona, Monteville and Lower Reivilo Formations in the Pering area and its relation to the Pering Zn-Pb metallogenesis. *Shell South Africa (Pty) Limited Metals Division. Technical Report No. 170.*

Tankard, A.J.; Jackson, M.P.A.; Erikson, K.A.; Hobday, D.K.; Hunter; D.R. and Minter, W.E.L. (1982). *Crustal Evolution of Southern Africa.* Springer-Verlag, New York, 523pp.

Tarutani, T.; Clayton, R.N. and Mayeda, T.K. (1969). The effect of polymorphism and magnesium substitution oxygen isotope fractionation between calcium carbonate and water. *Geochim. Cosmochim. Acta*, **33**, 987-996.

Taylor, G.H. (1979). Biogeochemistry of uranium minerals. *In*: Trudinger, P.A. and Swaine, D.J. (Eds.). *Biogeochemical Cycling of Mineral Forming Elements: Studies in Environmental Sciences (v.2)*. 485-514.

Ten Have, T. and Heijnen, W. (1985). *Geologie Mijnbouw*, **64**, 297-310.

Tyler, N. (1979). The stratigraphy of the Early-Proterozoic Buffalo Springs Group in the Thabazimbi area, west-central Transvaal. *Trans. Geol. Soc. S. Afr.*, **82**, 215-226.

Vajner, V. (1974). The tectonic development of the Namaqua mobile belt and its foreland parts in the Northern Cape. *Bull. Precam. Res. Unit, Univ. Cape Town*, **14**, 201pp.

Vehrenkamp, V.C. and Swart, P.K. (1988). Constraints and interpretation of $^{87}Sr/^{86}Sr$ ratios in Cenozoic dolomites. *Geophys. Res. Let.*, **14(4)**, 385-388.

Veizer, J. (1978). Secular variations in the composition of sedimentary carbonate rocks. II. Fe, Mn, Ca, Mg, Si and minor constituents. *Precambrian Res.*, **6**, 381-413.

Veizer, J.; Clayton, R.N.; Hinton, R.W.; Von Brunn, V.; Mason, T.R.; Buck, S.G. and Hoefs, J. (1990). Geochemistry of Precambrian carbonates: 3. Shelf seas and nonmarine environments in the Archean. *Geochim. Cosmochim. Acta*, **54**, 2717-2729.

Veizer, J.; Clayton, R.N. and Hinton, R.W. (1992). Geochemistry of Precambrian carbonates: 4. Early Paleoproterozoic (2.25 ± 0.25Ga) seawater. *Geochim. Cosmochim. Acta*, **56**, 875-885.

Walker, G.; Abumere, O.E. and Kamaluddin, B. (1989). Luminescence spectroscopy of Mn^{2+} centres in rock-forming carbonates. *Min. Mag.*, **53**, 201-211.

Walraven, F.; Armstrong, R.A. and Kruger, F.J. (1990a). A chronostratigraphic framework for the north-central Kaapvaal craton, the Bushveld Complex and Vredefort structure. *Tectonophysics*, **171**, 23-48.

Walraven, F.; Smith, C.B. and Kruger, F.J. (1990b). Age determination of the Zoetlief Group - a Ventersdorp correlate. *Geocongress '90, Extended Abstracts, Geol. Soc. South Africa, Cape Town*, **23**, 594-597.

Wang, Y. and Merino, E. (1992). Dynamic model of oscillatory zoning of trace elements in calcites: Double layer, inhibition, and self-organization. *Geochim. Cosmochim. Acta*, **56**, 587-596.

Wetzel, A. (1989). Influence of heat flow on ooze/chalk cementation: quantification from consolidation parameters in DSDP sites 504 and 505 sediments. *J. Sed. Petrol.*, **59**, 539-547.

Wheatley, C.J.V.; Whitfield, G.G.; Kenny, K.J. and Birch, A. (1986). The Pering carbonate-hosted zinc-lead deposit, Griqualand West. *In*: Anhaeusser, C.R. and Maske, S. (Eds.), *Mineral Deposits of Southern Africa*. Geol. Soc. S. Afr., Johannesburg, 891-900.

White, D.E. (1958). Liquid of inclusions in sulphides from Tristate (Missouri-Kansas-Oklahoma) is probably connate in origin [abs.], *Geol. Soc. Am. Bull.*, **69**, 1660.

White, D.E. (1965). Saline waters of sedimentary rocks: Fluids in subsurface environments - a symposium. *Amer. Assoc. Petr. Geol.*, Mem. **4**, 342-366.

White, D.F. (1981). Active geothermal systems and hydrothermal ore deposits. *In*: Skinner, B.J. (Ed.), *Economic Geology, 75th Anniversary Volume*. Lancaster Press, Lancaster, Pa, 392-423.

APPENDICES

APPENDIX 1

Geology, borehole reference log and number of samples collected from boreholes around Pering Mine.

Borehole: LB1.
Location: Letsila Belung.
Geology: Core drilled from Stromatolite Zone 2 (SZ2) of the Reivilo Formation to a depth of 316.88m through the Monteville Formation and LK1 of the Lokammona Formation.
Logged by: R. Swennen.
Samples: 19 (LB1A-LB1S).

Borehole: S26.
Location: Scheurfontein 785
Geology: Core drilled from Stromatolite Zone 3 (SZ3) of the Reivilo Formation to a depth of 209.3m through the Monteville Formation and LK1 of the Lokammona Formation.
Logged by: R. Swennen.
Samples: 31 (S26A-S26Y).

Borehole: KG1.
Location: Kokwaan 788.
Geology: Core drilled from Stromatolite Zone 1A (SZ1A) of the Reivilo Formation to a depth of 263.87m through the Monteville Formation and LK1, LK2 of the Lokammona Formation.
Logged by: K.G. Kartun, A. Birch.
R. Swennen.
Samples: 17 (KG1A-KG1P).

Borehole: DR1.
Location: Droogfontein.
Geology: Core drilled from vadose zone 77m above Stromatolite Zone 1A (SZ1A) of the Reivilo Formation to a depth of 338.21m through the Monteville Formation and LK1, LK2 of the Lokammona Formation.
Logged by: C. Halpin.
R. Swennen.
Samples: 26 (DR1A-DR1Z).

Borehole: TL1.
Location: Tlotcha 907.
Geology: Core drilled from 110m above Stromatolite Zone 1A (SZ1A) of the Reivilo Formation to a depth of 582.7m through the Monteville Formation and LK1-LK4 of the Lokammona Formation.
Logged by: K.G. Kartun.
R. Swennen.
Samples: 27 (TL1A-TL1X).

Borehole: RP1.
Location: Ruilputs 783.
Geology: Core drilled from 26.5m above Stromatolite Zone 1A (SZ1A) of the Reivilo Formation to a depth of 290.17m through the Monteville Formation and LK1, LK2 of the Lokammona Formation.
Logged by: F. Dooge, C. Halpin.
R. Swennen.
Samples: 21 (RP1A-RP1U).

Borehole: KF1.
Location: Kareefontein 784.
Geology: Core drilled from 12.6m above Stromatolite Zone 1 (SZ1) of the Reivilo Formation to a depth of 236.72m through the Monteville Formation and LK1, LK2 of the Lokammona Formation.
Logged by: C. Halpin.
R. Swennen.
Samples: 22 (KF1A-KF1V).

Borehole: KF2.
Location: Kareefontein 784.
Geology: Core drilled from 4.0m above Stromatolite Zone 2 (SZ2) of the Reivilo Formation to a depth of 245.80m through the Monteville Formation and LK1, LK2 of the Lokammona Formation.
Logged by: C. Halpin.
R. Swennen.
Samples: 23 (KF2A-KF2N).

APPENDIX 2

Chemical preparation of the carbonate samples from LB1 and S26 for Pb and Rb-Sr analysis.

^{87}Rb and ^{84}Sr spike of known isotopic concentration was accurately weighed into a clean, dry teflon beaker. The solution was then dried down and approximately 0.1g of sample weighed into the cooled beaker. The sample was dissolved in 6N HCl and left to dry. This allowed the spike and sample isotopic concentrations to mix.

2A. Pb Sample Preparation

Each sample was dissolved in 0.8N HBr and passed through small (250µl) natural lead, anion exchange columns. The separation and extraction of the Pb and remaining elements such as Rb and Sr was carried out using standard ion-exchange techniques. The procedure for Pb extraction is as follows:

(a) Place analytical grade Dowex AG1-X8, 100-200 mesh (chloride form) anion exchange resin into the cleaned columns;
(b) Clean the resin by passing distilled H_2O and 6N HCl through the columns separately, allowing each to pass through twice;
(c) Equilibrate the resin by passing 250µl (0.8N) HBr through each column;
(d) Pipette each dissolved sample into a column, and place the relevant teflon beaker under each column to collect the Sr, Rb and any other elements which pass through the column - dry down this sample under an infra-red lamp;
(e) Add 3ml of 0.8N HBr to each column and allow it to run into the teflon beaker;
(f) Collect the lead into a clean teflon beaker by passing 2ml 6N HCl through each column;
(g) Dry down the collected lead under an infra-red lamp.

Resin leaked through the ion-exchange columns which prevented the Pb being analysed in the mass-spectrometer. The lead was thus separated using an anodic electrodeposition technique. Platinum electrodes and a current of 300-400µA was used. The solutions (electrolytes) were continuously stirred with teflon-coated magnetic stirrers. The technique is as follows:

(a) Using a dilute copper solution as an electrolyte, allow a copper complex to deposit on the cathode over 2 hours;
(b) Clean the anode using concentrated HNO_3;
(c) Dissolve the sample in 25µl 0.3N HNO_3 and add approximately 5ml distilled water;
(d) Place the electrodes in the solution containing the sample;
(e) Allow the lead to deposit on the anode over 12 hours;
(f) Strip off the deposited lead from the anode using concentrated HNO_3;
(g) Dry down the collected lead solution under an infra-red lamp.

This double-stripping technique was necessary to ensure that pure lead was deposited on the anode. The copper-complex on the cathode ensures that all the lead is deposited on the anode.

2B. Rb-Sr Sample Preparation

The solution remaining after the Pb extraction procedure, containing the Rb, Sr and other trace elements, was dissolved in 1.5ml 2.59N HCl and centrifuged for half an hour. The supernatant (1ml) was passed through a 20cm cation-exchange column for the separation of Sr. The precipitate and supernatant remaining in the centrifuge tube was retained for Rb analysis. The separation and extraction of Sr was carried out using standard ion exchange techniques. Analytical grade Dowex AG 50W-X12, 200-400 mesh (hydrogen form) ion-exchange resin was used. The procedure is as follows:

(a) Backwash the columns with 2.59N HCl;
(b) Equilibrate the resin with 20ml 2.59N HCl;
(c) Add the sample solution (1ml);
(d) Wash the sample into the resin using three aliquots of 2ml 2.59N HCl each;
(e) Add between 60 and 80ml 2.59N HCl, depending on the particular column used;
(f) Collect the Sr with 20ml 2.59N HCl;
(g) Dry down the collected Sr under an infra-red lamp.

APPENDIX 3a

Calculation of fractionation correction factors using the ratios of the accepted lead standard (SRM-981) and the ratios determined for this standard at BPI by Dr F.J. Kruger. Samples were analysed with the Daly detecter (D) and the Faraday Cup (F) The filament current of each analysis is shown.

	Pb 206/204	Pb 207/204	Pb 208/204	Filament (A)
Accepted SRM-981	16.937	15.491	36.721	
Determined				
SRM-981a (D)	16.948	15.464	36.647	2.027
SRM-981a (F)	16.929	15.481	36.672	2.247
SRM-981b (D)	17.890	16.292	38.790	1.316
SRM-981b (F)	16.906	15.449	36.563	1.882
SRM-981c (D)	16.817	15.342	36.302	1.290
SRM-981c (F)	16.930	15.480	36.674	2.017
SRM-981d (D)	16.758	15.285	36.164	1.158
SRM-981d (F)	16.929	15.480	36.650	1.941

(A) TO CALCULATE THE CORRECTION FACTOR:

(1) divide each of the determined SRM-981 ratios by the accepted SRM-981 ratio;

SRM-981a (D)	1.001	0.998	0.998	2.027
SRM-981a (F)	1.000	0.999	0.999	2.247
SRM-981b (D)	1.056	1.052	1.056	1.316
SRM-981b (F)	0.998	0.997	0.996	1.882
SRM-981c (D)	0.993	0.990	0.989	1.290
SRM-981c (F)	1.000	0.999	0.999	2.017
SRM-981d (D)	0.989	0.987	0.985	1.158
SRM-981d (F)	1.000	0.999	0.998	1.941

Using the values with a filament current of >1.8 A (with the exception of SRM-981c (D) which was the only other acceptable Daly value other than SRM-981a (D)) calculate:

(2) Mean Daly (a+c/2)	0.997	0.994	0.993
(3) Mean Fday (a+b+c+d/2)	0.999	0.999	0.998
(4) Daly/Fday	0.998	0.996	0.995
(5) Mean Daly /Faraday	0.9962		

The correction factor Is therefore 1.0038
i.e. Faraday = Daly x 1.0038

(B) TO CALCULATE THE FRACTIONATION FACTOR:

(1) multiply the determined standard Daly values by 1.0038;

Standard No.	Pb 206/204	Pb 207/204	Pb 208/204
SRM-981a (D)	17.012	15.523	36.786
SRM-981a (F)	16.929	15.481	36.672
SRM-981b (D)			
SRM-981b (F)	16.906	15.449	36.563
SRM-981c (D)	16.881	15.400	36.440
SRM-981c (F)	16.930	15.480	36.674
SRM-981d (D)			
SRM-981d (F)	16.929	15.480	36.650

(2) calculate the mean of each lead ratio;

Mean	16.931	15.469	36.631

(3) divide each of the accepted SRM-981 ratios by each mean ratio.

Fractionation Factor	1.00034	1.00143	1.00246

FRACTIONATION CORRECTIONS:
(1) MULTIPLY EACH OF THE DALY VALUES BY 1.0038
(2) MULTIPLY THE FARADAY AND CALCULATED DALY RATIOS BY THE FRACTIONATION FACTOR FOR EACH RATIO.

APPENDIX 3b

Pb isotope ratios of the samples from S26 and LB1 before the fractionation corrections.
Daly and Faraday ratios.

BOREHOLE	SAMPLE NO.	DALY RATIOS			FARADAY RATIOS		
		Pb 206/204	Pb 207/204	Pb 208/206	Pb 206/204	Pb 207/204	Pb 208/204
S26	S26A-DOL	16.838	17.868	41.277	13.696	14.544	33.296
	S26A-C1	-	-	-	-	-	-
	S26A-C2	13.404	14.364	32.616	13.521	14.520	33.194
	S26B-DOL	13.812	14.794	33.661	13.615	14.521	33.130
	S26B-C2	13.467	14.427	33.177	13.566	14.544	33.209
	S26B-C3	13.531	14.502	33.080	13.557	14.553	33.218
	S26Gb-DOL	-	-	-	-	-	-
	S26Gb-C2	13.950	14.652	33.515	13.935	14.599	33.443
	S26L-DOL	13.932	14.530	33.262	13.970	14.597	33.488
	S26L-C2	13.625	14.499	33.133	13.663	14.545	33.334
	S26M-DOL	17.412	17.640	41.166	14.620	14.720	34.106
	S26M-C1	-	-	-	-	-	-
	S26M-C2	13.986	14.569	33.359	13.937	14.565	33.444
	S26M-C3	13.915	14.528	33.326	13.905	14.632	33.637
	S26N1-DOL	-	-	-	-	-	-
	S26N1-C1	17.763	16.156	37.451	-	-	-
	S26N1-C2	15.451	21.310	34.862	15.418	21.875	34.714
	S26N2-DOL	17.446	15.561	36.819	17.576	15.716	37.185
	S26N2-C1	17.822	15.628	37.471	-	-	-
	S26N2-C2	17.172	15.621	37.241	-	-	-
	S26X-DOL	17.602	19.798	40.661	14.888	16.699	34.242
	S26X-C2	14.110	15.970	33.411	14.110	15.973	33.471
	S26X-C3	13.688	14.487	33.061	13.827	14.671	33.485
LB1	LB1N-DOL	20.230	22.838	36.397	-	-	-
	LB1N-C2	15.319	24.301	34.801	-	-	-
	LB1N-C3	15.449	41.149	34.981	-	-	-
	LB1P-DOL	16.392	14.818	34.471	-	-	-
	LB1P-C2	17.801	21.128	36.828	-	-	-
	LB1R-DOL	-	-	-	-	-	-
	LB1R-C2	-	-	-	-	-	-
	LB1S-DOL	-	-	-	-	-	-
	LB1S-C2	18.371	25.898	35.242	-	-	-
	LB1S-C3	16.901	28.465	35.589	-	-	-

APPENDIX 3c

Pb Isotope ratios of the samples from S26 and LB1 after the fractionation corrections.
Daly and Faraday ratios.

BOREHOLE	SAMPLE NO.	DALY RATIOS			FARADAY RATIOS		
		Pb 206/204	Pb 207/204	Pb 208/206	Pb 206/204	Pb 207/204	Pb 208/204
S26	S26A-DOL	16.908	17.962	41.536	13.701	14.565	33.378
	S26A-C1	-	-	-	-	-	-
	S26A-C2	13.460	14.439	32.821	13.526	14.541	33.276
	S26B-DOL	13.869	14.871	33.872	13.620	14.542	33.212
	S26B-C2	13.523	14.503	33.385	13.571	14.565	33.291
	S26B-C3	13.587	14.578	33.287	13.562	14.574	33.300
	S26Gb-DOL	-	-	-	-	-	-
	S26Gb-C2	14.008	14.729	33.725	13.940	14.620	33.525
	S26L-DOL	13.990	14.606	33.471	13.975	14.618	33.570
	S26L-C2	13.681	14.575	33.341	13.668	14.566	33.416
	S26M-DOL	17.484	17.732	41.424	14.625	14.741	34.190
	S26M-C1	-	-	-	-	-	-
	S26M-C2	14.044	14.645	33.568	13.942	14.586	33.526
	S26M-C3	13.973	14.604	33.535	13.910	14.653	33.720
	S26N1-DOL	-	-	-	-	-	-
	S26N1-C1	17.837	16.241	37.686	-	-	-
	S26N1-C2	15.515	21.422	35.081	15.423	21.906	34.799
	S26N2-DOL	17.518	15.642	37.050	17.582	15.739	37.277
	S26N2-C1	17.896	15.710	37.706	-	-	-
	S26N2-C2	17.243	15.703	37.475	-	-	-
	S26X-DOL	17.675	19.902	40.916	14.893	16.723	34.326
	S26X-C2	14.168	16.054	33.620	14.115	15.996	33.553
	S26X-C3	13.745	14.563	33.268	13.832	14.692	33.567
LB1	LB1N-DOL	20.314	22.958	36.625	-	-	-
	LB1N-C2	15.382	24.428	35.019	-	-	-
	LB1N-C3	15.513	41.365	35.200	-	-	-
	LB1P-DOL	16.460	14.896	34.687	-	-	-
	LB1P-C2	17.875	21.239	37.059	-	-	-
	LB1R-DOL	-	-	-	-	-	-
	LB1R-C2	-	-	-	-	-	-
	LB1S-DOL	-	-	-	-	-	-
	LB1S-C2	18.447	26.034	35.463	-	-	-
	LB1S-C3	16.971	28.614	35.812	-	-	-

APPENDIX 3d

Difference between corrected
Daly and Faraday ratios.
[(Daly/Faraday x 100) - 100]

BOREHOLE	SAMPLE NO.	Pb 206/204	Pb 207/204	Pb 208/204
S26	S26A-DOL	23.41	23.32	24.44
	S26A-C1	-	-	-
	S26A-C2	-0.49	-0.70	-1.37
	S26B-DOL	1.83	2.27	1.99
	S26B-C2	-0.35	-0.43	0.28
	S26B-C3	0.19	-0.04	-0.04
	S26Gb-DOL	-	-	-
	S26Gb-C2	0.49	0.74	0.60
	S26L-DOL	0.11	-0.08	-0.30
	S26L-C2	0.10	0.06	-0.23
	S26M-DOL	19.55	20.29	21.16
	S26M-C1	-	-	-
	S26M-C2	0.73	0.41	0.12
	S26M-C3	0.45	-0.55	-0.55
	S26N1-DOL	-	-	-
	S26N1-C1	-	-	-
	S26N1-C2	0.59	-2.21	0.81
	S26N2-DOL	-0.36	-0.61	-0.61
	S26N2-C1	-	-	-
	S26N2-C2	-	-	-
	S26X-DOL	18.68	19.01	19.20
	S26X-C2	0.38	0.36	0.20
	S26X-C3	-0.63	-0.89	-0.89
LB1	LB1N-DOL	-	-	-
	LB1N-C2	-	-	-
	LB1N-C3	-	-	-
	LB1P-DOL	-	-	-
	LB1P-C2	-	-	-
	LB1R-DOL	-	-	-
	LB1R-C2	-	-	-
	LB1S-DOL	-	-	-
	LB1S-C2	-	-	-
	LB1S-C3	-	-	-
Galena		0.07	-0.15	-0.19

APPENDIX 3e

Galena Pb isotope data from the present study.
Pb and Rb-Sr isotope data from Duane et al.(1991).

		Pb 206/204	Pb 207/204	Pb 208/204
Original data	Daly	13.411	14.418	32.879
(Galena)	Faraday	13.452	14.494	33.067
Corrected data	Daly	13.467	14.494	33.085
(Galena)	Faraday	13.457	14.515	33.148
Galena data from		13.530	14.582	33.301
Duane et al.(1991)		13.430	14.537	33.236
		13.534	14.675	33.627

		Rb (ppm)	Sr (ppm)	Ro (87/86Sr)
Pering Mine data	Gangue carbonate	0.07	45.00	0.7305
Duane et al.(1991)	Reivilo Fmn.	1.88	13.80	0.7061
	Monteville Fmn.	0.48	11.30	0.7092

APPENDIX 4

Rb and Sr data for S26 and LB1.
(Calculations at 1900 Ma, 1 sigma error = 100.00,
Decay Constant = 1.42000E-0011, Students t = 2.00)
(Rb blank = 170 pg; Sr blank = 2ug)

BOREHOLE	SAMPLE NO.	Rb (ppm)	Sr (ppm)	87Rb/86Sr	87Sr/86Sr	Ro (87/86Sr)	95% conf.	Epsilon	95% conf.
S26	S26A-DOL	0.6870	16.5900	0.116324	0.707794	0.704813	0.005318	31.737	4.929
	S26A-C1	0.0269	14.1200	0.005509	0.702406	0.702255	0.000382	-1.827	5.433
	S26A-C2	0.0243	15.2400	0.004610	0.704500	0.704374	0.000352	29.378	4.006
	S26B-DOL	0.2370	12.8400	0.053400	0.707052	0.705592	0.002455	46.334	4.592
	S26B-C2	0.0508	45.1500	0.003262	0.729615	0.729526	0.000333	388.428	4.003
	S26B-C3	0.0110	46.9100	0.000680	0.737185	0.737148	0.000303	484.925	4.000
	S26Gb-DOL	0.0799	10.9400	0.021148	0.715791	0.715213	0.001009	182.649	14.103
	S26Gb-C2	0.0722	34.6400	0.006042	0.727785	0.727600	0.000406	359.007	4.009
	S26L-DOL	0.1880	10.5900	0.045909	0.709974	0.708719	0.002116	90.190	4.440
	S26L-C2	0.0718	43.3400	0.004801	0.752812	0.752681	0.000378	718.090	4.005
	S26M-DOL	0.5660	11.2000	0.146310	0.714700	0.710699	0.006685	118.385	8.078
	S26M-C1	0.0571	No strontium data could be obtained						
	S26M-C2	0.0393	12.7600	0.008906	0.717598	0.717352	0.000501	213.114	1.633
	S26M-C3	0.0114	84.6500	0.000391	0.749424	0.749413	0.000307	667.307	1.638
	S26N1-DOL	0.1200	11.3900	0.030497	0.712784	0.711980	0.001422	203.473	1.624
	S26N1-C1	0.0661	38.9800	0.004926	0.749631	0.749496	0.000380	670.753	1.626
	S26N1-C2	0.0457	62.3700	0.002131	0.781621	0.781583	0.000326	842.546	1.631
	S26N2-DOL	0.1650	13.9900	0.034143	0.713439	0.712505	0.001586	144.104	2.019
	S26N2-C1	0.0758	30.1400	0.007297	0.736918	0.736718	0.000449	488.832	1.628
	S26N2-C2	0.0574	73.0500	0.002283	0.750837	0.750775	0.000324	668.952	1.631
	S26X-DOL	0.0971	10.7000	0.026269	0.712873	0.712155	0.001234	139.111	1.845
	S26X-C2	0.0700	42.8300	0.004737	0.726489	0.726359	0.000367	341.348	1.626
	S26X-C3	0.0035	30.5900	0.000331	0.715048	0.715037	0.000292	172.371	1.638
LB1	LB1N-DOL	0.0381	16.1900	0.006458	0.719923	0.719748	0.000416	247.196	1.626
	LB1N-C2	0.0360	47.6000	0.002305	0.730361	0.730298	0.000316	397.422	1.630
	LB1N-C3	0.0188	184.4000	0.000280	0.723773	0.723765	0.000296	303.632	1.639
	LB1P-DOL	0.0350	10.7100	0.009458	0.711385	0.711108	0.000520	124.188	1.635
	LB1P-C2	0.0318	29.4000	0.003117	0.730677	0.730592	0.000331	401.605	1.628
	LB1R-DOL	0.0457	10.6800	0.012401	0.725119	0.724780	0.000639	318.859	1.851
	LB1R-C2	0.0611	31.1100	0.005701	0.742042	0.741870	0.000399	582.391	1.626
	LB1S-DOL	0.0566	23.4200	0.007402	0.727787	0.727585	0.000450	360.214	1.829
	LB1S-C2	0.0297	76.2200	0.001131	0.741038	0.741007	0.000307	549.890	1.835
	LB1S-C3	0.0120	26.9600	0.001292	0.747898	0.747861	0.000311	644.619	1.634

APPENDIX 5a

Carbon and oxygen isotope results.
S26 and LB1.
(σ: C-13 = <0.05; O-18 = <0.12)

BOREHOLE	SAMPLE NO.	DELTA C-13	DELTA O-18
S26	S26A-DOL	-0.38	-10.12
	S26A-C1	-0.29	-10.60
	S26A-C2	-0.51	-11.51
	S26B-DOL	-0.24	-10.34
	S26B-C2	-0.46	-14.04
	S26B-C3	-1.92	-11.45
	S26Gb-DOL	-0.72	-13.45
	S26Gb-C2	-0.56	-11.85
	S26L-DOL	-0.11	-10.63
	S26L-C2	0.43	-12.21
	S26M-DOL	-0.31	-10.94
	S26M-C1	0.06	-10.97
	S26M-C2	-0.45	-12.46
	S26M-C3	-1.62	-10.72
	S26N1-DOL	-0.24	-11.25
	S26N1-C1	-0.26	-11.25
	S26N1-C2	-0.56	-12.45
	S26N2-DOL	-0.36	-10.28
	S26N2-C1	-0.16	-10.78
	S26N2-C2	-0.84	-11.72
	S26X-DOL	0.43	-11.05
	S26X-C2	0.49	-13.24
	S26X-C3	-6.46	-8.93
LB1	LB1N-DOL	1.00	-10.37
	LB1N-C2	0.64	-12.52
	LB1N-C3	-0.06	-15.97
	LB1P-DOL	1.09	-10.42
	LB1P-C2	0.83	-10.99
	LB1R-DOL	1.64	-11.09
	LB1R-C2	1.13	-11.36
	LB1S-DOL	1.39	-9.81
	LB1S-C2	0.70	-11.13
	LB1S-C3	-0.48	-12.69

APPENDIX 5b

Temperature Calculations

SAMPLE NO	SMOW	T (K)	T (C)
LB1R-C2	19.15		
LB1R-QTZ	20.60	643.27	370.12
LB1S-C3	19.39		
LB1S-QTZ	20.16	882.73	609.60